
Function and regulation of Sgo1 during mitotic cell division in *Saccharomyces cerevisiae*

DISSERTATION DER FAKULTÄT FÜR BIOLOGIE
DER LUDWIG-MAXIMILIANS-UNIVERSITÄT MÜNCHEN



vorgelegt von

Andreas Wallek, M. Sc. Biochemie

Mai 2015

EIDESSTATTLICHE ERKLÄRUNG

Hiermit erkläre ich an Eides statt, dass ich die vorliegende Dissertation selbstständig und ohne unerlaubte Hilfe angefertigt habe. Ich habe weder anderweitig versucht, eine Dissertation einzureichen oder eine Doktorprüfung durchzuführen, noch habe ich diese Dissertation oder Teile derselben einer anderen Prüfungskommission vorgelegt.

München, den

.....

Promotionsgesuch eingereicht am: 12.05.2015

Datum der mündlichen Prüfung: 23.07.2015

Erster Gutachter: Prof. Dr. Stefan Jentsch

Zweiter Gutachter: Prof. Dr. Peter Becker

Die vorliegende Arbeit wurde zwischen Januar 2011 und Mai 2015 unter der Anleitung von Zuzana Storchová (Ph. D.) am Max-Planck-Institut für Biochemie in Martinsried durchgeführt.

Wesentliche Teile dieser Arbeit sind in folgender Publikation veröffentlicht und zusammengefasst:

Peplowska, K.*, Wallek, A. U.*, & Storchová, Z (2014). Sgo1 regulates both condensin and Ipl1/Aurora B to promote chromosome biorientation. *PLoS Genet.* **10**, e1004411.

*these authors contributed equally to this work

Note on results obtained in collaboration:

Generation of data and graphs depicted in Fig. 10A, 12, 13C and 20 was performed by Dr. Karolina Peplowska in the group of Zuzana Storchová.

Summary	1
1 Introduction	2
1.1 Cellular safeguarding mechanisms prevent genomic instability during mitosis	2
1.1.1 Cohesin and condensin complexes maintain the structure of mitotic chromosomes and sister chromatid cohesion	3
1.1.2 The spindle assembly checkpoint (SAC) monitors the attachment of chromosomes to the mitotic spindle.....	7
1.1.3 The chromosomal passenger complex (CPC) contributes to chromosome biorientation through regulating the kinetochore-microtubule interface	9
1.2 Shugoshin proteins are essential for faithful chromosome segregation.....	14
1.2.1 A conserved domain organization is characteristic of Shugoshin proteins	14
1.2.2 The role of Shugoshin and its binding partner PP2A in meiotic chromosome segregation	15
1.2.3 Shugoshin proteins contribute to the fidelity of mitotic chromosome segregation	18
2 Aim of this study	20
3 Results	21
3.1 Cell cycle-dependent regulation of Sgo1 protein levels	21
3.1.1 The C-terminus of Sgo1 mediates its cell cycle-dependent protein expression profile	21
3.1.2 Mapping of degradation signals in the C-terminal domain of Sgo1 reveals one essential element.....	22
3.1.3 Mutation of a putative SUMO-binding motif stabilizes Sgo1 protein levels	23
3.1.4 Cell cycle-dependent regulation of Sgo1 protein levels is not essential for its function in mitotic chromosome segregation.....	25
3.2 Localization of Sgo1 via its conserved basic region.....	26
3.2.1 Mutation of the conserved basic region interferes with Sgo1's localization leading to defective chromosome segregation.....	26
3.2.2 Mps1 overexpression causes a synthetic growth defect in cells expressing mislocalized Sgo1	28
3.3 The function of Sgo1's coiled-coil domain in mitosis.....	30
3.3.1 The coiled-coil domain of Sgo1 mediates the interaction with Rts1 <i>in vitro</i>	30
3.3.2 Sgo1 is required for the centromeric enrichment of Rts1 in mitotic cells	31
3.3.3 Rts1 is required for faithful chromosome segregation during mitosis	32
3.3.4 Rts1 and its interaction with Sgo1 at centromeres are crucial for the detection and/or the repair of syntelic chromosome attachments.....	33
3.3.5 Genetic analysis of <i>sgo1</i> mutants lacking the interaction with Rts1.....	35

3.4 SMC protein complexes as downstream targets of Sgo1 and Rts1	36
3.4.1 The centromeric enrichment of cohesin is not affected by <i>SGO1</i> deletion	36
3.4.2 Sgo1 is essential to maintain a centromeric pool of condensin complexes in mitotic cells	37
3.4.3 The centromeric pool of condensin functions in the detection and/or repair of incorrect chromosome attachments	39
3.4.4 Sgo1 and Rts1 contribute to the compaction of centromeric chromatin during mitosis	41
3.5 The chromosomal passenger complex (CPC) as downstream target of Sgo1	42
3.5.1 Ipl1/Aurora B phosphorylation has to be precisely balanced for functional repair of syntelic attachments	42
3.5.2 Sgo1 maintains adequate levels of centromeric Ipl1/Aurora B in mitotic cells	44
3.5.3 Overexpression of CPC proteins partially rescues chromosome segregation defects in cells lacking Sgo1	45
3.5.4 Overexpression of CPC proteins does not rescue the defective repair of syntelic attachments of condensin mutants	47
4 Discussion	49
4.1 Cell cycle-dependent regulation of Sgo1 protein levels during mitosis	49
4.2 Phosphorylation-dependent localization of Shugoshin proteins in mitosis	51
4.3 Sgo1 and PP2A function together in mitotic chromosome segregation	54
4.4 Sgo1-dependent enrichment of centromeric condensin allows the repair of incorrect chromosome attachments	55
4.5 Sgo1 regulates Ipl1/Aurora B levels at centromeres	57
5 Material and methods	62
5.1 Material	62
5.1.1 Chemicals, consumables, equipment and commercially available kits	62
5.1.2 Enzymes	63
5.1.3 Oligonucleotides	63
5.1.4 Plasmids	66
5.1.5 Bacterial strains and culture conditions	68
5.1.6 Yeast strains and culture conditions	68
5.1.7 Antibodies	73
5.2 Molecular biology methods	75
5.2.1 Polymerase chain reaction (PCR)	75
5.2.2 PCR-based introduction of point mutations	76

5.2.3 Restriction hydrolysis	76
5.2.4 Ligation.....	77
5.2.5 Sequencing	77
5.2.6 DNA agarose electrophoresis	78
5.2.7 Purification of plasmid DNA from <i>E. coli</i>	78
5.2.8 Transformation of chemical competent <i>E. coli</i> cells	78
5.2.9 Transformation of <i>S. cerevisiae</i>	79
5.2.9 Extraction of genomic DNA from <i>S. cerevisiae</i>	79
5.2.10 Sensitivity of yeast mutants towards microtubule poisons and protein overexpression.....	80
5.2.11 Induction of cell cycle arrest and synchronization of <i>S. cerevisiae</i> cultures.....	80
5.3 Protein biochemistry techniques	81
5.3.1 TCA precipitation of cellular proteins	81
5.3.2 SDS-PAGE.....	81
5.3.3 Immunoblotting.....	82
5.3.4 <i>in vitro</i> binding analysis of Sgo1 and purified PP2A complexes	82
5.4 Chromatin immunoprecipitation (ChIP) followed by quantitative PCR	83
5.5 Fluorescence microscopy to visualize GFP/RFP-tagged proteins	85
6 References	87
Abbreviations	102
Acknowledgements.....	105
Curriculum Vitae	106

Summary

In order to segregate sister chromatids equally to daughter cells, all chromosomes have to be attached to microtubules of the mitotic spindle in a bioriented manner. During the gradual establishment of chromosome biorientation, intermediate attachments that do not manifest tension across the kinetochores of sister chromatids are turned over by the activity of the conserved kinase Ipl1/Aurora B. In budding yeast this quality control of chromosome attachments depends on the presence of the conserved Shugoshin (Sgo1) protein.

In this study, we investigate the regulation of Sgo1 during mitotic cell division to understand its molecular contribution to this quality control mechanism. We show that cell cycle-dependent degradation of Sgo1 during late stages of mitosis is dispensable for the repair of incorrect chromosome attachments and chromosome biorientation. We further identify Sgo1 to be crucial for the enrichment of Rts1 (the regulatory subunit of the protein phosphatase 2A complex) on centromeric regions of chromosomes, which lack tension between sister chromatids. Accordingly, we show that both, the precise localization of Sgo1 and the interaction with Rts1 are important to achieve chromosome biorientation after induction of incorrect chromosome attachments.

Moreover, we show that Sgo1 is essential to maintain a centromeric pool of condensin complexes in mitotic cells. The compaction of centromeric chromatin is impaired upon deletion of *SGO1* or inhibition of condensin function resulting in a failure to detect or repair tensionless chromosome attachments. In parallel, Sgo1 aids the turnover of such attachments by stabilizing the protein levels of Ipl1/Aurora B on kinetochores during mitosis in budding yeast. We propose that Sgo1 acts as binding hub that modulates the conformation of centromeric chromatin via condensin and sustains adequate amounts of the repair kinase Ipl1/Aurora B on kinetochores to ensure faithful chromosome segregation.

1 Introduction

Symmetric distribution of the genetic information into the daughter cells is fundamental for all organisms in order to stably proliferate. Thus, elaborate safeguarding mechanisms have evolved in prokaryotic as well as eukaryotic cells allowing them to segregate their replicated genetic material faithfully and to maintain genome stability over many generations. Malfunction of these molecular control mechanisms and its key components leads to asymmetric distribution of the genetic material, thus creating daughter cells with varying chromosome content. Such deviations from the typical chromosome number are called aneuploidy and its physiological effects are highly deleterious for most organisms. In human cells aneuploidy is closely linked to tumour formation, miscarriages and severe developmental disorders, such as Down's syndrome. Understanding how cells maintain genomic stability on the molecular level will provide important insights regarding the causes and consequences of aneuploidy and related diseases.

1.1 Cellular safeguarding mechanisms prevent genomic instability during mitosis

During mitosis the replicated DNA is compacted into distinct chromosomes and the chromosome mass is equally distributed by the spindle apparatus, which is a highly ordered structure based on a dynamic microtubule network (reviewed in Bouck *et al.*, 2008). The following chapters introduce a set of key aspects, which are necessary to faithfully distribute the replicated sister chromatids between the two poles of the mitotic spindle. First, we describe the mode of action of structural maintenance of chromosomes (Smc) protein complexes, such as cohesin and condensin. These complexes determine the conformation of mitotic chromosomes and maintain the cohesion of duplicated sister chromatids until late stages of mitosis. Next, we focus on the spindle assembly checkpoint (SAC) and how it couples cell cycle progression with the attachment status of chromosomes to the mitotic spindle. We further summarize current knowledge about how the chromosomal passenger complex (CPC) monitors the kinetochore-microtubule interface, which physically links mitotic chromosomes to the spindle apparatus. The CPC and its effector kinase Ipl1/Aurora B constitute the cellular repair machinery, which allows the release and thus, the repair of incorrect chromosome attachments.

If not indicated with an abbreviation to specify the source organism (*Dm* = *Drosophila melanogaster*, *Hs* = *Homo sapiens*, *Ms* = *Mus musculus*, *Sc* = *Saccharomyces cerevisiae*, *Sp* = *Schizosaccharomyces pombe*, *Xl* = *Xenopus laevis*), all protein or gene names in this study refer to the budding yeast *S. cerevisiae*.

1.1.1 Cohesin and condensin complexes maintain the structure of mitotic chromosomes and sister chromatid cohesion

Eukaryotic organisms generate genetically identical daughter cells through alternating cycles of DNA replication or synthesis (S phase) and DNA partitioning during mitosis (M phase). The cohesin complex is an essential factor maintaining the cohesion of duplicated sister chromatids until they are equally partitioned between the two daughter cells by the mitotic spindle. The molecular structure of the cohesin complex is closely related to this function. The core of the cohesin complex is formed by two proteins of the structural maintenance of chromosomes (SMC) family, Smc1 and Smc3 (reviewed in Nasmyth & Hearing, 2009). Monomeric Smc3 folds into a rod-like structure, which results from a long intramolecular coiled-coil domain that is capped by globular domains on each end (Haering *et al.*, 2002). One of these globular domains, the so called hinge domain, interacts with its counterpart of Smc1, thus forming a heterodimer that can be visualized as “open V”-shaped structures by electron microscopy (Haering *et al.*, 2002). Both arms of the V-shaped structure are capped by a second globular domain, which is comprised of the C- and N-termini of Smc1 and Smc3, respectively (Melby *et al.*, 1998; Haering *et al.*, 2002). These globular domains form two individual ATP nucleotide binding domains (NBDs) of the ABC family of ATPases (Melby *et al.*, 1998; Haering *et al.*, 2002).

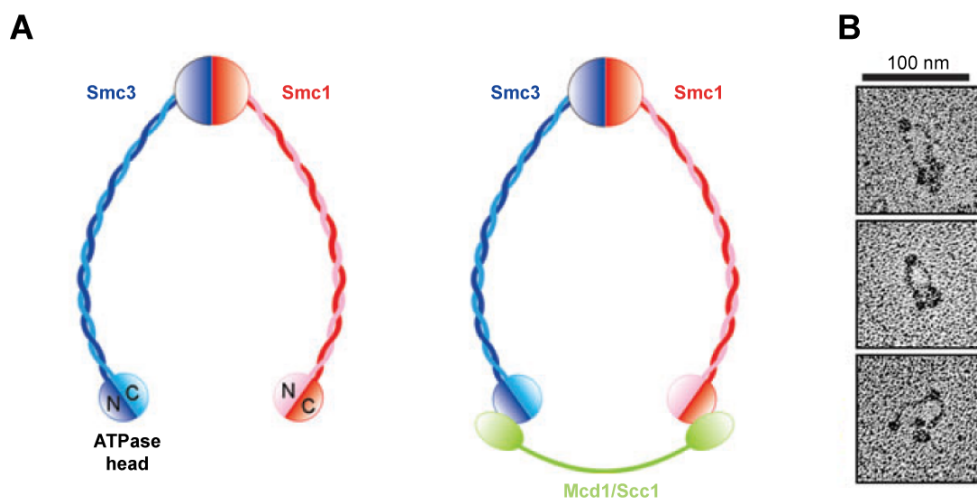


Figure 1. Scheme of dimeric SMC protein and trimeric cohesin complexes

(A) Smc1 and Smc3 form a V-shaped heterodimer via an interaction of their hinge domains. N- and C-termini of each SMC subunit form a globular ATPase head domain by folding back on each other in an intramolecular coiled-coil rod. Both globular head domains contact the kleisin subunit Mcd1/Sccl to assemble a closed ring-like structure, which might embrace DNA double strands (figure adapted from Xiong & Gerton, 2009). (B) Electron micrographs of soluble cohesin complexes exemplifying their open V-shaped and ring-like structures *in vitro* (figure adapted from Nasmyth & Haering, 2005).

A third protein is necessary to connect these globular domains generating a ring-like structure that potentially embraces replicated DNA strands (Gruber *et al.*, 2003). Members of this protein family have been named kleisins, which stands for closure in Greek to emphasize their function in the cohesin

complex. The interaction between the Smc1/3 heterodimer and the mitotic kleisin subunit Scc1/Mcd1 has been studied extensively in budding yeast. The N-terminus of Scc1/Mcd1 contacts the ATPase head domain of Smc3, whereas its C-terminus interacts with Smc1 (see Figure 1; Haering *et al.*, 2002). Based on its molecular structure and its dimensions the cohesin ring seems sufficient to embrace the two copies of a duplicated DNA double helix. The observed structure of the cohesin complex imposes an intriguing model how its cohesive force is achieved. Elegant studies confirmed recently that such a topological binding of cohesin complexes can be observed on small circular minichromosomes purified from budding yeast and in an *in vitro* assembled reaction (Ivanov & Nasmyth, 2005; Murayama & Uhlmann, 2014). Linearization of the minichromosome or cleavage of one cohesin subunit abolishes this interaction in both experimental setups, hence arguing for topological DNA binding.

To serve its function as a cohesion factor for sister chromatids, the cohesin complex has to associate with chromosomes. The initial loading of cohesin on chromosomes is mediated by a separate complex consisting of Scc2 and Scc4 (Ciosk *et al.*, 2000). The molecular details of this loading mechanism are currently unknown. However, the opening of the cohesin ring seems to be important for this process (Ocampo-Hafalla & Uhlmann, 2011). Previous studies revealed that only cohesin loaded during S phase on chromosomes maintains cohesion between sister chromatids (Uhlmann & Nasmyth, 1998). This finding suggests that in addition to chromosome binding, the cohesin complex has to be activated in order to establish its cohesive force. Indeed, establishment of cohesion is directly linked to DNA replication via the proliferating cell nuclear antigen (PCNA) protein that tethers the establishment factor Eco1 to the replication machinery (Moldovan *et al.*, 2006). The acetyltransferase Eco1 acetylates residues located in the globular head domain of Smc3 and this modification locks the pre-loaded cohesin complex in a cohesive state (Ben-Shahar *et al.*, 2008; Unal *et al.*, 2008; Zhang *et al.*, 2008; Rowland *et al.*, 2009). Once established, sister chromatid cohesion is maintained until all chromosomes become correctly attached to the mitotic spindle in metaphase.

After the establishment of chromosome biorientation, the cohesive population of cohesin molecules has to be removed in a coordinated manner to allow the segregation of sister chromatids. The resolution of sister chromatid cohesion is a non-reversible process; hence its faithful execution is crucial for cells to prevent chromosome missegregation and aneuploidy. One key factor controlling the regulated loss of cohesin is a highly conserved, heterodimeric complex of Pds1 (securin) and Esp1 (separase; Cohen-Fix *et al.*, 1996; Ciosk *et al.*, 1998). Esp1 has been identified as a cysteine protease that cleaves the cohesin subunit Scc1/Mcd1 thereby releasing cohesin from chromosomes (Uhlmann *et al.* 1999, 2000). In order to avoid premature cleavage of cohesin, the proteolytic activity of Esp1 is restrained by binding of its inhibitor Pds1. Degradation of the potent Esp1-inhibitor Pds1 is initiated by the E3 ubiquitin ligase activity of the anaphase promoting complex/cyclosome (APC/C; Cohen-Fix *et al.*, 1996). This complex is targeted by the spindle assembly checkpoint (SAC) to couple the attachment status of chromosomes with the timely loss of sister chromatid cohesion and cell cycle progression. The intricate signalling network of the SAC will be discussed later in more detail.

In addition to cohesin, a second complex, which is called condensin, is essential to determine the shape of mitotic chromosomes. Overall, condensin complexes are structurally related to cohesin and assemble into a similar molecular structure (reviewed in Nasmyth & Haering, 2005). In contrast to cohesin, two functionally different condensin complexes (condensin I and condensin II) can be found in most eukaryotic organisms (reviewed in Hirano, 2012). The core of the condensin complex is formed by a heterodimer of two SMC proteins, Smc2 and Smc4 (reviewed in Nasmyth & Haering, 2005). Each SMC protein folds into a rod-shaped coiled-coil molecule that is capped by two globular domains. Analogous to the cohesin complex, these SMC proteins use their hinge domains to make contact with each other forming an open-V shaped structure (Figure 1). Two different sets of regulatory subunits bind to this SMC heterodimer resulting in the assembly of functionally different condensin I and II complexes. Each set of regulatory subunits consists of one member of the kleisin protein family and two proteins containing HEAT repeat domains. In budding as well as in fission yeast only one set of regulatory proteins has been identified, which might reflect evolutionary adaptations in these fungi containing relatively small genomes (Hirano, 2012; Table 1).

Table 1. Subunit composition of different condensin complexes in vertebrates, *S. cerevisiae* and *S. pombe*

Condensin subunit	Vertebrates	<i>S. cerevisiae</i>	<i>S. pombe</i>
Smc2	CAP-E	Smc2	Cut14
Smc4	CAP-C	Smc4	Cut3
condensin I			
kleisin	CAP-H	Brn1	Cnd2
HEAT repeat protein A	CAP-D2	Ycs4	Cnd1
HEAT repeat protein B	CAP-G	Ycg1	Cnd3
condensin II			
kleisin	CAP-H2	—	—
HEAT repeat protein A	CAP-D3	—	—
HEAT repeat protein B	CAP-G2	—	—

Condensin contributes to several aspects of nuclear and chromosomal architecture as well as chromosome segregation in eukaryotes (reviewed in Hirano 2012; Thadani *et al.*, 2012). The assembly of condensed, mitotic chromosomes is probably condensin's most prominent and eponymous function, as it was shown with sperm chromatin in *Xenopus* egg extracts (Hirano & Mitchison, 1994). How condensin achieves the full compaction of mitotic chromosomes and contributes to their faithful segregation remains unexplained on the molecular level. In order to gain insight into its various contributions, two groups independently mapped condensin binding sites via genome-wide chromatin immunoprecipitation (ChIP) approaches in budding yeast (Wang *et al.*, 2005; D'Ambrosio *et al.* 2008a). Both studies revealed that condensin is enriched around centromeres and on ribosomal DNA (rDNA) besides other specialized chromatin regions.

Condensin recruitment to rDNA depends on Csm1 and Lrs4, two members of the monopolin complex (Johzuka & Horiuchi, 2009). The authors of this study showed that monopolin recruits condensin in order to maintain the structural integrity as well as the number of rDNA repeats. Moreover, condensin was shown to be important for the efficient decatenation of the replicated rDNA locus by topoisomerase II in order to prevent anaphase bridges during chromosome segregation (D'Ambrosio *et al.*, 2008b). This function is just one example of how condensin contributes to the fidelity of chromosome segregation during anaphase. Another example is the separation of sister chromatids in anaphase, which is actively promoted by chromosome recoiling (Renshaw *et al.*, 2010). This study revealed that a pool of functional cohesin molecules escapes the cleavage by separase at the onset of anaphase and resides on chromosome arms. The chromosomes undergo alternating cycles of stretching and recoiling while they are pulled to the poles of the mitotic spindle. Renshaw and colleagues showed that recoiling of chromatin stretches is important for the removal of residual cohesin complexes and the execution of sister chromatid separation in a timely manner. Strikingly, chromosome recoiling depends on functional condensin complexes located on the arms of anaphase chromosomes. Such a mode of action is consistent with the finding that condensin becomes hyperphosphorylated upon entry into anaphase (St-Pierre *et al.*, 2009). The budding yeast polo-like kinase Cdc5 phosphorylates all three regulatory subunits and their modification significantly increases the capability of condensin to introduce supercoils into relaxed plasmid DNA *in vitro*. All these examples emphasize that condensin contributes to chromosome segregation during anaphase, likely by introducing DNA supercoils to decatenate sister chromatids.

However, recent studies provide evidence that condensin participates in the process of chromosome segregation also before the onset of anaphase. This function seems to be rather related to condensin enrichment on centromeric chromatin. Correspondingly, it was shown that condensin maintains the integrity of centromeres in budding as well as in fission yeast and vertebrates (Ribeiro *et al.*, 2009; Stephens *et al.*, 2011; Tada *et al.*, 2011). The depletion of Smc2 reduces the stiffness of centromeric chromatin in vertebrate cells, thereby increasing the average distance between sister kinetochores (Ribeiro *et al.*, 2009). Although the kinetochores seem to be fully functional and intact under these conditions, the cells show a persistent activation of the SAC. Likewise, inactivation of condensin in budding yeast affects the compaction state of centromeric and pericentric chromatin in metaphase (Stephens *et al.*, 2011). The authors of this study further showed that functional cohesin and condensin as well as appropriate amounts of histone H3 are necessary for wild type compaction of centromeric regions. Based on these findings the authors speculate that cohesin and condensin act on centromeric chromatin to form a molecular (mitotic) spring, which counteracts the forces of the mitotic spindle. A similar mechanism might work in fission yeast. Tada and colleagues reported that inactivation of the centromeric pool of condensin leads to increased rates of merotelic attachments and sensitivity towards microtubule poisons (Tada *et al.*, 2011). This study also provides evidence that condensin acts during metaphase to facilitate error-free chromosome segregation in yet another model organism. These findings provide evidence that condensin contributes to several molecular mechanisms, which act before and after the initiation of sister chromatid cohesion in order to facilitate error-free chromosome segregation.

1.1.2 The spindle assembly checkpoint (SAC) monitors the attachment of chromosomes to the mitotic spindle

One major criterion for faithful chromosome segregation is that all chromosomes have to attach to microtubules emanating from the mitotic spindle before the segregation machinery starts to pull sister chromatids to the spindle poles. The attachment of microtubules to chromosomes is mediated by large protein complexes, also known as kinetochores. These protein complexes assemble on centromeric DNA, provide the binding platform for microtubules and translate the poleward-directed microtubule forces into chromosome movement (reviewed in Yamagishi *et al.*, 2014; Cheeseman, 2014). Kinetochores consist of more than 100 different proteins, which form a highly-ordered macromolecular complex on the underlying centromeric chromatin. These specific regions vary strongly within eukaryotes and lack uniform DNA sequences or structures. Site-specific incorporation of non-canonical nucleosomes seems to be the only unifying feature of most eukaryotic centromeres identified so far. Canonical histone H3 is substituted by a 17 kDa protein, called CENP-A (Cse4 in budding yeast), in such nucleosomes deposited at human centromeres (Palmer *et al.*, 1987, 1991). Ectopic expression of the budding yeast CENP-A homolog Cse4 can complement the knock-down of endogenous CENP-A in human cells (Wieland *et al.*, 2004). Furthermore, knock-down experiments in human cells showed that CENP-A is necessary for the recruitment of several kinetochore subcomplexes to centromeric DNA including members of the SAC network (Liu *et al.*, 2006). Moreover, Cse4 is crucial for the integrity of centromeric DNA and faithful chromosome segregation in budding yeast, which relies on functional kinetochores (Stoler *et al.*, 1995; Meluh *et al.*, 1998). These studies imply that the incorporation of a non-canonical histone H3 variant at centromeric DNA is essential for the formation of functional kinetochores. They further establish this epigenetic modification as a general mechanism that defines the position of the microtubule attachment site on chromosomes.

Cells have to monitor these chromosomal attachment sites for occupancy with spindle microtubules in order to prevent chromosome missegregation. To this end cell cycle progression has to be coupled to the attachment status of each kinetochore. The SAC, an intricate signalling network, delays the entry into anaphase as long as one single kinetochore remains unattached to the mitotic spindle (reviewed in Lara-Gonzales *et al.*, 2012; Musacchio & Salmon, 2007). To address such a scenario experimentally cells can be treated with chemical compounds, which depolymerise the mitotic spindle. The use of these microtubule poisons, such as benomyl or nocodazole, allowed the identification of crucial checkpoint genes in budding yeast (Hoyt *et al.*, 1991; Li & Murray, 1991). These studies identified the genes *BUB1*, *BUB3*, *MAD1*, *MAD2*, *MAD3* (*BUBR1* in vertebrates) as core components of the checkpoint response. The protein kinase Mps1 supports these core components and its kinase activity can establish the checkpoint response even in the absence of spindle damage (Hardwick *et al.*, 1996; Weiss & Winey, 1996). Mechanistic aspects of the SAC network seem to be strikingly conserved from budding yeast to higher eukaryotes despite their different requirements for efficient chromosome segregation (Vleugel *et al.*, 2012).

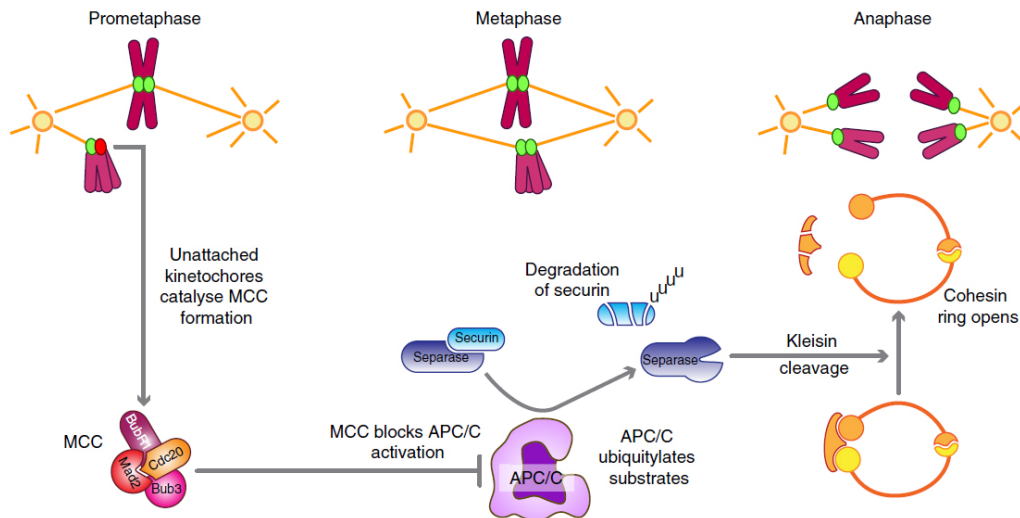


Figure 2. The release of chromatin-bound cohesin is coupled to the attachment of chromosomes to the mitotic spindle by the spindle assembly checkpoint (SAC) network

Unattached kinetochores contribute to the generation of mitotic checkpoint complexes (MCCs), which bind and tether Cdc20 the co-factor of the anaphase promoting complex/cyclosome (APC/C) during mitosis. Hence, the APC/C cannot ubiquitinate securin/Pds1 and separase/Esp1 is kept inactive. Once all kinetochores are captured by microtubules emanating from the mitotic spindle, the formation of MCCs ceases and Cdc20 is released. Cdc20 binds to the APC/C, which in turn marks securin/Pds1 for proteasomal degradation. The destruction of securin/Pds1 leads to the activation of separase/Esp1, which finally cleaves the cohesin subunit Scc1/Mcd1 to dissolve sister chromatid cohesion (figure adapted from Lara-Gonzales *et al.*, 2012).

Recent studies revealed that the checkpoint kinase Mps1 phosphorylates the constitutive kinetochore component Spc105/KNL1 in yeast as well as in human cells (London *et al.*, 2012; Shepperd *et al.*, 2012; Yamagishi *et al.*, 2012). This modification seems to generate the assembly platform for the other SAC components around centromeres thereby engaging the checkpoint. A complex of the protein kinase Bub1 and the checkpoint component Bub3 recognizes and binds phosphorylated Spc105. As a consequence of this interaction, the heterodimeric Bub1/Bub3 complex associates with kinetochores (London *et al.*, 2012). Despite extensive research, the exact function of the Bub1/Bub3 complex in checkpoint signalling still remains elusive (Hauf, 2013). Notably, it was shown that the kinase activity of Bub1 is dispensable for SAC activation in response to unattached kinetochores, but critical for its activation in response to reduced sister chromatid cohesion (Fernius & Hardwick, 2007). In addition, the Bub1/Bub3 complex is necessary for the accumulation of the SAC components Mad1 and Mad2 on unattached kinetochores (Gillet *et al.*, 2004). Recent evidence suggests that Bub1 acts as a receptor of Mad1 on unattached kinetochores and that this interaction is actively promoted by Mps1 phosphorylation in budding yeast (London & Biggins, 2014). The Mad1/Mad2 moieties in turn catalyse the reaction that generates the mitotic checkpoint complex (MCC), which is the effector of the spindle checkpoint (Figure 2).

The MCC is formed by binding of Mad2, Mad3 (BubR1) and Bub3 to the APC/C activator Cdc20 (Hardwick *et al.*, 2000; Hwang *et al.*, 1998; Primorac & Musacchio, 2013). Thus, the inhibitory signal created by the SAC is due to the sequestration of the APC/C co-activator Cdc20. The large ubiquitin

ligase APC/C ubiquitylates its major substrates (securin/Pds1 and mitotic cyclins) to mark them for proteasomal degradation only when it is bound to Cdc20 (reviewed in Peters, 2006). *In vitro* experiments indicate that the association of the APC/C with MCCs further restrains the access to its substrates (Herzog *et al.*, 2009). Recent structural analysis of the MCC revealed that the recognition sites of Cdc20, which are important for ubiquitylation by the APC/C, are occupied by Mad3 within the MCC (Chao *et al.*, 2012). This observation supports the hypothesis that Mad3 contributes to the inhibition of the APC/C by acting as a pseudosubstrate of its activator Cdc20 (Burton & Solomon, 2007). The formation of MCCs relies on the conformational change of Mad2 molecules from their inactive open form (O-Mad2) to a closed conformation state (C-Mad2). Mad2 can only bind to Cdc20 in its closed conformation, thereby initiating the formation of the MCC. A Mad1-C-Mad2 tetramer bound to unattached kinetochores acts as a catalyst for the conformational change of additional, unbound O-Mad2 molecules in a prion-like manner (De Antoni *et al.*, 2005; Simonetta *et al.*, 2009). This chaperone-like function of the Mad1-C-Mad2 complex rapidly increases the levels of C-Mad2, which in turn is competent to bind Cdc20, thus, inhibiting the APC/C and cell cycle progression. Such a mechanism explains also how one single unattached kinetochore as the sole source of C-Mad2 molecules can yield sufficient amounts of MCCs to halt cell cycle progression. This elegant mechanism couples the attachment status of individual chromosomes directly to sister chromatid cohesion and cell cycle progression.

1.1.3 The chromosomal passenger complex (CPC) contributes to chromosome biorientation through regulating the kinetochore-microtubule interface

Unattached kinetochores actively contribute to the formation of MCCs and the resulting cell cycle arrest. But even when all chromosomal attachment sites are occupied, faithful chromosome segregation is not always ensured, because faulty attachments can be formed (Figure 3). In budding yeast each kinetochore is captured exactly by one spindle microtubule (Winey *et al.*, 1995). In case that both sister kinetochores become attached to spindle microtubules emanating from the same spindle pole (syntelic attachment), the SAC would not be activated and yet chromosome segregation would lead to the formation of aneuploid daughter cells. Syntelic attachments are less frequent in higher eukaryotes due to the fact that several microtubules make contact with one single kinetochore. However, another configuration challenges the fidelity of chromosome segregation in these organisms as spindle microtubules from opposite poles become attached to the same kinetochore. Such connections are called merotelic attachments and likewise interfere with the fidelity of chromosome segregation. Chromatids that are merotelically attached do not segregate with the bulk chromatin mass, but stay behind as lagging chromosomes (Cimini *et al.*, 2001). An additional layer of control is therefore required to repair syntelic as well as merotelic attachments in order to prevent the unequal distribution of the replicated genetic material. This control mechanism targets the kinetochore-microtubule interface and likely detects whether the established attachment yields appropriate tension between sister chromatids. Only when sister kinetochores are connected to opposing spindle poles

(i. e. chromosome biorientation), the microtubule-generated forces can pull the sister chromatids apart from each other. Since these forces are opposed by cohesin complexes loaded along chromosomes, tension is applied to sister chromatids. Microtubule-generated forces fail to establish appropriate tension between sister chromatids when they are attached syntelically and merotelically, respectively.

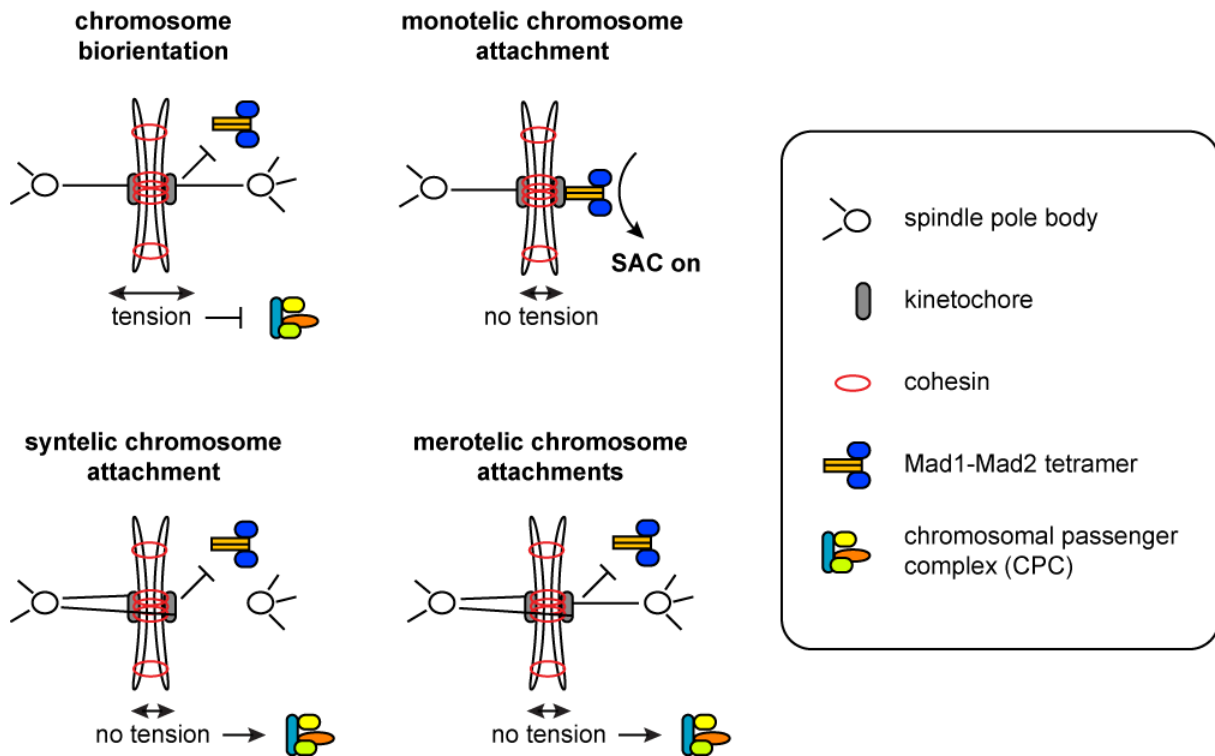


Figure 3. Scheme of chromosome attachments occurring during mitosis

Chromosome biorientation, which is required for the equal distribution of genetic material, directly blocks SAC activation and yields appropriate tension between sister chromatids. Monotelic attachments occur naturally during the establishment of chromosome biorientation and halt cell cycle progression through SAC activation. This response is initiated through binding of Mad1-Mad2 tetramers to unattached kinetochores, which is inhibited in syntelic and merotelic chromosome attachments. These attachment types are characterized by reduced tension between sister chromatids. Reduced tension likely initiates the resolution of these attachments, which is facilitated through the chromosomal passenger complex (CPC) and its effector kinase Aurora B/Ipl1.

In budding yeast, two kinetochore subcomplexes are most important to form a functional kinetochore-microtubule interface, which allows the translation of microtubule-generated forces into sister chromatid tension. Structural analysis revealed that the oligomeric Dam1 complex can form ring-like structures around microtubules (Miranda *et al.*, 2005; Westermann *et al.*, 2005). Strikingly, these ring-like structures can slide along encircled microtubules and move processively with depolymerising microtubule ends (Westermann *et al.*, 2006). Biochemical analysis revealed that Dam1 complexes weakly bind to purified Ndc80, which is another constitutive member of budding yeast kinetochores (Shang *et al.*, 2003). This observation is in line with another study suggesting that Dam1 and Ndc80 complexes are mainly discrete, although a weak association of can be detected (Janke *et al.*, 2002; Tien *et al.*, 2010). Nevertheless, both kinetochore complexes act highly cooperative on pre-assembled

microtubules *in vitro* (Lampert *et al.*, 2010; Tien *et al.*, 2010). Two studies reported independently that Dam1 and Ndc80 complexes assemble efficiently on dynamic microtubule ends *in vitro*. Moreover, Dam1 acts as a processivity factor for Ndc80 and confers microtubule plus end-tracking ability to this complex (Lampert *et al.*, 2010; Tien *et al.*, 2010). These results suggest that Ndc80 complexes specifically bind Dam1 complexes that are assembled on the plus ends of spindle microtubules in order to connect kinetochores with the mitotic spindle (Figure 4; Lampert & Westermann, 2011).

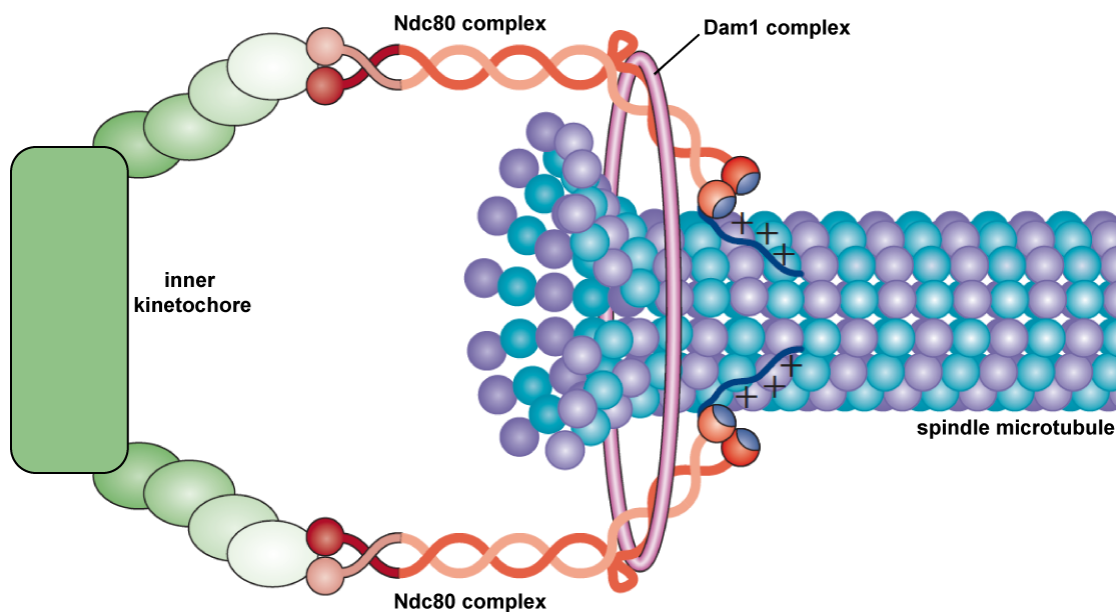


Figure 4. Model of the kinetochore-microtubule interface in *S. cerevisiae*

The kinetochore component Ndc80 interacts with Dam1 oligomers forming a ring-like structure, which tracks the plus ends of microtubules. The association of Ndc80 and Dam1 molecules at the end of spindle microtubules likely couples the kinetochore to the mitotic spindle to translate microtubule-generated forces into chromosome movement. Moreover, the strength of this interaction is regulated by Aurora B/Ipl1 phosphorylation allowing the release of faulty chromosome attachments (figure adapted from Lampert & Westermann, 2011).

The Ndc80-Dam1 interaction is therefore not only crucial for the actual coupling of chromosomes to the mitotic spindle, but also may provide the interface for the repair of incorrect attachments. In this context it is important to note that the affinity between Ndc80 and Dam1 complexes depends on their phosphorylation by Ipl1, which is the budding yeast homolog of mammalian Aurora B kinases (Lampert *et al.*, 2010; Tien *et al.*, 2010; Shang *et al.*, 2003). Aurora B/Ipl1 is the catalytic component of the chromosomal passenger complex (CPC), which additionally contains the three regulatory subunits INCENP/Slh15, survivin/Bir1 and borealin/Nbl1 (reviewed in Ruchaud *et al.*, 2007; Carmena *et al.*, 2012). In general, the CPC is conceived as a master regulator of mitotic chromosome segregation and its various functions are executed via phosphorylation of different substrates by the Aurora B/Ipl1 kinase (Carmena *et al.*, 2012).

The influence of Aurora B/Ipl1 on the stability of kinetochore-microtubule connections in *S. cerevisiae* had been reported even before its direct effect on the interaction between Ndc80 and Dam1 complexes was revealed (Biggins *et al.*, 1999). Aurora B/Ipl1, together with INCENP/Sli15, was later shown to actively promote chromosome bi-orientation in budding yeast (Tanaka *et al.*, 2002). The authors of this study proposed that initial attachments of kinetochores to spindle microtubules are turned over by Ipl1 activity until chromosome biorientation is achieved, which eventually stabilizes these connections. Indeed, Ipl1 was shown to directly phosphorylate several kinetochore components, such as Dam1 and Spc34 (Cheeseman *et al.*, 2002). The authors further confirmed that *dam1* mutants, which are resistant to Ipl1 phosphorylation, missegregate chromosomes with elevated frequencies resembling the phenotype of *ipl1* mutants. Strikingly, this chromosome segregation defect is consistent with the effect of Ipl1 phosphorylation on the interaction of Dam1 and Ndc80 complexes *in vitro* (Lampert *et al.*, 2010; Tien *et al.*, 2010). In addition to budding yeast, Aurora B/Ipl1 seems to perform a very similar role in vertebrates. The human analogue of Ndc80 (*HsHec1*) is phosphorylated by Aurora B/Ipl1 *in vitro* and the mutation of the identified residues results in an increase of stretched centromeres and merotelic attachments (Deluca *et al.*, 2006). These phenotypes indicate that the lack of Aurora B/Ipl1 phosphorylation leads to stabilized kinetochore-microtubule attachments. Moreover, Aurora B/Ipl1 phosphorylation further counteracts the interaction of kinetochores with the Ska complex in human cells, which is the functional analogue of the budding yeast Dam1 complex (Chan *et al.*, 2012; Welburn *et al.*, 2009). Although mechanistic details may vary in different species, these results emphasize that Aurora B/Ipl1 phosphorylation plays a central and highly conserved role in regulating the stability of kinetochore-microtubule attachments.

Although the contribution of Aurora B/Ipl1 and the CPC to the resolution of incorrect chromosome attachments has been broadly accepted, it remains unclear how tension affects kinetochore structure and how the CPC can detect this changes to discriminate between incorrect and correct attachments. Extensive research on the details of Aurora B/Ipl1 kinase activation as well as CPC localization in various model organisms yielded first molecular insights into the nature of this cellular error correction machinery. This research further suggests that the spatio-temporal distribution of Aurora B/Ipl1 kinase activity and substrate accessibility are key determinants of the repair of syntelic and merotelic attachments.

One crucial aspect of functional error repair is that it requires the controlled activation of Aurora B/Ipl1. The physical association of INCENP/Sli15 with Aurora B/Ipl1 heavily stimulates its kinase activity *in vitro* and might represent the initial step of kinase activation *in vivo* (Honda *et al.*, 2003). Accordingly, INCENP/Sli15 itself is phosphorylated *in vitro* by Aurora B/Ipl1 and this modification further increases the kinase activity of human Aurora B/Ipl1 and its homolog in *C. elegans* (Bishop & Schumacher, 2002; Honda *et al.*, 2003). Another parameter that affects the kinase activity of Aurora B/Ipl1 is the clustering of CPC molecules in a certain cellular context. Recent studies revealed that Aurora B/Ipl1 kinase activity forms a gradient that is centred on overlapping microtubules in the spindle midzone, where CPC molecules become clustered during anaphase (Fuller *et al.*, 2008). Such a phosphorylation gradient intriguingly suggests that spatial separation from the kinase might be a crucial mechanism to regulate the phosphorylation status of Aurora B/Ipl1 substrates. Using a

fluorescence resonance energy transfer (FRET-) based sensor, Liu and colleagues showed that phosphorylation of Aurora B/Ipl1 targets at the kinetochore-microtubule interface also depends on the spatial separation from the kinase during metaphase in human cells (Liu *et al.*, 2009). The phosphorylation of such substrates further depends on their localization within kinetochores and their relative distance to the kinase, which is located at the inner centromere (Welburn *et al.*, 2010). Importantly, changes in Aurora B/Ipl1 phosphorylation of substrates also depend on their relative position in the kinetochore when tension between sister chromatids is applied and the substrates are pulled away from Aurora B/Ipl1 (Welburn *et al.*, 2010). These findings are consistent with a mechanism in which Aurora B/Ipl1 activity in general forms a gradient, which radially expands from a centre with the highest density of CPC molecules. Thus, the relative distance of substrates to this centre of this gradient determines their phosphorylation state.

The centre of such a phosphorylation gradient must be precisely determined in order to ensure appropriate control of kinetochore-microtubule attachments. As a consequence, the activity and localization of CPC molecules on centromeres is critical for functional correction of faulty attachments. In order to provide stringent control of the CPC and its effector Aurora B/Ipl1, several mechanisms might target the individual subunits of this complex. The crystal structure of a ternary complex of human INCENP/Sli15, survivin/Bir1 and borealin/Nbl1 revealed that these proteins interact in a three helix bundle with each other (Jeyaprakash *et al.*, 2007). The integrity of this helix bundle is critical for the localization of the human CPC at centromeres (Jeyaprakash *et al.*, 2007). In *X. laevis*, fission yeast and human cells, CPC binding to centromeric chromatin is further regulated via phosphorylation of histone H3 (Wang *et al.*, 2010; Kelly *et al.* 2010; Yamagishi *et al.*, 2010). Threonine 3 of histone H3 located in the nucleosomes of centromeric regions is phosphorylated by haspin kinases and this modification increases the binding affinity of H3 towards survivin/Bir1 (Wang *et al.*, 2010; Yamagishi *et al.*, 2010). However, this mode of localization represents only one way of how eukaryotic cells ensure CPC binding to centromeres. Recently, a second mechanism contributing to CPC enrichment at centromeres was discovered in fission yeast and human cells (Kawashima *et al.*, 2007; Tsukahara *et al.*, 2010; Yamagishi *et al.*, 2010). This second pathway relies on the interaction of CPC subunits with members of the conserved family of Shugoshin proteins and will be discussed in the following chapters. Since CPC enrichment is highest at the intersection of the activities of both pathways, they seem to act synergistically to precisely localize Aurora B/Ipl1 (Yamagishi *et al.*, 2010). This elaborate control of Aurora B/Ipl1 localization emphasizes how important this conserved function is for faithful chromosome segregation.

1.2 Shugoshin proteins are essential for faithful chromosome segregation

1.2.1 A conserved domain organization is characteristic of Shugoshin proteins

Shugoshin (Japanese for “guardian spirit”) proteins were named to reflect their biological function in chromosome segregation (Kitajima *et al.*, 2004). The founding member of this class (Mei-S332) was identified first in *D. melanogaster* mutants that fail to maintain sister chromatid cohesion during meiosis (Kerrebrock *et al.*, 1992). In agreement with this suggested function, it has been shown that GFP-tagged Mei-S332 localizes to centromeric regions of meiotic chromosomes until the onset of anaphase II in flies (Kerrebrock *et al.*, 1995). The molecular mechanism of Mei-S332 in cohesion protection remained unidentified until counterparts of Mei-S332 were found in other eukaryotes, such as fission and budding yeast (Katis *et al.*, 2004; Kitajima *et al.*, 2004; Marston *et al.*, 2004). Shugoshin proteins have been discovered in all eukaryotes studied so far, but the number of paralogs differs between species (Gutiérrez-Caballero *et al.*, 2012). *S. cerevisiae* and *D. melanogaster* encode one single Shugoshin protein, whereas *S. pombe*, *X. laevis*, *M. musculus* and *H. sapiens* encode two different versions. Shugoshins do not share high sequence conservation, but they nevertheless perform similar functions during chromosome segregation (Gutiérrez-Caballero *et al.*, 2012).

Despite their low sequence similarity, two highly conserved elements are characteristic for all Shugoshin proteins (Kitajima *et al.*, 2004; Tang *et al.*, 1998). One of these elements, a conserved stretch of mostly basic amino acid residues at the C-terminus of Mei-S332, has been found to be essential for its centromeric localization in *Drosophila* (Tang *et al.*, 1998). This basic region also facilitates the centromeric enrichment of Shugoshin proteins in human cells and fission as well as budding yeast (Kawashima *et al.*, 2010). In these organisms, the kinetochore-bound SAC kinase Bub1 phosphorylates histone H2A within centromeric chromatin (Kawashima *et al.*, 2010). This histone modification is recognized and bound by the conserved basic region of Shugoshin proteins. As a consequence, Shugoshin proteins become enriched around centromeric chromatin during early stages of meiosis as well as mitosis (Kawashima *et al.*, 2010). Notably, there are also other pathways that contribute to the correct localization of Shugoshin proteins. The functional interaction of *SpSgo1* with the heterochromatin protein *SpSwi6* is necessary to ensure for full centromeric enrichment of *SpSgo1* and proper chromosome segregation during meiosis (Yamagishi *et al.*, 2008). The heterochromatin protein *HsHP1α* likewise contributes to the maintenance of *HsSgo1* on mitotic chromosomes in human cells (Yamagishi *et al.*, 2008). In budding yeast, centromeric enrichment of Sgo1 molecules also depends on the activity of a second SAC kinase Mps1 (Storchová *et al.*, 2011). Therefore, it remains to be tested whether Mps1 affects directly the localization of Sgo1 or indirectly through its role in directing Bub1 to kinetochores (London *et al.*, 2012). Taken together, there seems to be one conserved major pathway for the localization of Shugoshin proteins that relies on the interaction of the conserved basic region and phosphorylated histone H2A at centromeric chromatin. In addition, there might be other mechanisms, which contribute to and fine-tune the recruitment of Shugoshin proteins in a species-dependent manner.

The second conserved element of Shugoshin proteins is a coiled-coil domain located at the N-terminus. Pioneering studies on Mei-S332 in *Drosophila* already suggested that this domain might be important to make contact with other proteins (Tang *et al.*, 1998). This hypothesis was indeed confirmed by experiments showing that a heterotrimeric complex of the protein phosphatase 2A (PP2A) only binds fragments of HsSgo1 containing the coiled-coil domain (Tang *et al.*, 2006). As Shugoshin proteins also co-purify PP2A complexes from human and yeast cellular extracts, this interaction seems to be an evolutionary conserved feature of Shugoshin's coiled-coil domain (Kitajima *et al.*, 2006; Riedel *et al.*, 2006; Tang *et al.*, 2006). The publication of a crystal structure containing the coiled-coil domain of human HsSgo1 and HsPP2A raised further evidence for the direct interaction of this domain with other proteins (Xu *et al.*, 2009). The coiled-coil domains of two individual HsSgo1 molecules form a homodimer, which in turn provides the surface to make contact with two subunits of the heterotrimeric PP2A complex. Individual PP2A complexes are comprised of one scaffolding (A), one regulatory (B) and one catalytic subunit (C; reviewed in Shi, 2009). Commonly, the regulatory subunit of PP2A targets the complex to other proteins and confers specificity towards certain substrates. The crystal structure of HsSgo1 and PP2A further revealed that the helical coiled-coil domains of HsSgo1 homodimer contact the regulatory and the catalytic subunit with several amino acids directly (Xu *et al.*, 2009). These direct interactions might explain why HsSgo1, SpSgo1 and ScSgo1 were found to co-purify PP2A complexes containing only one specific class of regulatory subunits (B'/B56 in human cells, SpPar1 in fission yeast and ScRts1 in budding yeast; Kitajima *et al.*, 2006; Riedel *et al.*, 2006). Remarkably, the introduction of one single point mutation replacing asparagine 61 with isoleucine (N51I in budding yeast) in the coiled-coil domain of HsSgo1 abolished its interaction with PP2A (Xu *et al.*, 2009). This finding might explain why mutants of Mei-S332 containing an equivalent mutation lose the ability to protect centromeric cohesin in *Drosophila* (Tang *et al.*, 1998). Similar phenotypes upon introduction of these mutations were also observed in mouse oocytes and meiotic budding yeast cells (Xu *et al.*, 2009). In summary, these findings suggest an evolutionary conserved mechanism in which Shugoshin proteins bind to centromeric chromatin via their basic region and in turn recruit PP2A via their coiled-coil domain. Together with PP2A, Shugoshin proteins might affect different substrates at centromeres, which will be discussed in the following paragraphs.

1.2.2 The role of Shugoshin and its binding partner PP2A in meiotic chromosome segregation

The replicated genetic information of diploid cells is segregated twice during meiosis (reductional segregation or meiosis I and equational segregation or meiosis II, respectively) in order to form haploid gametes. During meiosis I, homologous chromosomes are segregated to the opposing poles of the meiotic spindle. Subsequently, sister chromatids become segregated in meiosis II in a manner that resembles mitosis. To maintain the stable sequence of reductional and equational chromosome segregation several adaptations of the chromosome segregation machinery are necessary. One striking difference between meiotic and mitotic chromosome segregation is the composition of cohesin

complexes. The Scc1/Mcd1 kleisin subunit of mitotic cohesin complexes is substituted by the structurally related protein Rec8 in the meiotic counterpart of budding yeast cells (Klein *et al.*, 1999). Orthologs of budding yeast Rec8 were identified by sequence similarity in fission yeast and human cells emphasizing the highly conserved nature of meiosis-specific cohesin complexes (Parisi *et al.*, 1999). Pioneering studies using budding and fission yeast analyzed the regulation and function of this meiosis-specific cohesin complex. These studies are summarized in the following paragraphs revealing how Rec8-containing cohesin complexes contribute to the orderly progression of meiotic chromosome segregation as part of a mechanism, which seems to be conserved throughout eukaryotes.

Rec8 starts to accumulate in cells upon the induction of premeiotic DNA replication and localizes as part of the meiotic cohesin complex along the longitudinal axis of chromosomes until the initiation of anaphase I (Klein *et al.*, 1999). The bulk of Rec8-containing cohesin is removed from chromosome axes during anaphase I, but a small fraction of Rec8 is maintained at centromeres until anaphase II (Klein *et al.*, 1999). Notably, both fractions are equally important for faithful execution of meiosis in budding as well as in fission yeast (Klein *et al.*, 1999, Watanabe & Nurse, 1999). In both organisms, the larger fraction of cohesin along chromosomes axes is removed through proteolytic cleavage of Rec8 by the endopeptidase separase during reductional segregation (Buonomo *et al.*, 2000; Kitajima *et al.*, 2003). Therefore, proteolytic cleavage of cohesin by separase is obviously a highly conserved and common feature of mitotic as well as meiotic cell division, which coordinates the segregation of chromosomes (Uhlmann *et al.*, 2000). In addition, the distinct behaviour of the two separate pools of meiotic cohesin complexes might provide the basis for the step-wise loss of cohesion, first between homologue chromosomes and subsequently between sister chromatids. Such a molecular model predicts the existence of cellular factors that protect the centromeric pool of cohesin from separase-dependent cleavage during reductional segregation (Klein *et al.*, 1999; Watanabe & Nurse, 1999).

In agreement with such a protective function, fission yeast SpSgo1 localizes to centromeres to prevent the premature loss of SpRec8 during anaphase I (Kitajima *et al.*, 2004). To establish Shugoshin proteins as conserved protectors of meiotic cohesion complexes, the authors searched for members of this protein family in other eukaryotes. In agreement with independent studies, Kitajima and colleagues found that the putative Sgo1 protein in budding yeast indeed protects centromeric cohesin complexes during meiosis as well (Katis *et al.*, 2004; Kitajima *et al.*, 2004; Marston *et al.*, 2004). Mechanistic aspects of this protective function were revealed by two studies showing that SpSgo1 interacts with the heterotrimeric protein phosphatase complex 2A (PP2A) and recruits it to centromeres in meiotic cells (Kitajima *et al.*, 2006; Riedel *et al.*, 2006). Such a Shugoshin-dependent recruitment of PP2A occurs also in human cells during mitosis and is mediated by the B'B56 regulatory subunit of the phosphatase complex (SpPar1 in fission yeast; Rts1 in budding yeast; Kitajima *et al.*, 2006). The artificial recruitment of PP2A to meiotic cohesin complexes causes the dephosphorylation of SpRec8 and blocks meiotic chromosome segregation (Riedel *et al.*, 2006). These findings led to the proposal that phosphorylation of Rec8, which is counteracted by PP2A, primes it for proteolytic cleavage by separase/Esp1. Intriguingly, such a phosphorylation-dependent

mechanism regulates the cleavage of the mitotic cohesin member Scc1/Mcd1 by separase (Alexandru *et al.*, 2001).

According to this hypothesis, the phosphorylation of *SpRec8* by the fission yeast casein kinase 1 was shown to be indeed necessary for the efficient cleavage of *SpRec8* by separase during meiosis (Ishiguro *et al.*, 2010). Consistently, the authors of this study found that excessive phosphorylation of *SpRec8* at centromeric regions by casein kinase 1 leads to premature loss of *SpRec8* resembling the phenotype of cells lacking *SpSgo1*. In addition, Katis and colleagues found that in *S. cerevisiae* Rec8 cleavage also depends on its phosphorylation by Hrr25, the budding yeast casein kinase 1 (Katis *et al.*, 2010). The replacement of Rec8 phosphoacceptor sites with alanine significantly reduced and delayed its proteolytic cleavage (Katis *et al.*, 2010). Taken together, these data imply the existence of a conserved pathway in which Shugoshin proteins contribute to the protection of meiosis-specific cohesin complexes by facilitating the centromeric localization of PP2A. The activity of PP2A at centromeric chromatin in turn shields meiotic cohesin complexes from proteolytic cleavage by dephosphorylating Rec8 (Figure 5).

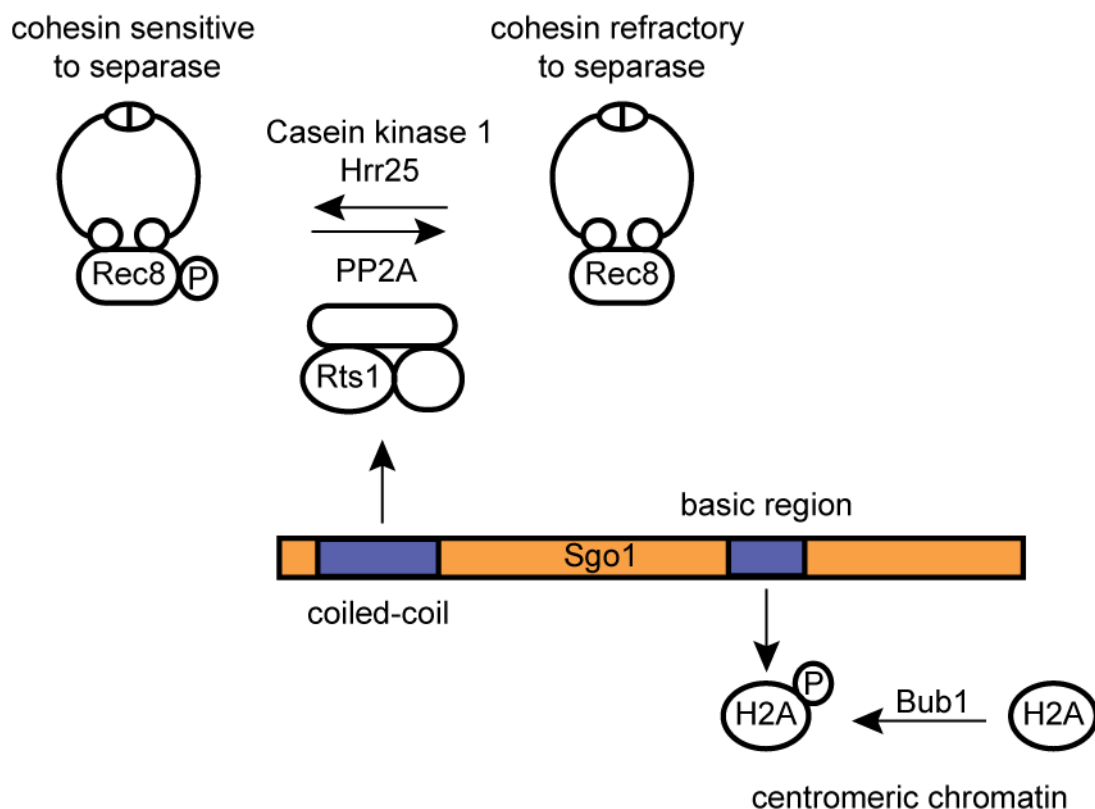


Figure 5. Schematic representation of the domain architecture of budding yeast Sgo1 and the function of these domains in the protection of centromeric cohesin during meiotic cell division

The phosphorylation of histone H2A by Bub1, which is localized to centromeric chromatin, creates the receptor site for the conserved basic region of Sgo1. Once localized to centromeres, the N-terminal coiled-coil of Sgo1 interacts with the regulatory subunit (Rts1) of protein phosphatase 2A (PP2A) complexes facilitating the recruitment of PP2A. PP2A in turn counteracts the phosphorylation of the cohesin member Rec8 by Hrr25; hence rendering centromeric cohesin complexes refractory to proteolytic cleavage by separase during reductional segregation.

1.2.3 Shugoshin proteins contribute to the fidelity of mitotic chromosome segregation

In addition to the protection of centromeric cohesin molecules during meiosis, Shugoshin proteins also play an important role during mitotic cell division. Whereas the meiotic function is highly conserved in eukaryotes, the functions of Shugoshin proteins during mitotic cell division seem to differ in various species (Gutiérrez-Caballero *et al.*, 2012). In analogy to meiosis, Shugoshin proteins are necessary to prevent premature loss of sister chromatid cohesion of mitotic chromosomes in human cells (Salic *et al.*, 2004). Notably, the major fraction of cohesin molecules in these cells is removed during prophase from chromosome arms (Waizenegger *et al.*, 2000). The removal of this cohesin fraction does not depend on proteolytic cleavage of Scc1/Mcd1, but on the kinase activity of the polo like kinase 1 in *Xenopus* egg extracts (Sumara *et al.*, 2002; Waizenegger *et al.*, 2000). This so-called prophase pathway is essential to coordinate the step-wise loss of cohesin molecules from the chromosomes of vertebrates. Only a minor fraction of cohesin bound to centromeric chromatin escapes the prophase pathway, which is finally removed by proteolytic cleavage of Scc1/Mcd1 at the onset of anaphase (Waizenegger *et al.*, 2000). Further research identified *HsSgo1* as the factor, which specifically protects this pool of cohesin from its removal during prophase in human cells (Kitajima *et al.*, 2005; McGuinness *et al.*, 2005).

The molecular mechanism by which *HsSgo1* protects the centromeric pool of cohesin differs between mitotic and meiotic chromosome segregation, although both rely on the recruitment of PP2A (Kitajima *et al.*, 2006; Liu *et al.*, 2013a; Riedel *et al.*, 2006; Tang *et al.*, 2006). Phosphorylation of *HsSgo1* by cyclin-dependent kinase 1 (Cdk1) enables a direct interaction between *HsSgo1*-PP2A and cohesin molecules (Hara *et al.*, 2014; Liu *et al.*, 2013a). PP2A in turn dephosphorylates a factor named sororin, which associates with chromatin-bound cohesin in human cells (Liu *et al.*, 2013a; Schmitz *et al.*, 2007). *HsSgo1*-mediated dephosphorylation of sororin strengthens its stable association with cohesin complexes (Liu *et al.*, 2013a). This interaction restrains the access of the cohesion antagonizing factor Wapl and therefore prevents the premature loss of cohesin complexes from centromeric chromatin (Liu *et al.*, 2013a; Nishiyama *et al.*, 2010). The structural analysis of *HsSgo1* bound to cohesin complexes further revealed that *HsSgo1* directly competes with Wapl to make contact with the cohesin subunits SA2 and Scc1/Mcd1 (Hara *et al.*, 2014). Therefore, a minor fraction of cohesin complexes escapes the Wapl-mediated removal through the dual function of *HsSgo1* during pro- and prometaphase in human cells.

In lower eukaryotes, such as *S. cerevisiae* or *S. pombe*, a step-wise loss of cohesin molecules has not unambiguously been detected and therefore the existence of the prophase pathway still remains a matter of debate in these organisms (Gutiérrez-Caballero *et al.*, 2012; Marston, 2014; Schmidt *et al.*, 2009). Sister chromatid cohesion is not defective in budding yeast cells lacking Sgo1 suggesting that Sgo1 is dispensable for the protection of centromeric cohesin during mitosis (Indjeian *et al.*, 2005). The distribution of cohesin complexes along mitotic chromosomes is also not affected by Sgo1 in *S. cerevisiae*, which is in agreement with this notion (Kiburz *et al.*, 2005). Nevertheless, mitotic chromosome segregation is defective in budding yeast cells lacking Sgo1 suggesting that it performs

other functions than protecting cohesin from its premature removal from chromosomes (Katis *et al.*, 2004; Indjeian *et al.*, 2005). Accordingly, *sgo1* Δ cells fail to halt cell cycle progression in response to incorrect chromosome attachments (Indjeian *et al.*, 2005; Jin *et al.*, 2012). As the absence of Sgo1 does not alter the intrinsic bias of sister chromatids to achieve chromosome biorientation, these findings led to the proposal that Sgo1 senses the absence of tension on a pair of sister kinetochores, which are incorrectly attached to the mitotic spindle (Indjeian *et al.*, 2005; Indjeian & Murray, 2007). Thus, Sgo1's molecular functions that contribute to sense and/or repair incorrect chromosome attachments in budding yeast still have to be identified.

Research performed in other organisms provides first insights into such potential functions in the repair of incorrect chromosome attachments. In vertebrate cells, *HsSgo2* interacts with the mitotic centromere-associated kinesin (MCAK or KIF2C; Tanno *et al.*, 2010). MCAK is a potent microtubule depolymerising enzyme regulating the detachment of kinetochores from the mitotic spindle (Wordeman *et al.*, 2007). This detachment is believed to be a critical prerequisite for the gradual establishment of chromosome biorientation. In human cells, *HsSgo2* is phosphorylated by the Aurora B/Ipl1 kinase and this modification enables the enrichment of MCAK at the kinetochore-microtubule interface (Huang *et al.*, 2007; Tanno *et al.*, 2010). Hence, depletion of *HsSgo2* leads to increased rates of incorrect chromosome attachments through the loss of properly localized MCAK (Huang *et al.*, 2007). These findings suggest that repairing incorrect chromosome attachments during mitosis might be another common function of Shugoshin proteins besides the protection of cohesin molecules.

In addition to localizing MCAK, Shugoshin proteins contribute to the repair of incorrect chromosome attachments by a second pathway in several organisms. In this second branch, Shugoshin proteins act as centromeric receptors for the CPC and its effector kinase Aurora B/Ipl1. Like MCAK, the CPC controls the stability of kinetochore-microtubule attachments and allows the detachment of incorrect chromosome attachments as already mentioned before. Thus, achieving sufficient levels of centromeric Aurora B/Ipl1 through the recruitment by Shugoshin proteins might enable the efficient repair of incorrect attachments. Indeed, *SpSgo2* and *HsSgo1*, respectively interact with CPC proteins and these interactions are required for proper enrichment of Aurora B/Ipl1 at centromeres in fission yeast and human cells (Kawashima *et al.*, 2007; Tsukahara *et al.*, 2010). In both organisms, these interactions are facilitated by Cdk1-dependent phosphorylation of the respective CPC binding partner (Tsukahara *et al.*, 2010). Hence, Shugoshin-dependent recruitment of CPC molecules complements initial CPC enrichment mediated by histone H3 phosphorylation (Wang *et al.*, 2010; Kelly *et al.* 2010; Yamagishi *et al.*, 2010). Obviously, the regulation of Aurora B/Ipl1 is highly critical for the repair of incorrect chromosome attachments, because two redundant pathways exist to ensure proper CPC levels at centromeres. Notably, the deletion of Sgo1 does not abrogate the centromeric localization of Aurora B/Ipl1 in *S. cerevisiae* (Storchová *et al.*, 2011). Thus, it remains to be tested whether such a dual mechanism for CPC recruitment exists in budding yeast as well.

2 Aim of this study

In this study we addressed how Sgo1 facilitates the repair of incorrect chromosome attachments in budding yeast.

1. To gain first insights we analysed whether cell cycle dependent regulation of Sgo1, its correct subcellular localization or the interaction with known binding partners, such as Rts1 (PP2A), are required for this function. To this end, we mapped the domains and elements required for each of these specific functions on Sgo1. We further introduced point mutations in the identified elements to test which of these aspects of Sgo1's regulation are critical for the repair of incorrect chromosome attachments.

2. To determine how Sgo1 affects chromosome segregation, we analyzed the localization of cohesin and condensin complexes in cells lacking Sgo1. In addition, we tested if the structural integrity of centromeric chromatin during mitosis depends on Sgo1. We also tested whether Rts1 (as downstream factor of Sgo1) is required for the localization of condensin complexes and the maintenance of centromeric chromatin conformation.

3. Finally, we investigated whether Sgo1 is important for the localization of the CPC effector kinase Aurora B/Ipl1 to centromeric chromatin. We also tested the requirement for functional Rts1 in this process. In addition, we evaluated putative crosstalk between condensin and CPC molecules on centromeric chromatin, which both contribute to the repair of incorrect chromosome attachments.

Together, these experiments allowed us to draw new conclusions about Sgo1's regulation and its molecular function in the context of mitotic chromosome segregation.

3 Results

3.1 Cell cycle-dependent regulation of Sgo1 protein levels

3.1.1 The C-terminus of Sgo1 mediates its cell cycle-dependent protein expression profile

Sgo1 protein levels are regulated in a cell cycle-dependent manner in budding yeast and peak in mitosis (Indjeian *et al.*, 2005). In order to understand whether this expression profile is important for the function of Sgo1, we wanted to find a mutation within Sgo1 that interferes with its cell cycle-dependent regulation. To generate such a mutant we first determined the position of elements required for protein degradation within Sgo1. To this end, we followed the expression of a C-terminally truncated fragment of Sgo1 lacking the last 250 amino acids (Sgo1 Δ C) and wild type Sgo1 both fused to a C-terminal tandem affinity purification (TAP-) tag during one synchronous cell cycle. Whereas wild type Sgo1 was absent in G1 cells and degraded after mitosis, we observed that the levels of truncated Sgo1 Δ C remained constant throughout the whole cell cycle (Figure 6A). This observation shows that the C-terminus of Sgo1 containing the last 250 amino acids mediates its degradation.

To exclude that mislocalization of the truncated fragment impairs its degradation and thus, causes the stabilization of protein levels, we determined the localization of Sgo1 Δ C fused to a C-terminal enhanced green fluorescent protein (eGFP-) tag by fluorescence microscopy. We detected Sgo1-eGFP as well as Sgo1 Δ C-eGFP in the nuclei of yeast cells (Figure 6B). In contrast to wild type Sgo1-eGFP, which could only be observed in budding cells as one distinct focus, we found Sgo1 Δ C-eGFP dispersed in the nuclei of all cells independently of the cell cycle stage (Figure 6B). The diffused nuclear localization pattern of Sgo1 Δ C-eGFP is probably caused by the lack of the conserved basic region, which is located in the 250 missing amino acids and mediates the enrichment on centromeric chromatin (Kawashima *et al.*, 2010). As we found both wild type Sgo1 as well as Sgo1 Δ C within nuclei of yeast cells, we speculate that the impaired degradation of Sgo1 Δ C does not result from localization to the wrong cellular compartment.

Based on these results we conclude that elements in the last 250 amino acids of Sgo1 are necessary for its cell cycle-dependent regulation. To confirm this function of the last 250 amino acids, we compared the protein levels of wild type Sgo1-TAP and Sgo1 Δ N-TAP (lacking the first 340 amino acids) expressed from the endogenous *SGO1* promoter over one synchronous cell cycle. We found that both proteins cannot be detected in G1 cells, whereas they peak in cells with high levels of mitotic cyclin B (Clb2) before they are degraded upon the exit of mitosis (Figure 6C). In contrast to Sgo1 Δ C-TAP, we observed in total lower expression levels of Sgo1 Δ N-TAP in comparison to wild type Sgo1 (compare Figure 6A and Figure 6C). Thus, we conclude that the C-terminal 250 amino acids of Sgo1 contain all elements, which are required as well as sufficient for its cell cycle-dependent regulation.

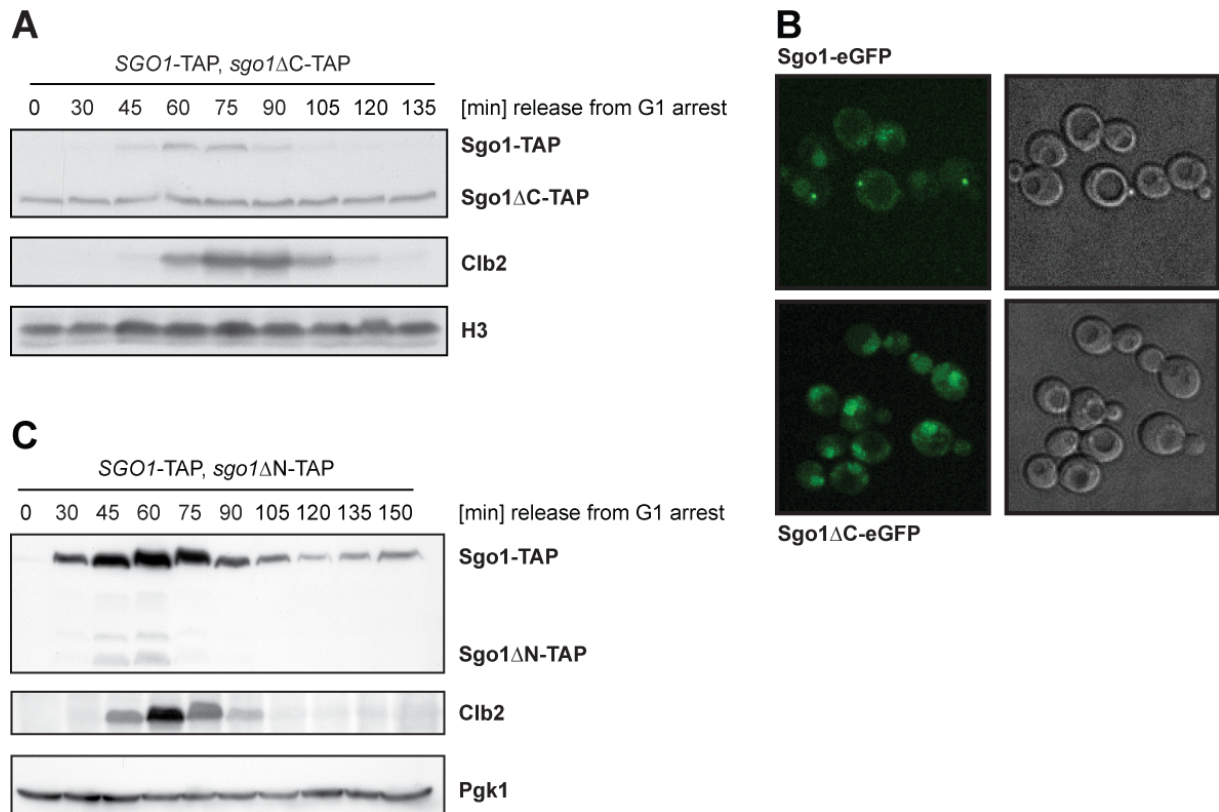


Figure 6. The C-terminal domain of Sgo1 (last 250 amino acids) mediates its cell cycle-dependent degradation and its centromeric enrichment

(A) Cells expressing wild type Sgo1-TAP as well as C-terminally truncated Sgo1ΔC-TAP (amino acids 1 – 340) under control of its endogenous promoter were arrested with α -factor at a final concentration of 20 μ M and released into one synchronous cell-cycle (see experimental procedures). Samples were withdrawn at indicated time points after the washout of α -factor and the corresponding levels of wild type and mutant Sgo1-/Sgo1ΔC-TAP were analysed by immunoblotting (histone H3 used as loading control; mitotic cyclin Clb2 used as control for cell cycle progression). (B) The localization of wild type Sgo1-eGFP and C-terminally truncated Sgo1ΔC-eGFP (amino acids 1 – 340) was determined by fluorescence microscopy in asynchronous cells (left panels). The morphology of yeast cells was monitored by differential interference contrast (DIC) microscopy (right panels). (C) The protein levels wild-type Sgo1-TAP as well as N-terminally truncated Sgo1ΔN-TAP (amino acids 341 – 590) were monitored by immunoblotting throughout one synchronous cell cycle (Pgk1 used as loading control; mitotic cyclin Clb2 used as control for cell cycle progression). The experiment was performed as described in (A).

3.1.2 Mapping of degradation signals in the C-terminal domain of Sgo1 reveals one essential element

The last 250 amino acids of Sgo1, which are essential for its cell cycle-dependent degradation (Figure 6C), contain several putative recognition sites for ubiquitylation by the APC/C marking it for subsequent proteasomal degradation. However, none of these sites perfectly matches the sequences identified in *bona fide* APC/C substrates, such as securin/Pds1 or mitotic cyclin Clb2. Thus, to map and identify elements mediating the cell cycle-dependent degradation of Sgo1, we designed a series of Sgo1 truncations containing Sgo1ΔC (amino acids 1 – 340) and additional residues of the last 250 amino acids (Figure 7A; fragment B encoding amino acids 341 – 370, fragment C encoding amino acids 391 – 490 and fragment D encoding amino acids 491 – 590). We expressed these alleles with a

C-terminal TAP-tag in asynchronous and G1-arrested cells and determined the levels of the corresponding fragment. Strikingly, we found that only fragment Sgo1 Δ C+CD-TAP is not present in detectable levels in G1-arrested cells, resembling wild type Sgo1 (compare Figure 7B and Figure 6A). As neither fragment C nor fragment D by itself was sufficient to mediate Sgo1 degradation in G1, we conclude that amino acids directly located at the transition of fragment C and D are essential for the cell cycle-dependent regulation of Sgo1 protein levels.

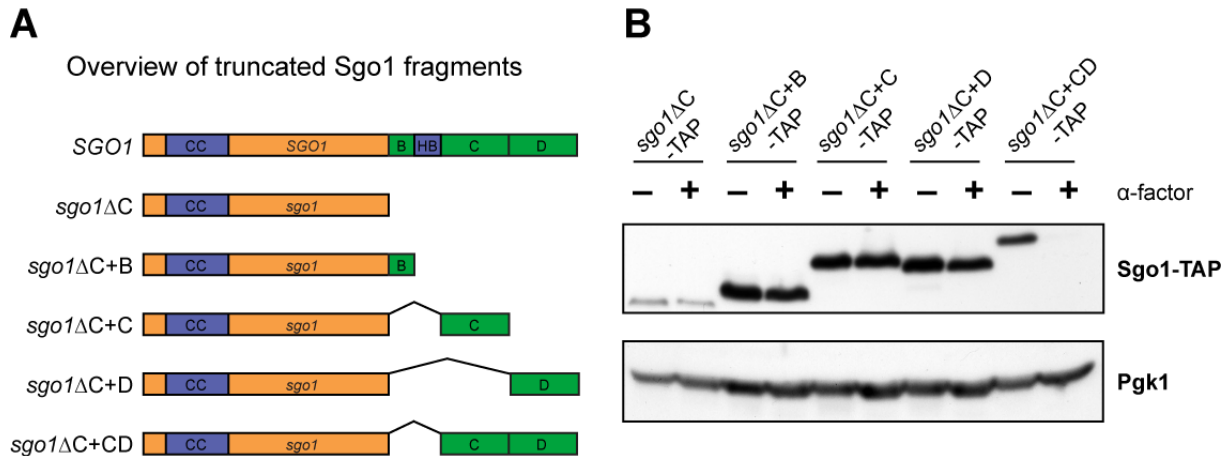


Figure 7. Cell cycle-dependent degradation of Sgo1 relies on one stretch of amino acids located around leucine 490 within the C-terminus

(A) Schematic overview representing the structure of truncated Sgo1 fragments, which were tested for cell cycle-dependent protein stability in G1-arrested cells. (B) TAP-tagged Sgo1 fragments were expressed from the endogenous *SGO1* promoter in exponentially growing (- α -factor) or G1-arrested cells (+ α -factor). The corresponding Sgo1 levels were analysed by immunoblotting (Pgk1 used as loading control).

3.1.3 Mutation of a putative SUMO-binding motif stabilizes Sgo1 protein levels

The prediction of linear motifs based on the eukaryotic linear motif (ELM) resource database revealed that a putative small ubiquitin-like modifier- (SUMO-) interacting motif (SIM) spans the transition of the Sgo1 fragments C and D (amino acids 489 – 493: LLDIT) (Dinkel *et al.*, 2014). To test the relevance of this motif for cell cycle-dependent degradation of Sgo1, we replaced leucine 489 as well as leucine 490 with alanine in an N-terminal truncation of Sgo1 (sgo1 Δ N L489,490A-TAP) in order to impair the interaction with SUMO. We then compared the protein levels of wild type Sgo1 Δ N-TAP and mutant Sgo1 Δ N L489,490A-TAP expressed under control of the constitutive *ADH1* promoter in cells arrested in mitosis and G1. We detected significantly higher levels of the mutant protein in comparison to wild type Sgo1 Δ N-TAP independently of the cell cycle stage (Figure 8A). Moreover, we detected similar amounts of mutant Sgo1 Δ N L489,490A-TAP in asynchronous, mitotic and G1-arrested cells (Figure 8A), indicating that cell cycle-dependent regulation of Sgo1 is bypassed upon mutation of the putative SUMO-binding motif.

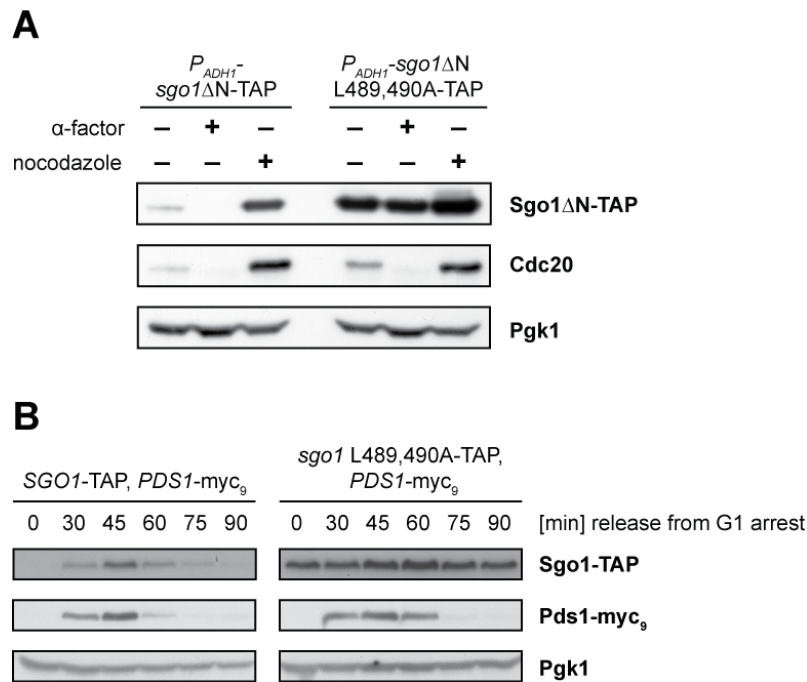


Figure 8. Mutation of a putative SUMO-interacting motif (SIM) blocks the cell cycle-regulated degradation of Sgo1

(A) Truncated versions of Sgo1ΔN-TAP with (*sgo1ΔN* L489,490A) or without (*sgo1ΔN*) mutation of the putative SUMO-interacting motif (SIM) were expressed under control of the constitutive *ADH1* promoter. Corresponding protein levels in exponentially growing, G1-arrested (+ α-factor) and metaphase-arrested cells (+ nocodazole) were analysed by immunoblotting (Pgk1 used as loading control; Cdc20 used as control for metaphase arrest). (B) Cells expressing wild type Sgo1-TAP or the putative SIM mutant (*sgo1* L489,490A-TAP) under control of its endogenous promoter were arrested with α-factor at a final concentration of 20 μM and released into one synchronous cell-cycle (see experimental procedures). Samples were withdrawn at indicated time points and the corresponding levels of wild-type and mutant Sgo1 -TAP were analysed by immunoblotting (Pgk1 used as loading control; Pds1-myc₉ used as control for cell cycle progression).

To further confirm this hypothesis, we followed the expression of full-length Sgo1-TAP containing the L489A and L490A amino acid substitutions under control of the endogenous *SGO1* promoter over one synchronous cell cycle. As expected, the protein levels of mutant Sgo1-TAP (*sgo1* L489,490A-TAP) remained constant throughout the whole cell cycle, whereas wild type Sgo1 is only present in mitosis resembling the expression profile of Pds1 (Figure 8B). This observation confirms that the predicted SUMO-binding motif is necessary for the timely degradation of Sgo1. In contrast to our results obtained with the truncated versions of Sgo1, which were expressed under control of the *ADH1* promoter, we observed similar levels of full-length Sgo1 independently of the mutation of the putative SIM (compare Figure 8A and Figure 8B). Thus, Sgo1 degradation might not be completely blocked by the mutation of the SUMO-binding motif, but rather delayed or impaired.

3.1.4 Cell cycle-dependent regulation of Sgo1 protein levels is not essential for its function in mitotic chromosome segregation

Next, we analyzed whether cell cycle-dependent regulation of Sgo1 protein levels affects its function in mitotic chromosome segregation. To this end we expressed the non-degradable Sgo1 mutant (*sgo1* L489,490A-TAP) in cells lacking endogenous Sgo1 and tested their response upon exposure to microtubule poisons. We found that cells expressing the non-degradable Sgo1 mutant can proliferate like wild type cells on plates containing low doses of the microtubule poison nocodazole. Cells lacking Sgo1 (*sgo1* Δ) in contrast are sensitive to this chronic exposure (Figure 9A). Thus, degradation of Sgo1 at the end of mitosis seems dispensable for accurate mitotic chromosome segregation in budding yeast.

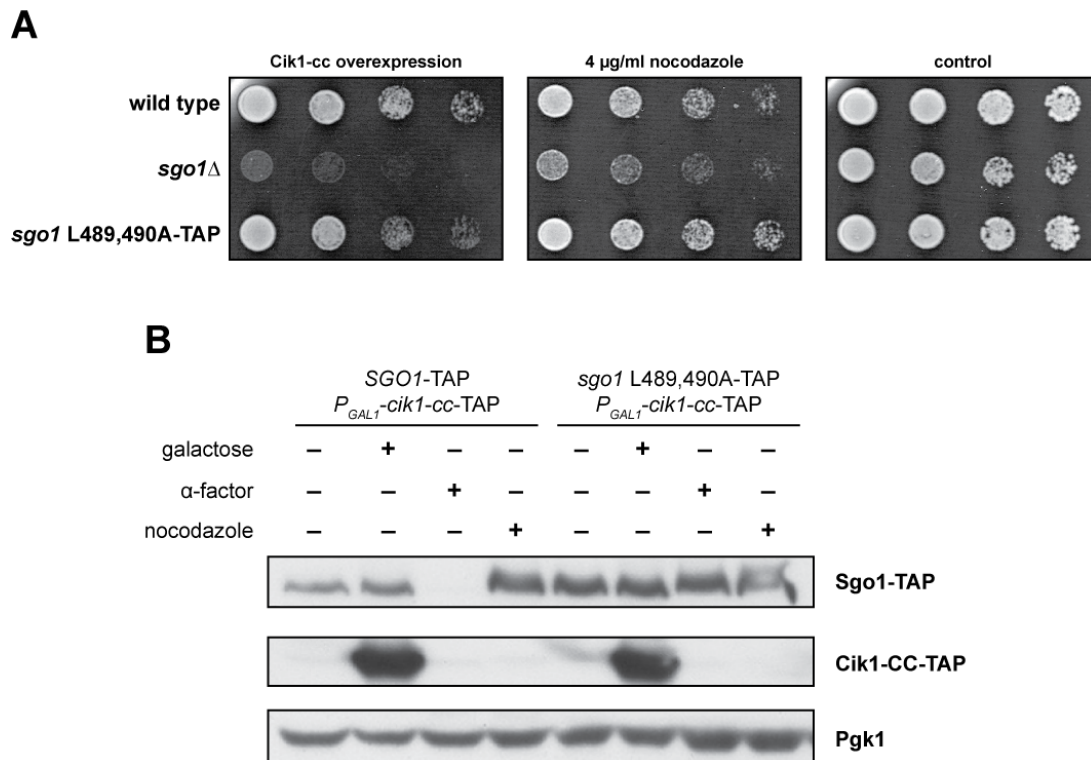


Figure 9. Cell cycle-dependent degradation of Sgo1 is not essential for proper chromosome segregation in mitosis

(A) The sensitivity of wild type cells as well as cells expressing no Sgo1 (*sgo1* Δ) or non-degradable, TAP-tagged Sgo1 (*sgo1* L489,490A-TAP) to microtubule poisons (4 μ g/ml nocodazole) and to Cik1-cc overexpression, which triggers the formation of syntelic attachments at high frequencies, was analyzed. Tenfold serial dilutions of yeast cultures were spotted on plates containing galactose to induce overexpression of Cik1-cc-TAP or plates supplemented with 4 μ g/ml nocodazole and incubated at 25 °C. (B) The overexpression of Cik1-cc-TAP was induced through addition of galactose to a final concentration of 2% in asynchronous yeast cultures expressing wild type (SGO1-TAP) or non-degradable Sgo1 (*sgo1* L489,490A-TAP). The protein levels of TAP-tagged Cik1-cc as well as wild type and non-degradable Sgo1 in G1-arrested (+ α -factor) and mitotic cells (+ nocodazole) were determined by immunoblotting (Pgk1 used as loading control).

As Sgo1 becomes delocalized from centromeric chromatin upon the establishment of tension between sister chromatids, we tested whether impaired degradation of Sgo1 leads to a defect in chromosome biorientation (Nerusheva *et al.*, 2014). To this end, we induced syntelic attachments in wild type cells, cells lacking Sgo1 and cells expressing the non-degradable Sgo1 mutant by constant overexpression of the coiled-coil domain of Cik1 (Cik1-cc; amino acids: 81 – 360) fused to a C-terminal TAP-tag (Figure 9B). Cik1-cc overexpression leads to the formation of syntelic attachments at high frequencies, and both detection and efficient correction are required to ensure cell proliferation under these conditions (Jin *et al.*, 2012). Whereas cells lacking Sgo1 (*sgo1* Δ) failed to proliferate due to massive chromosome missegregation, wild type cells and the *sgo1* L489,490A mutant grew under these conditions (Figure 9A; Jin *et al.*, 2012). These results suggest that degrading Sgo1 upon mitotic exit is not essential for the repair of syntelic attachments and for chromosome biorientation.

3.2 Localization of Sgo1 via its conserved basic region

3.2.1 Mutation of the conserved basic region interferes with Sgo1's localization leading to defective chromosome segregation

Having established that cell cycle-dependent degradation of Sgo1 is not essential for its function in mitotic cell division, we asked whether accurate localization of Sgo1 contributes to it. The enrichment of Sgo1 on centromeres depends on the interaction of its conserved basic region (amino acids 364 – 391) with phosphorylated histone H2A (Kawashima *et al.*, 2010; Kitajima *et al.*, 2004). Notably, a *sgo1* mutant containing one single amino acid exchange within this region (T379I in *sgo1-100*) fails to halt cell cycle progression in response to incorrect chromosome attachments (Indjeian *et al.*, 2005). To analyze whether the loss of function of this *sgo1* mutant is caused by the inability to localize to centromeres, we replaced threonine 379 with aspartic acid (*sgo1* T379D) within the conserved basic region to compensate the positive charges of several basic residues within the vicinity of threonine 379. Next, we compared the localization of this mutant protein fused to a C-terminal GFP-tag with wild type Sgo1-GFP by fluorescence microscopy. In contrast to wild type Sgo1-GFP, which was enriched between the spindle pole bodies (marked by Spc29 fused to a C-terminal red fluorescent protein-(RFP-) tag), we observed a diffused nuclear signal of Sgo1 T379D-GFP in mitotic cells (Figure 10A; data from K. Peplowska). In summary, we showed that mutations within the conserved basic region interfere with the accurate localization of Sgo1 to centromeres, as previously published (Kawashima *et al.*, 2010).

To confirm that centromeric enrichment of Sgo1 is indeed crucial for its function, we tested the sensitivity of the *sgo1* T379D mutant to microtubule poisons. We found that cells expressing mislocalized Sgo1 (*sgo1* T379D-TAP) are not able to proliferate upon chronic exposure to benomyl (Figure 10B). To further confirm this result, we created another *sgo1* mutant in which we deleted most of the conserved basic region (*sgo1* Δ HB lacking amino acids 371 – 390) to abolish centromeric enrichment. As expected, these mutants were as sensitive as *sgo1* T379D or *sgo1* Δ cells to chronic

exposure to benomyl (Figure 10B). These findings emphasize that localizing Sgo1 to centromeric chromatin via its conserved basic region is necessary for its correct function. Together with our analysis of the localization of the *sgo1* T379D mutant, they further provide an explanation why the *sgo1-100* mutant containing the T379I substitution fails to block mitotic exit in the presence of incorrect chromosome attachments (Indjeian *et al.*, 2005). In agreement with this hypothesis, we found that *sgo1* Δ HB mutants cannot proliferate upon overexpression of Cik1-cc, which induces syntelic attachments at high frequencies (data not shown). This finding further emphasizes that centromeric Sgo1 is essential for the detection and/or repair of syntelic attachments.

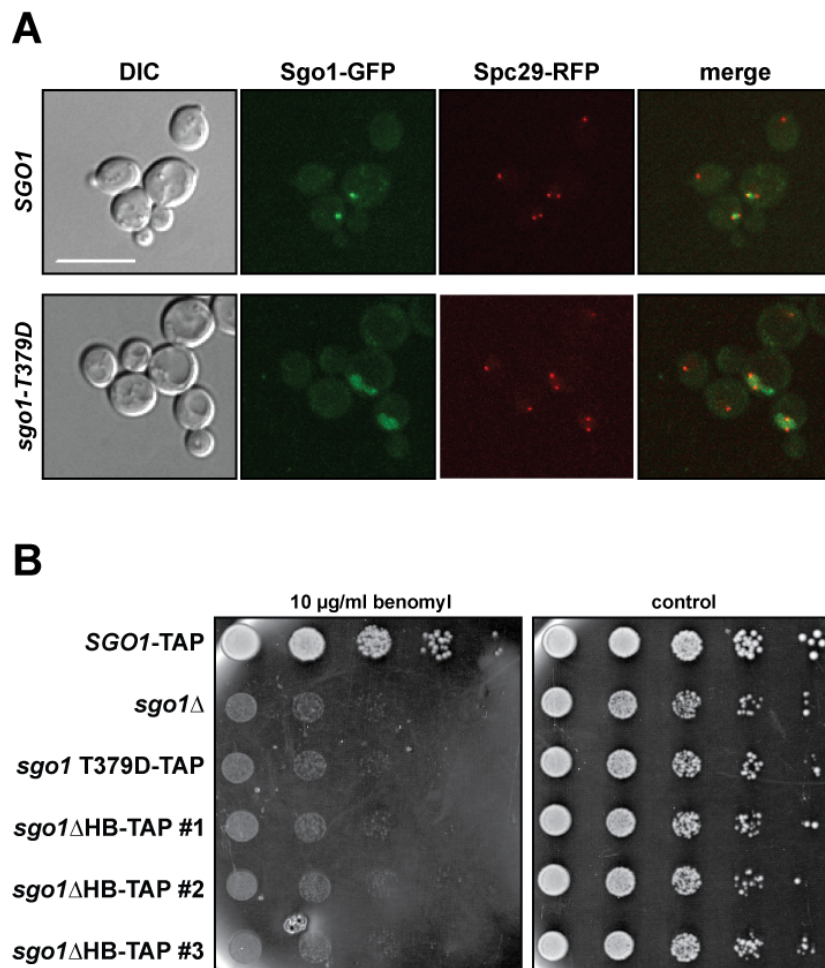


Figure 10. The conserved basic region of Sgo1 facilitates its centromeric enrichment and is essential for its function in mitosis

(A) The localization wild type Sgo1-GFP and mutant Sgo1 T379D-GFP was determined by fluorescence microscopy in exponentially growing cells. The morphology of the corresponding yeast cells was monitored by differential interference contrast (DIC) microscopy (left panels) and the poles of the mitotic spindle were visualized through fluorescence microscopy of RFP-tagged Spc29. The right panels (merge) show an overlay of RFP- and GFP-signals (data from K. Peplowska). (B) The sensitivity of wild type cells (SGO1-TAP) as well as cells expressing no Sgo1 (*sgo1* Δ) or mislocalized Sgo1 (*sgo1* T379D-TAP and *sgo1* Δ HB-TAP) to microtubule poisons (10 μ g/ml benomyl) was analyzed. Tenfold serial dilutions of yeast cultures were spotted on plates containing 10 μ g/ml benomyl or no microtubule poisons (control) and incubated at 25 $^{\circ}$ C.

3.2.2 Mps1 overexpression causes a synthetic growth defect in cells expressing mislocalized Sgo1

A recent study from our laboratory showed that the chromosome segregation defect of *sgo1Δ* cells can be partially rescued by ectopic overexpression of Mps1 from a high copy number plasmid (Storchová *et al.*, 2011). The overexpression of Mps1 is believed to constitutively activate the SAC signalling cascade even in the absence of spindle damage (Hardwick *et al.*, 1996), which might bypass the inability to sense and/or repair incorrect chromosome attachments of *sgo1Δ* cells. To confirm this result, we analysed whether the benomyl sensitivity of *sgo1Δ* cells is also alleviated when Mps1 is overexpressed from the inducible *GAL1* promoter. Consistent with our previous results, we found that the benomyl sensitivity of *sgo1Δ* cells is indeed reduced upon ectopic expression of Mps1 (Figure 11A). As Mps1 kinase activity might directly contribute to the centromeric localization of Sgo1 (Storchová *et al.*, 2011), we further analyzed whether the defect of cells expressing mislocalized Sgo1 (*sgo1* T379D-TAP) is also rescued by increased expression levels of Mps1. Remarkably, Mps1 overexpression did not alleviate, but further increased the sensitivity of cells expressing mislocalized Sgo1 towards microtubule poisons (Figure 11A).

As ectopic Mps1 expression further impaired the proliferation of the *sgo1* T379D mutant in the presence of benomyl, we analysed whether elevated levels of Mps1 by itself are sufficient to cause a synthetic growth defect in cells expressing mislocalized Sgo1. Thus, we overexpressed Mps1 in wild type and *sgo1Δ* cells as well as in three different mutants expressing mislocalized Sgo1 (*sgo1* T379D-TAP, *sgo1Δ*HB-TAP and *sgo1Δ*C-TAP). Mps1 overexpression slightly impaired the proliferation of *sgo1Δ* cells and mutants expressing C-terminally truncated Sgo1 (*sgo1Δ*C-TAP containing amino acids 1 – 340) in comparison to wild type (Figure 11B). Mislocalized Sgo1 mutants containing only a single amino acid substitution within the conserved basic region (*sgo1* T379D-TAP) or a small internal deletion of the conserved basic region (*sgo1Δ*HB-TAP) in contrast showed a more pronounced growth defect under these conditions (Figure 11B). Based on these findings, we conclude that elevated protein levels of Mps1 cause indeed a synthetic growth defect in cells expressing mislocalized Sgo1. As the *sgo1Δ*C mutant lacks this phenotype, we reason that this growth defect is mediated by elements other than the conserved basic region within the last 250 amino acids of Sgo1.

In order to investigate the molecular mechanism that causes this synthetic growth defect, we tested whether constitutive SAC activation accounts for the observed phenotype. To this end, we deleted *MAD2*, which is a core component of the mitotic checkpoint complex (MCC) that tethers Cdc20 and blocks mitotic progression (Hwang *et al.*, 1998; Hardwick *et al.*, 2000), in cells expressing mislocalized Sgo1 (*mad2Δ sgo1* T379D-TAP) and the corresponding wild type background. Thus, a functional SAC response cannot be established in these cells even when Mps1 is overexpressed (Hardwick *et al.*, 1996). We found that Mps1 overexpression is sufficient to cause the synthetic growth defect in cells expressing mislocalized Sgo1 in the absence of Mad2 (*mad2Δ sgo1* T379D-TAP; Figure 11C). Based on this observation, we conclude that elevated levels of Mps1 cause a SAC-independent growth defect in the presence of mislocalized Sgo1.

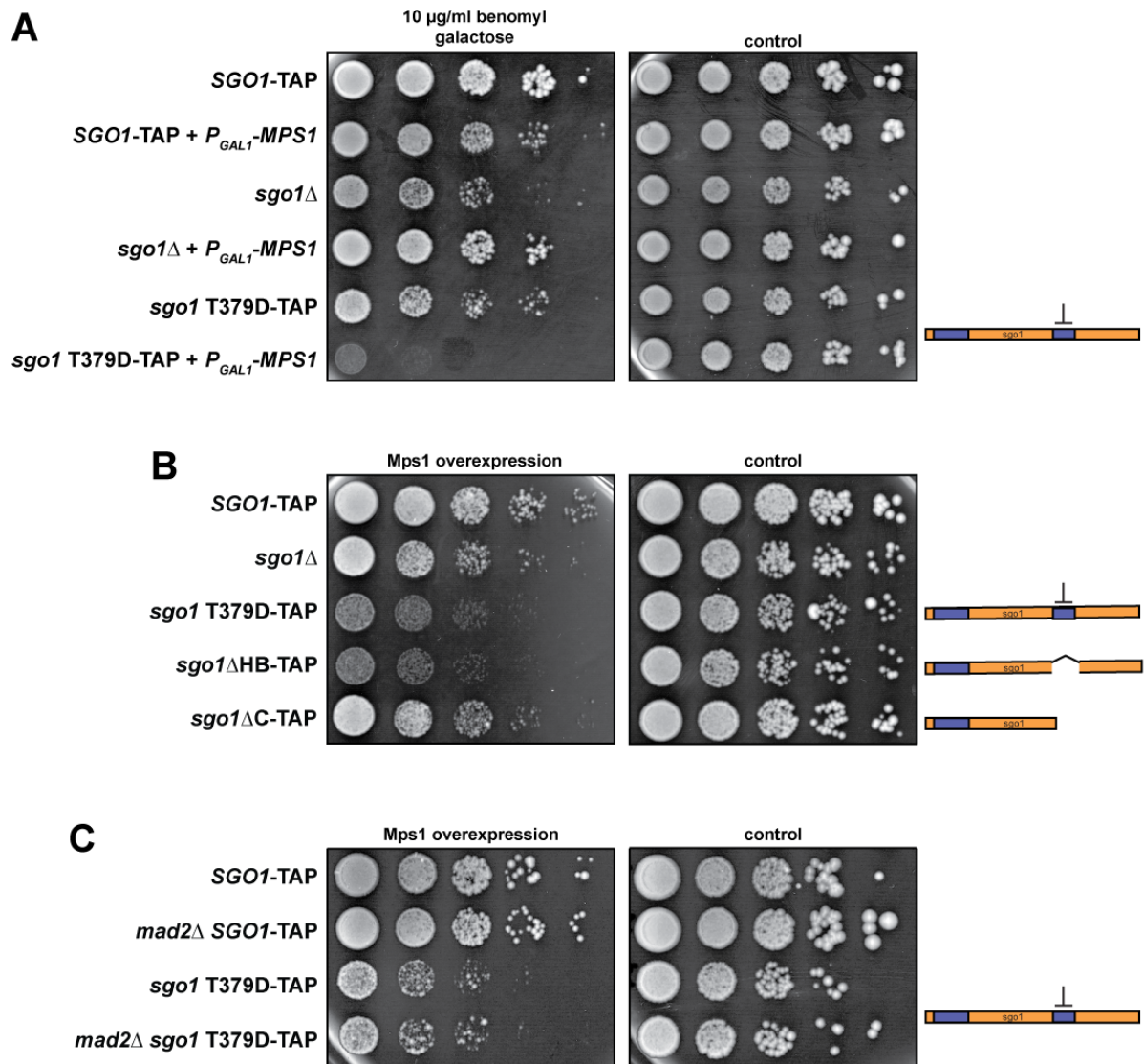


Figure 11. Ectopic expression of Mps1 causes a SAC-independent synthetic growth defect in cells expressing mislocalized Sgo1

(A) The effect of Mps1 overexpression on the sensitivity of cells lacking Sgo1 (*sgo1*Δ) or expressing mislocalized Sgo1 (*sgo1* T379D-TAP) towards microtubule poisons was analyzed. Tenfold serial dilutions of yeast cultures were spotted on plates containing 10 µg/ml benomyl and 2% galactose to induce Mps1 overexpression from the *GAL1* promoter in the indicated strains (+ *P_{GAL1}*-*MPS1*). Control plates without benomyl contained 2% glucose as carbon source to repress transcription of *MPS1*. (B) The sensitivity of cells expressing mislocalized Sgo1 (*sgo1* T379D-TAP, *sgo1*ΔHB-TAP and *sgo1*ΔC-TAP) towards ectopic Mps1 overexpression was analyzed. Tenfold serial dilutions of yeast cultures were spotted on plates containing 2% galactose to induce Mps1 overexpression from the *GAL1* promoter in all tested strains. Control plates contained 2% glucose as carbon source to repress transcription of *MPS1*. (C) The effect of Mps1 overexpression on SAC-deficient mutants (*mad2*Δ) expressing wild type (*SGO1*-TAP) or mislocalized Sgo1 (*sgo1* T379D-TAP) was evaluated. The experiment was performed as described in (B).

3.3 The function of Sgo1's coiled-coil domain in mitosis

3.3.1 The coiled-coil domain of Sgo1 mediates the interaction with Rts1 *in vitro*

The interaction of human PP2A complexes and *HsSgo1* is disrupted upon the introduction of the N61I mutation within its coiled-coil domain (Xu *et al.*, 2009). To verify that the equivalent mutant allele (*sgo1* N51I) of budding yeast Sgo1 shows the same behaviour, we recapitulated the *in vitro* binding assay using the yeast homologue. To this end we purified PP2A containing TAP-tagged Rts1 from mitotic yeast extract. We incubated purified PP2A with C-terminally truncated wild type or mutant Sgo1 Δ C containing the N51I substitution. Subsequently, we immunoprecipitated the Sgo1 Δ C fragments via their His-tag and tested whether the PP2A subunit Rts1-TAP binds to Sgo1 under these conditions. Whereas mutant Sgo1 Δ C N51I failed to co-purify Rts1-TAP, we detected binding of Rts1-TAP to Sgo1 Δ C containing the wild type version of the coiled-coil domain (Figure 12; data from K. Peplowska). This result is consistent with studies suggesting that the interaction of Sgo1 and PP2A complexes depends on the coiled-coil domain of Shugoshin proteins and is highly conserved throughout eukaryotes (Kitajima *et al.*, 2006; Riedel *et al.*, 2006). Moreover, these *in vitro* binding experiments further validate that the *sgo1* N51I allele is suitable to study the involvement of PP2A and Rts1 in the function of Sgo1 during chromosome segregation in mitosis.

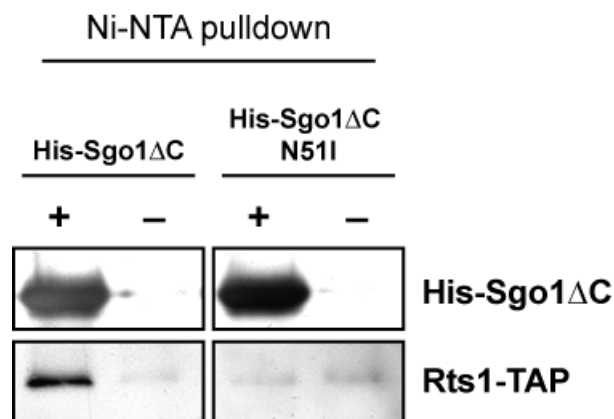


Figure 12. The coiled-coil domain of Sgo1 is critical for the *in vitro* interaction of Sgo1 with PP2A complexes containing the Rts1 subunit

Heterotrimeric PP2A complexes were purified from mitotic lysates of *S. cerevisiae* via Rts1-TAP fusion proteins using calmodulin-coupled agarose and eluted through addition of EDTA. Equal amounts of PP2A were incubated with recombinant His-Sgo1 Δ C fragments (amino acids 1–340, expressed in *E. coli*) bound to Ni-NTA agarose beads. Agarose-bound proteins were eluted by boiling in SDS sample buffer and subjected to SDS-PAGE followed by Western blot analysis to detect bound PP2A subunits (data from K. Peplowska).

3.3.2 Sgo1 is required for the centromeric enrichment of Rts1 in mitotic cells

Sgo1 recruits PP2A in order to protect centromeric sister chromatid cohesion during meiosis (Riedel *et al.*, 2006). Therefore, we asked whether PP2A localization in mitosis also depends on Sgo1. To address this question, we performed chromatin immunoprecipitation (ChIP) experiments followed by quantitative polymerase chain reaction (qPCR) to determine the centromeric enrichment of Rts1, the B' regulatory subunit of PP2A in budding yeast. In mitotic wild type cells, Rts1-FLAG was more than 15-fold enriched on chromatin proximal to the point centromere of chromosome 1 (CEN1) in comparison to an unspecific control locus on the arm of chromosome 10 (*MDV1*; Figure 13A).

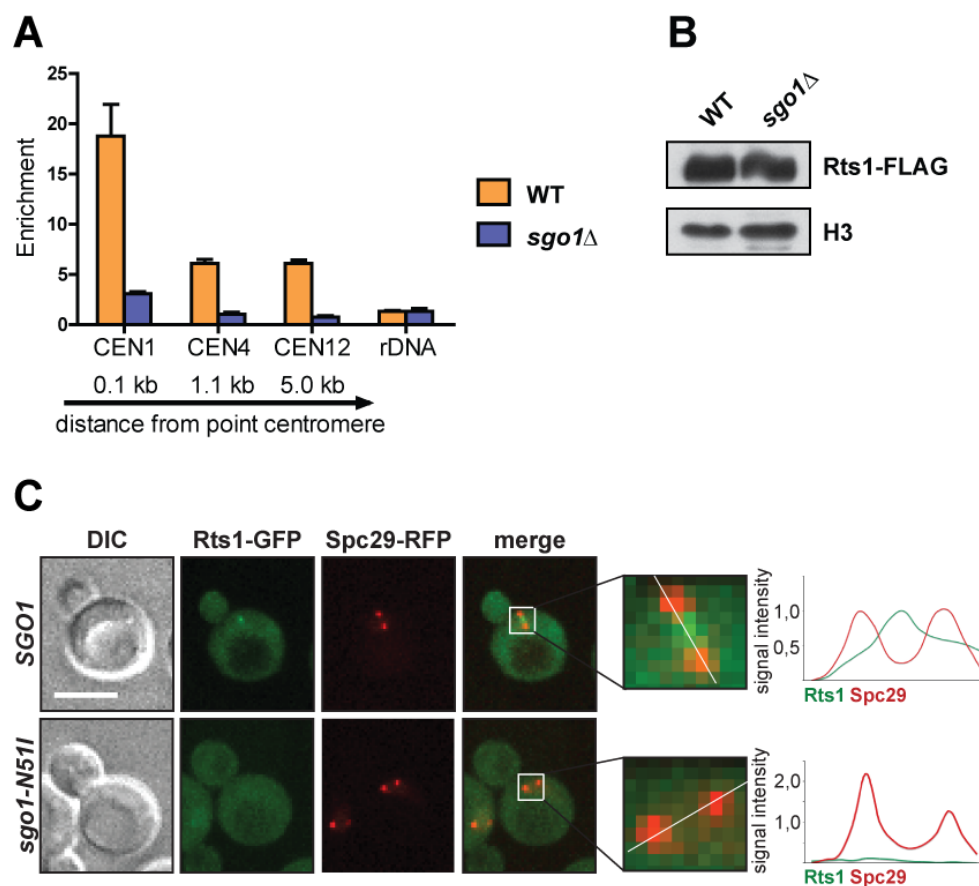


Figure 13. Rts1 enrichment on centromeric chromatin relies on Sgo1 and its N-terminal coiled-coil domain in mitotic cells

(A) Enrichment of FLAG-tagged Rts1 on centromeric/pericentromeric DNA (0.1 kb away from CEN1, 1.1 kb away from CEN4 and 5.0 kb away from CEN12) and on rDNA (NTS1-2) in nocodazole-arrested wild type and *sgo1*Δ cells was determined by ChIP followed by qPCR. Enrichment was calculated from normalization to the levels of Rts1-FLAG bound to an unspecific locus on the arm of chromosome 10 (*MDV1*). Error bars represent the standard error of the mean. (B) The levels of FLAG-tagged Rts1 in exponentially growing wild type and *sgo1*Δ cells were analyzed by Western blot analysis (histone H3 used as loading control). (C) The localization of Rts1-GFP in wild type cells (*SGO1*) or in cells expressing the *sgo1* N51I allele (*sgo1-N51I*) was determined by fluorescence microscopy. The poles of the mitotic spindle were visualized through fluorescence microscopy of RFP-tagged Spc29. Plots on the right show histograms of the signal intensity across the white line in the insets. Bar – 5 μm (data from K. Peplowska).

We further observed a five-fold enrichment of Rts1 on chromatin more distal from the point centromeres (1.1 and 5.0 kb) of chromosome 4 and 12, respectively. Notably, we failed to detect this centromeric enrichment of Rts1 in cells lacking Sgo1 (*sgo1* Δ ; Figure 13A). We conclude that Sgo1 is necessary for the recruitment of the PP2A subunit Rts1 to centromeres during mitosis, as the steady state levels of Rts1 were not affected by the deletion of *SGO1* (Figure 13B). Our finding is consistent with previous ChIP experiments showing that the correct localization of Sgo1 is critical for recruitment of Rts1 to centromeres in meiosis of *S. cerevisiae* (Yu & Koshland, 2008).

To extend our analysis, we determined the localization of Rts1-GFP in wild type cells and the *sgo1* N51I mutant by fluorescent microscopy. In agreement with our ChIP-qPCR experiments, we detected increased amounts of Rts1-GFP between the spindle pole bodies in wild type cells during mitosis (data from K. Peplowska; Figure 13C). This pool of Rts1-GFP was absent in cells expressing the *sgo1* N51I allele. Taken together, our results show that Sgo1 is essential for the centromeric enrichment of the PP2A subunit Rts1 during mitosis. The recruitment of Rts1 is likely mediated by a direct interaction between Sgo1 and PP2A complexes, which depends on the coiled-coil domain of Sgo1.

3.3.3 Rts1 is required for faithful chromosome segregation during mitosis

Having established that centromeric enrichment of Rts1 is a common feature of both meiotic as well as mitotic chromosome segregation, we investigated whether Rts1 also facilitates Sgo1's function in mitosis. First, we tested the sensitivity of cells lacking Rts1 (*rts1* Δ) or expressing the *sgo1* N51I allele (*sgo1* N51I-TAP) towards microtubule poisons. Like *sgo1* Δ cells, both mutants were sensitive to chronic exposure to nocodazole (Figure 14A). As reported earlier, we also consistently observed that the sensitivity of *rts1* Δ mutants was not as pronounced as for *sgo1* Δ (Xu *et al.*, 2009). Similarly, cells expressing the *sgo1* N51I allele exhibited a milder phenotype than *sgo1* Δ mutants.

Next, we addressed what is causing the increased sensitivity towards microtubule poisons in the tested strains. Mutants of *bona fide* SAC genes fail to maintain a mitotic arrest in response to microtubule poisons and are therefore sensitive to such drugs (Hoyt *et al.*, 1991; Li & Murray, 1991). One possible explanation is that a defective SAC is causing the observed phenotypes of cells lacking Rts1 (*rts1* Δ). Therefore, we tested whether these cells fail to maintain a mitotic arrest upon complete depolymerisation of the spindle microtubules by high doses of nocodazole. We released wild type and *rts1* Δ cells from a G1-arrest into a synchronous cell cycle in the presence of nocodazole and followed cell cycle progression by determining the levels of budding yeast securin Pds1. Wild type as well as *rts1* Δ cells maintained high levels of Pds1 in the presence of nocodazole even 3 hours after the release from the G1 arrest (Figure 14B). This finding suggests that cells lacking Rts1 are capable of establishing a stringent mitotic arrest in response to unattached kinetochores. Thus, the observed nocodazole sensitivity cannot be explained by a major SAC defect in cells lacking Rts1. Consistently, *sgo1* Δ and *sgo1* N51I mutants also maintain robust activation of the SAC under these conditions (Indjeian *et al.*, 2005; Peplowska *et al.*, 2014).

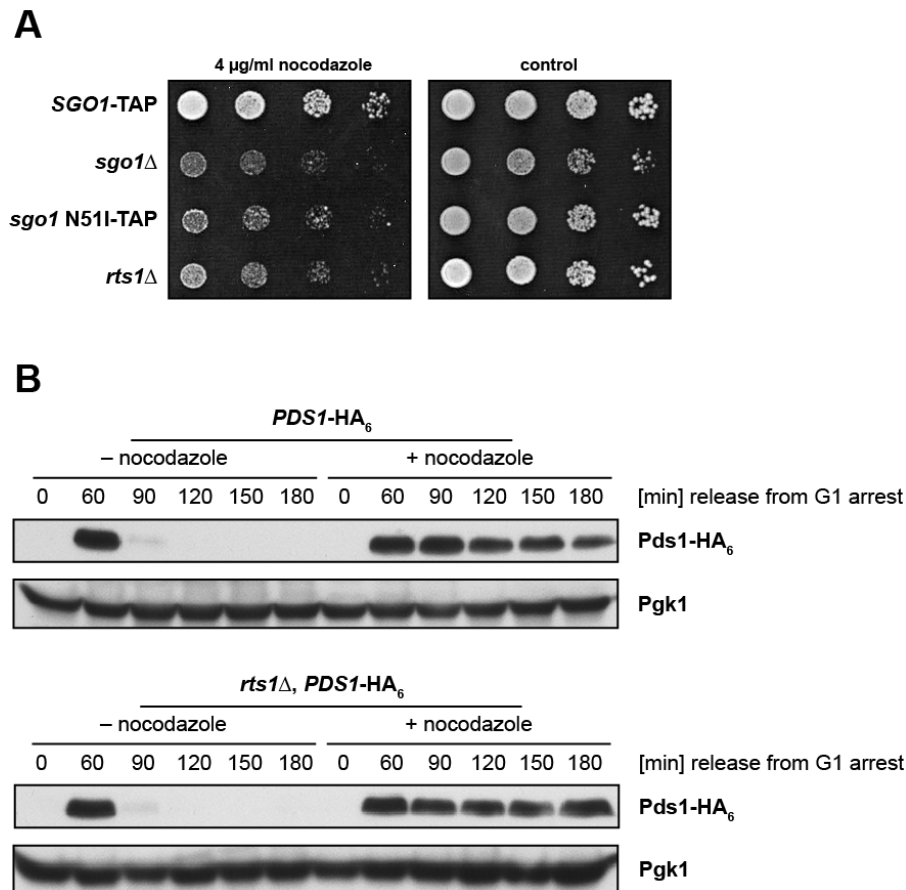


Figure 14. Cells lacking Rts1 are defective in chromosome segregation despite functional checkpoint response triggered by unattached kinetochores

(A) The sensitivity of wild type cells (*SGO1*-TAP) as well as of cells expressing no Sgo1 (*sgo1*Δ), no Rts1 (*rts1*Δ) or the *sgo1* N51I allele (*sgo1* N51I-TAP) to microtubule poisons (4 μg/ml nocodazole) was analyzed. Tenfold serial dilutions of yeast cultures were spotted on plates containing 4 μg/ml nocodazole or no microtubule poisons (control). (B) Wild type and *rts1*Δ cells expressing HA-tagged Pds1 were arrested with α-factor and released into a synchronous cell cycle in the absence as well as in the presence of 25 μg/ml nocodazole (see experimental procedures). Samples were withdrawn at indicated time points and the corresponding levels of HA-tagged Pds1 were analysed by immunoblotting (Pgk1 used as loading control).

3.3.4 Rts1 and its interaction with Sgo1 at centromeres are crucial for the detection and/or the repair of syntelic chromosome attachments

To determine the role of Rts1 in chromosome segregation, we next tested whether it is important for the detection and repair of syntelic attachments. To this end, we induced syntelic chromosome attachments by constitutive overexpression of the coiled-coil domain of Cik1 in cells lacking Rts1 or in the *sgo1* N51I mutant. Consistent with a previous study that introduced this genetic tool, we observed that *sgo1*Δ cells are highly sensitive towards the constitutive overexpression of Cik1-cc (Figure 15A; Jin *et al.*, 2012). Cells lacking Rts1 or expressing the *sgo1* N51I allele also failed to grow efficiently under these conditions indicating that the repair of syntelic attachments or the establishment of chromosome biorientation is impaired (Figure 15A).

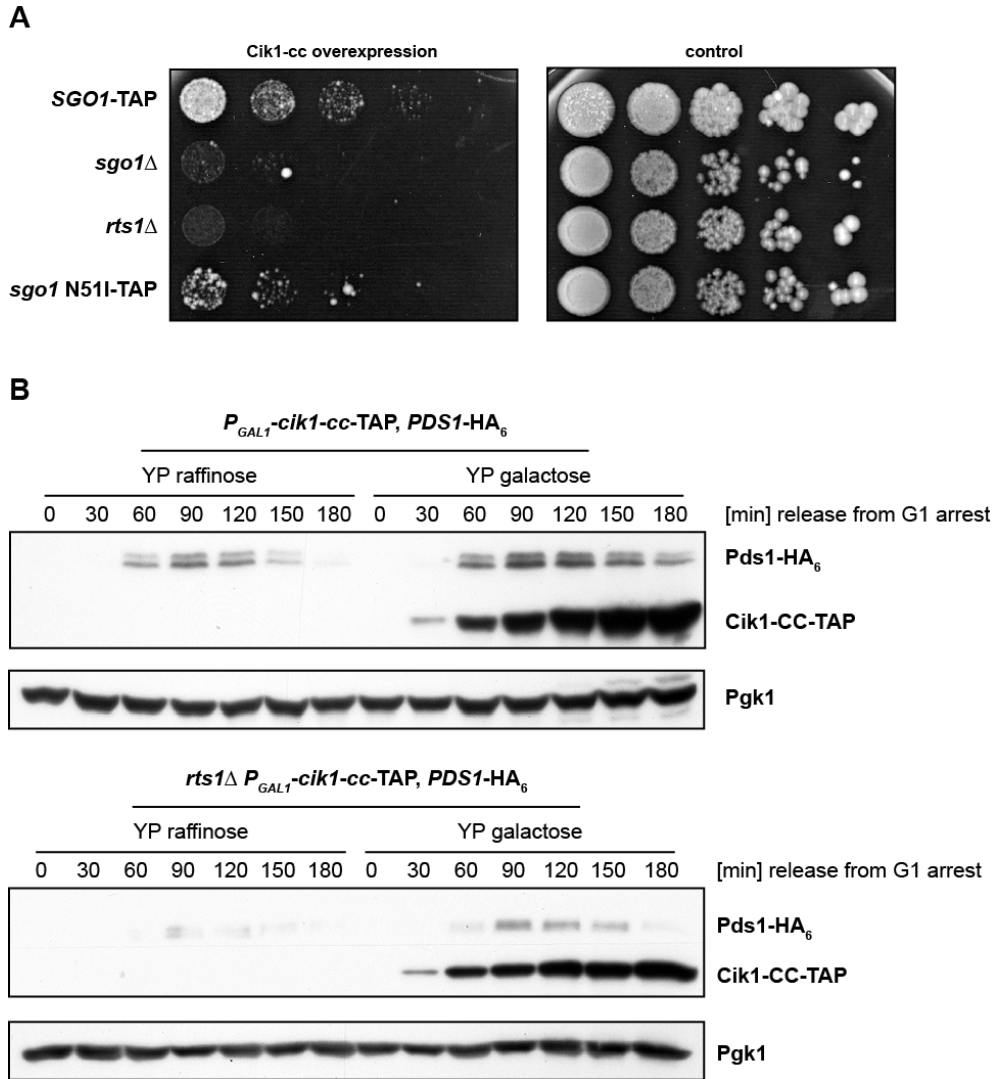


Figure 15. Rts1 and its correct localization facilitated by Sgo1 are essential for cell viability upon the induction of syntelic chromosome attachments

(A) The sensitivity of wild type cells (SGO1-TAP) as well as of cells expressing no Sgo1 (*sgo1*Δ), no Rts1 (*rts1*Δ) or the *sgo1* N51I allele (*sgo1* N51I-TAP) to Cik1-cc overexpression, which triggers the formation of syntelic attachments at high frequencies, was analyzed. Tenfold serial dilutions of yeast cultures were spotted on plates containing either 2% galactose to induce or 2% glucose to repress Cik1-cc expression (control) and incubated at 25 °C. (B) Wild type and *rts1*Δ cells expressing HA-tagged Pds1 were arrested with α-factor and released into a synchronous cell cycle in the absence (YP raffinose) as well as in the presence of 2% galactose (YP galactose) to induce Cik1-cc-TAP expression (see experimental procedures). Samples were withdrawn at indicated time points and the corresponding levels of HA-tagged Pds1 were analysed by immunoblotting (Pgk1 used as loading control).

We further tested whether inducing syntelic attachments by Cik1-cc overexpression affects the timing of mitosis. To this end, we released G1 arrested cells into a synchronous cell cycle with (YP galactose) and without (YP raffinose) induction of Cik1-cc expression and monitored the protein levels of Pds1. Consistent with previous experiments, we observed a stabilization of Pds1 at later time points in cells upon Cik1-cc overexpression indicating that syntelic attachments are detected and repaired through the activity of the CPC (YP galactose; Figure 15B; Jin *et al.*, 2012). *Sgo1*Δ cells lack this response and therefore we analysed the kinetics of Pds1 degradation in *rts1*Δ mutants to determine

whether these cells show the same phenotype (Jin *et al.*, 2012). Pds1 was degraded with a similar timing in *rts1Δ* mutants independently of Cik1-cc overexpression (Figure 15B). Thus, we conclude that cells lacking Rts1, like *sgo1Δ* mutants, fail to detect and/or repair syntelic attachments. These findings further indicate that Rts1 might cooperate with Sgo1 to ensure faithful chromosome segregation during mitosis in budding yeast.

3.3.5 Genetic analysis of *sgo1* mutants lacking the interaction with Rts1

During our analysis to identify *sgo1* mutants, which are not degraded in a cell cycle dependent manner, we noticed that expressing C-terminally truncated Sgo1ΔC in *sgo1Δ* cells weakly alleviates the sensitivity to microtubule poisons (Figure 16A). As we were interested whether Sgo1 cooperates with Rts1 during mitosis, we introduced the N51I mutation into C-terminally truncated Sgo1ΔC (*sgo1ΔC* N51I-TAP) to abolish the interaction of this fragment with Rts1. We then analysed the proliferation of cells expressing this mutant fragment of Sgo1 in the presence of microtubule poisons. As expected, we found that this mutant is as sensitive as *sgo1Δ* cells to chronic exposure to benomyl indicating that the interaction with Rts1 is crucial for the partial rescue phenotype of Sgo1ΔC (Figure 16A). This finding raises further evidence supporting our notion that Rts1 and Sgo1 act together during mitosis.

In addition, we performed genetic experiments using *sgo1* mutants, which express mislocalized, full-length Sgo1, to validate the cooperation with Rts1 during mitotic cell division. These mutants (*sgo1* T379D and *sgo1ΔHB*) showed a SAC-independent growth defect upon ectopic expression of the protein kinase Mps1 (Figure 11B; Figure 16B). As we failed to detect this growth defect in *sgo1Δ* cells, we speculate that Mps1 overexpression becomes detrimental in cells in which mislocalized Sgo1 targets its potential downstream factor Rts1 (and PP2A) to the wrong cellular binding site. Therefore, our hypothesis that Rts1 contributes to the function of Sgo1 predicts that disrupting this interaction should alleviate the observed synthetic growth defect. In order to test this assumption, we created a *sgo1* allele, which fails to interact with Rts1 and is not enriched on centromeric chromatin (*sgo1* N51I, T379D). Consistent with our hypothesis, this mutant lacked the synthetic growth defect like *sgo1Δ* cells, when Mps1 was ectopically overexpressed (Figure 16B).

In summary, our genetic and biochemical analysis of *sgo1* mutants containing the N51I amino acid substitution argues that Sgo1 binds Rts1 and thus, recruits it to centromeric chromatin during mitosis. Our results further suggest a mechanism in which Sgo1 localizes its downstream factor Rts1, which at least partially executes Sgo1's function in mitotic chromosome segregation.

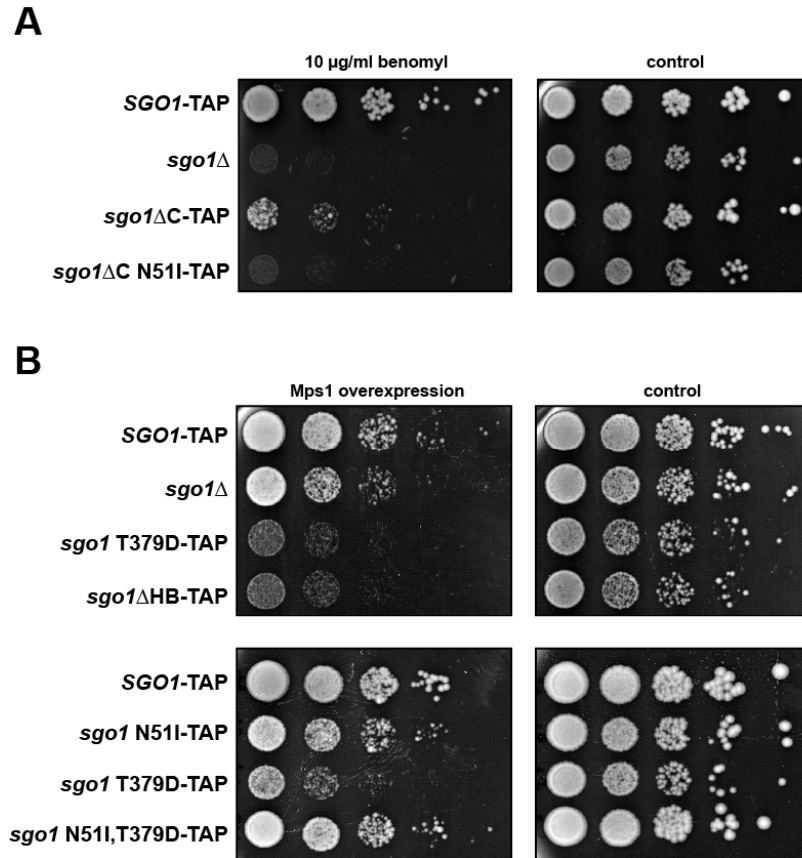


Figure 16. The dominant negative function of mislocalized Sgo1 depends on the integrity of its N-terminal coiled-coil domain

(A) The sensitivity of cells lacking Sgo1 (*sgo1Δ*) or expressing truncated versions of Sgo1 containing the wild type (*sgo1ΔC-TAP*) or a mutant version (*sgo1ΔC N51I-TAP*) of the coiled-coil domain towards microtubule poisons was analyzed. Tenfold serial dilutions of yeast cultures were spotted on plates containing 10 µg/ml benomyl or no microtubule poisons (control). (B) The sensitivity of cells expressing mislocalized Sgo1 (*sgo1 T379D-TAP* and *sgo1ΔHB-TAP*) as well as cells expressing mislocalized Sgo1, which fails to interact with Rts1 (*sgo1 N51I,T379D-TAP*), towards Mps1 overexpression was analyzed. Tenfold serial dilutions of yeast cultures were spotted on plates containing 2% galactose to induce Mps1 overexpression from the *GAL1* promoter in all tested strains. Control plates contained 2% glucose as carbon source to repress transcription of *MPS1*.

3.4 SMC protein complexes as downstream targets of Sgo1 and Rts1

3.4.1 The centromeric enrichment of cohesin is not affected by *SGO1* deletion

In meiosis, Sgo1 recruits PP2A via an interaction with Rts1 to protect centromeric cohesion of sister chromatids (Kitajima *et al.*, 2006; Riedel *et al.*, 2006). Since we found that Sgo1 recruits Rts1 in a similar manner to centromeres during mitosis (Figure 13A, C), we considered the possibility that cohesin complexes might also be the substrate of Sgo1 (and Rts1/PP2A) during mitotic chromosome segregation. Thus, we analysed the enrichment of the cohesin subunit Mcd1/Sccl on centromeric chromatin in mitotic cells using ChIP followed by qPCR. Mcd1/Sccl was up to 20-fold enriched on centromeric DNA in comparison to an unspecific control locus (Figure 17A). The Mcd1/Sccl enrichment declined with increasing distances from the point centromeres of budding yeast

chromosomes. Strikingly, the deletion of *SGO1* did not alter the chromosomal enrichment of Mcd1/Sccl in this assay, indicating that abundance and distribution of cohesin complexes around centromeres is not affected by Sgo1 in budding yeast mitosis. Accordingly, the steady state levels of Mcd1/Sccl are comparable in wild type and *sgo1* Δ cells (Figure 17B). Complementing results were obtained by fluorescence microscopy, which revealed that the localisation of the cohesin subunit Smc3-GFP is also not affected by *SGO1* deletion (Peplowska *et al.*, 2014). Our findings are consistent with a previous publication showing that chromosomal association of Mcd1/Sccl does not depend on Sgo1 during mitotic cell division (Kiburz *et al.*, 2005). Moreover, these findings explain why mitotic cells lacking Sgo1 have no major cohesion defect in contrast to *sgo1* Δ cells undergoing meiotic cell division (Indjeian *et al.*, 2005). Taken together, cohesin complexes and sister chromatid cohesion are not regulated by Sgo1 during mitosis in budding yeast as it is in vertebrate cells (McGuinness *et al.*, 2005).

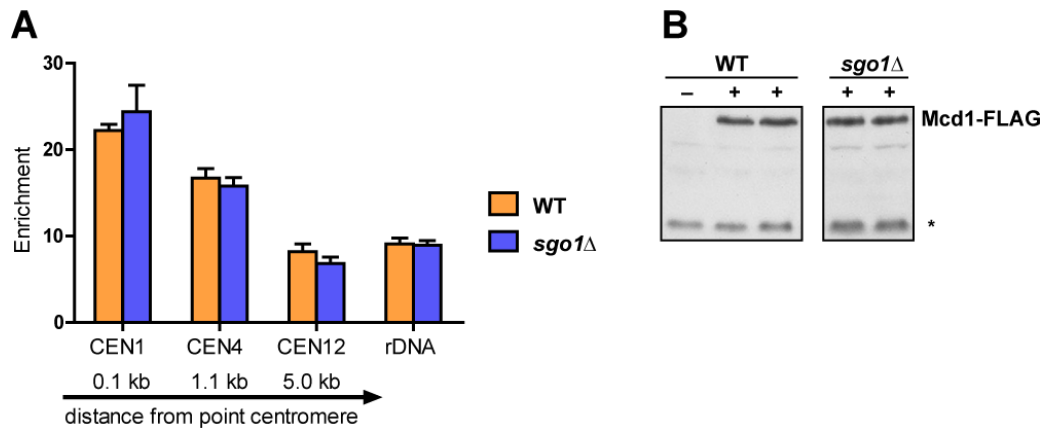


Figure 17. The chromatin enrichment and the protein levels of the cohesin subunit Mcd1/Sccl are not affected by Sgo1

(A) Enrichment of FLAG-tagged Mcd1/Sccl on centromeric/pericentromeric DNA (0.1 kb away from CEN1, 1.1 kb away from CEN4 and 5.0 kb away from CEN12) and on rDNA (NTS1-2) in nocodazole-arrested wild type and *sgo1* Δ cells was determined by ChIP followed by qPCR. Enrichment was calculated from normalization to the levels of Mcd1/Sccl-FLAG bound to an unspecific locus on the arm of chromosome 10 (*MDV1*). Error bars represent the standard error of the mean. (B) The levels of FLAG-tagged Mcd1/Sccl in exponentially growing wild type and *sgo1* Δ cells (two independent clones of each genetic background) were analyzed by Western blot analysis (asterisk indicates an unspecific cross reaction of the anti-FLAG antibody, which was used as loading control).

3.4.2 Sgo1 is essential to maintain a centromeric pool of condensin complexes in mitotic cells

Since we found no evidence that Sgo1 affects centromeric cohesin, we aimed to identify other targets of Sgo1, which might contribute to its function in the repair of syntelic attachments. The condensin complex might be such a putative downstream target, as it co-localizes with Sgo1 at centromeric chromatin and affects the structural integrity of these regions in budding yeast (Bachellier-Basi *et al.*, 2008; Wang *et al.*, 2005; D'Ambrosio *et al.* 2008a; Stephens *et al.*, 2011). The high similarity of

condensin and cohesin, a *bona fide* substrate of Sgo1 and PP2A (see Introduction), further supports this assumption. In order to test whether the localization of condensin complexes is affected by Sgo1, we performed ChIP experiments followed by qPCR. We determined the enrichment of the condensin subunit Smc2 on centromeres and on rDNA in nocodazole-arrested wild type and *sgo1* Δ cells (Figure 18A). Consistent with previous studies on the localization of condensin, Smc2 was indeed up to eightfold enriched on rDNA and centromeric chromatin in wild type cells (Figure 18A; Bachellier-Basi *et al.*, 2008; Wang *et al.*, 2005; D'Ambrosio *et al.* 2008a). Similar as for Rts1 and Mcd1/Scc1, we observed that the level of Smc2 enrichment declined with increasing distance from the point centromere. The deletion of *SGO1* greatly reduced the level of Smc2 enrichment on all tested loci proximal to point centromeres. Strikingly, Smc2 binding to rDNA was not reduced upon *SGO1* deletion in comparison to wild type cells (Figure 18A). We rather observed an increase of Smc2 on rDNA indicating that two separate mechanisms exist, which are differentially targeting condensin to centromeres and to rDNA. These findings are also in line with the localization of Smc2 and another condensin subunit Ycg1 determined by fluorescence microscopy in our laboratory (data from K. Peplowska; Peplowska *et al.*, 2014). A previous study on the localization of condensin in budding yeast further showed that the individual subunits of the pentameric complex always co-localize at rDNA and at pericentromeric regions (Bachellier-Basi *et al.*, 2008). Based on this uniform behaviour of the complex members, we conclude that Sgo1 is crucial to maintain a centromeric pool of condensin complexes until the initiation of anaphase in budding yeast.

Considering the role of Rts1 as potential downstream-factor of Sgo1 in mitotic chromosome segregation (Figure 13), we next asked whether Rts1 might also be important for the centromeric enrichment of condensin. To address this question, we performed the same ChIP assay as for *sgo1* Δ cells analyzing the levels of Smc2 enrichment on centromeric chromatin in *rts1* Δ cells. In comparison to wild type cells, we found less Smc2 bound to centromeric/pericentromeric chromatin in *rts1* Δ cells (Figure 18B). However, this observed reduction of Smc2 enrichment on centromeric chromatin (58% of wild type levels) was not as pronounced as for cells lacking Sgo1. Consistent with our analysis of *sgo1* Δ cells, we observed no reduction, but rather a small increase of Smc2 bound to rDNA upon deletion of *RTS1* (Figure 18B).

In order to exclude the possibility that the observed reduction of centromeric Smc2 in our ChIP assays simply reflects reduced protein levels, we determined the steady state levels of FLAG-tagged Smc2 in cells lacking Sgo1 or Rts1. As we observed no variations of FLAG-tagged Smc2 in wild type and *sgo1* Δ /*rts1* Δ cells, we conclude that the enrichment of Smc2 for each analyzed locus correlates with the amount of condensin bound to the corresponding genomic region (Figure 18C). Based on the observation that Smc2 is less abundant on centromeric chromatin in *sgo1* Δ than in *rts1* Δ cells, we speculate that Sgo1 is essential for centromeric enrichment of condensin and Rts1 likely supports Sgo1 in this function.

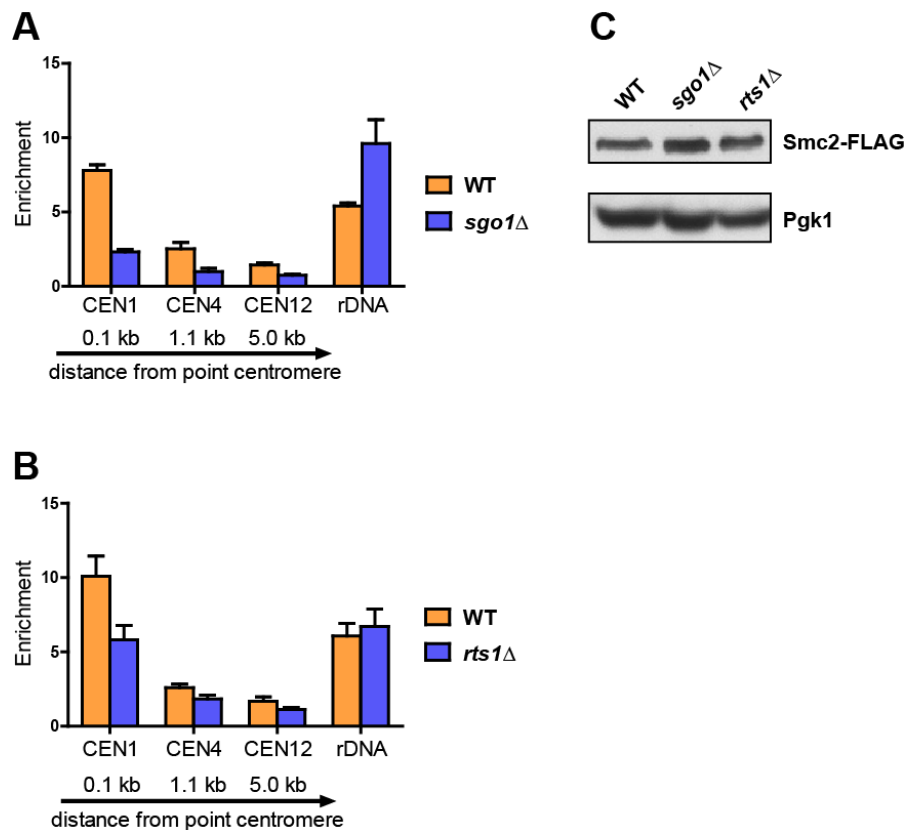


Figure 18. Sgo1 is essential to maintain a pool of the condensin subunit Smc2 at centromeric chromatin

(A) Enrichment of FLAG-tagged Smc2 on centromeric/pericentromeric DNA (0.1 kb away from CEN1, 1.1 kb away from CEN4 and 5.0 kb away from CEN12) and on rDNA (NTS1-2) in nocodazole-arrested wild type and *sgo1*Δ cells was determined by ChIP followed by qPCR. Enrichment was calculated from normalization to the levels of Smc2-FLAG bound to an unspecific locus on the arm of chromosome 10 (*MDV1*). Error bars represent the standard error of the mean. (B) Enrichment of FLAG-tagged Smc2 on centromeric/pericentromeric DNA and on rDNA in wild type and *rts1*Δ cells was determined by ChIP followed by qPCR. Experiments were performed as described in (A). Error bars represent the standard error of the mean. (C) The levels of FLAG-tagged Smc2 in exponentially growing wild type, *sgo1*Δ and *rts1*Δ cells were analyzed by Western blot analysis (Pgk1 used as loading control).

3.4.3 The centromeric pool of condensin functions in the detection and/or repair of incorrect chromosome attachments

Sgo1 maintains adequate levels of condensin at centromeric regions of chromosomes, which have not yet achieved chromosome biorientation (Figure 18A; Verzijlbergen *et al.*, 2014; Nerusheva *et al.*, 2014). This observation suggests a functional role for condensin in the establishment of correct microtubule-kinetochore attachments before sister chromatids are segregated during anaphase. To test this hypothesis, we induced the formation of syntelic attachments by Cik1-cc overexpression in mutants containing temperature-sensitive (ts) alleles of two essential condensin subunits (*smc2-8* and *ycg1-10*). Even at non-restrictive temperatures these cells failed to proliferate under constitutive Cik1-cc overexpression (Figure 19A), arguing for a contribution of condensin activity to the detection and/or repair of syntelic chromosome attachments. However, condensin acts also on rDNA repeats and thereby influences the timing of chromosome segregation during anaphase (D'Ambrosio *et al.*, 2008b;

St-Pierre *et al.*, 2009). Interfering with this anaphase-specific function might also cause the observed lethality in response to Cik1-cc overexpression. To test this possibility, we induced syntelic attachments in a yeast strain, which has been reported to be mostly deficient for condensin function in anaphase chromosome condensation (strain D1225; St-Pierre *et al.*, 2009). This strain expresses phosphorylation-resistant variants of the regulatory subunits Brn1, Ycg1 as well as Ycs4 and has a major defect in the formation of properly condensed rDNA loci in anaphase-arrested cells (St-Pierre *et al.*, 2009). Strikingly, these mutations did not affect the growth of cells under constitutive induction of syntelic chromosome attachments (Figure 19A). This finding argues for a hitherto unknown function of condensin during the establishment of chromosome biorientation before cells enter anaphase.

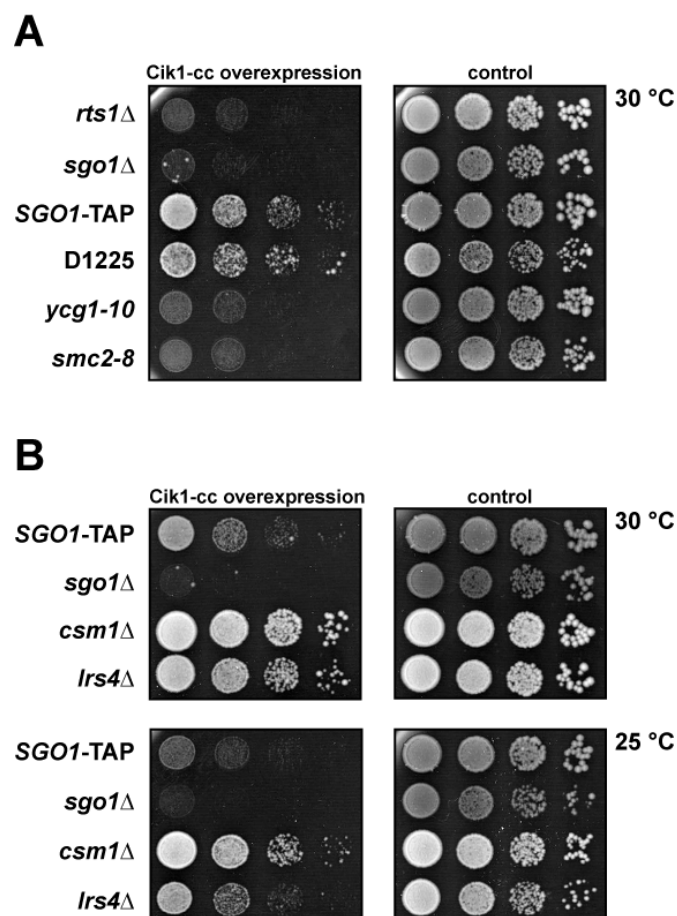


Figure 19. Functional condensin is essential for cell viability upon induction of syntelic attachments

(A) The sensitivity of wild type cells (*SGO1-TAP*) and condensin mutants (D1225, *ycg1-10*, *smc2-8*) to Cik1-cc overexpression, which triggers the formation of syntelic attachments at high frequencies, was analyzed. The yeast strain D1225 expresses phosphorylation-deficient mutants of the condensin subunits Ycg1, Ycs4 and Brn1, which impair the function of condensin specifically during anaphase. The condensin mutants *smc2-8* and *ycg1-10* contain temperature sensitive alleles of the corresponding gene affecting all functions of condensin. Tenfold serial dilutions of yeast cultures were spotted on plates containing either 2% galactose to induce or 2% glucose to repress Cik1-cc expression (control) and incubated at 25 °C. (B) The sensitivity of wild type cells (*SGO1-TAP*) and monopolin mutants (*csm1*Δ, *lrs4*Δ) to Cik1-cc overexpression was analyzed. Experiment was performed as described in (A) and the plates were incubated at the indicated temperatures.

A second line of evidence further supports this hypothesis. Yeast cells lacking the monopolin complex members Csm1 or Lrs4 fail to efficiently localize condensin to specific loci within the rDNA (Johzuka & Horiuchi, 2009). This defective condensin loading on rDNA likely interferes with the correct condensation of rDNA during anaphase. If the impairment of this function causes the observed lethality of the temperature-sensitive condensin mutants (*smc2-8* and *ycg1-10*) upon induction of syntelic attachments, *csm1Δ* and *lrs4Δ* cells should also be sensitive to Cik1-cc overexpression. However, these mutants were not affected by the induction of syntelic attachments when the cells were grown at 30 °C (Figure 19B).

Notably, we found that the proliferation of *lrs4Δ* cells was slightly impaired upon Cik1-cc overexpression at lower temperatures (25 °C; Figure 19B). A recent study determining the localisation of condensin by fluorescence microscopy revealed that Smc4 levels at centromeres are reduced to 80% of wild type levels in *lrs4Δ* mutants (Snider *et al.*, 2014). We conclude that this minor loss of condensin from centromeres causes the observed weak sensitivity to Cik1-cc overexpression, because *csm1Δ* and *lrs4Δ* mutants are otherwise equally compromised in the loading of condensin to rDNA (Johzuka & Horiuchi, 2009). In summary, our genetic analysis suggests that condensin functions in the detection and/or repair of incorrect chromosome attachments independently of its role in anaphase.

3.4.4 Sgo1 and Rts1 contribute to the compaction of centromeric chromatin during mitosis

As condensin mutants failed to proliferate upon Cik1-cc overexpression similarly like cells lacking Sgo1 (Figure 19A), we asked whether *sgo1Δ* mutants show phenotypes resembling cells lacking functional condensin. Recently, it has been published that condensin mutants fail to maintain the proper structure of centromeric chromatin (Stephens *et al.*, 2011). As Sgo1 contributes to condensin localization on centromeres (Figure 18; Verzijlbergen *et al.*, 2014; Nerusheva *et al.*, 2014), we assumed that *sgo1* and *rts1* mutants should show a defect in the maintenance of correct centromeric structures as well. Thus, we analyzed the compaction of a tetracycline operator (TetO) sequence integrated 1 kb away from the point centromere of chromosome 4 through visualization using a tetracycline repressor- (TetR-) GFP fusion protein. Up to 90% of analysed wild type cells showed a single GFP focus, which sometimes split due to so called kinetochore-breathing during the establishment of chromosome biorientation (data from K. Peplowska; Figure 20; He *et al.*, 2000; Stephens *et al.*, 2011). We found that only a minor population of wild type cells showed an increased stretching of centromeric chromatin (data from K. Peplowska; Figure 20; Stephens *et al.*, 2011). The fraction of cells with stretched centromeric chromatin was increased up to 40% for *sgo1Δ* mutants. We further observed similar rates of stretched centromeric chromatin in cells expressing *sgo1* N51I or lacking Rts1. The observed frequencies of stretched chromatin are comparable to published experiments using the temperature sensitive *brn1-9* mutant and therefore resembling a condensin deficient phenotype (Stephens *et al.*, 2011). Taken together, we conclude that Sgo1 maintains a pool of condensin that shapes the structure of centromeric chromatin. We further hypothesize that this

structural integrity is important for the detection of tension between sister chromatids upon establishment of chromosome biorientation. Such an interpretation would also explain why condensin mutants fail to repair syntelic attachments.

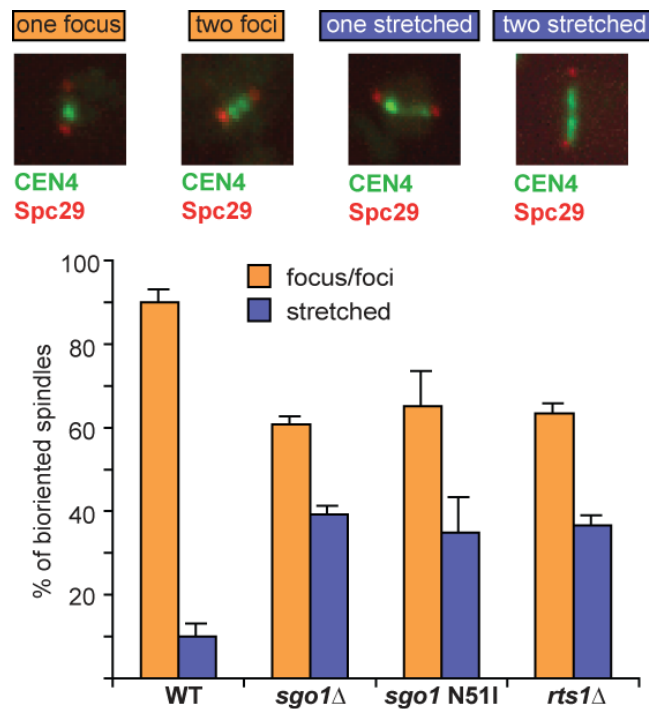


Figure 20. Loss of centromeric condensin increases stretching of centromeric chromatin in mitotic cells

Stretching of centromeric DNA in wild type cells compared with cells that lack Sgo1 (*sgo1*Δ) or fail to localize Rts1 to the centromeric region (*rts1*Δ and *sgo1-N51I*) was analyzed by fluorescence microscopy of CEN4. CEN4 was visualized through binding of a TetR-GFP fusion protein to TetO-repeats integrated 1 kb away from the point centromere of chromosome 4. Only pre-anaphase spindles (SPB distance <2 μm, spindle located in the mother cell) were scored. Top – examples of scored categories (data from K. Peplowska).

3.5 The chromosomal passenger complex (CPC) as downstream target of Sgo1

3.5.1 Ipl1/Aurora B phosphorylation has to be precisely balanced for functional repair of syntelic attachments

The phosphorylation of kinetochore components by Ipl1/Aurora B is essential for the turnover of incorrect chromosome attachments (reviewed in Carmena *et al.*, 2012). Accordingly, we tested whether a temperature sensitive mutant of Ipl1/Aurora B (*ipl1-321*) is sensitive to the induction of syntelic attachments by Cik1-cc overexpression. In agreement with a previous study, we found that *ipl1-321* cells failed to proliferate upon Cik1-cc overexpression even at permissive temperatures (Figure 21A; Jin *et al.*, 2012). The proliferation defect of *ipl1-321* cells, which we even observed at non-restrictive temperatures, might be due to generally reduced kinase activity of the mutant protein

(Jin *et al.*, 2012; Kotwaliwale *et al.*, 2007; Makrantonis & Stark, 2009). Thus, we analysed the phosphorylation of histone H3 on serine 10 by Ipl1/Aurora B in wild type and *ipl1-321* cells using an antibody against this phospho-epitope (Hendzel *et al.*, 1997; Hsu *et al.*, 2000). Even at room temperature (RT) *ipl1-321* cells displayed lower levels of H3 phosphorylation in comparison to wild type cells (Figure 21B). This effect was even more pronounced at the restrictive temperature (37 °C) and H3 phosphorylation was virtually abolished under these conditions in *ipl1-321* cells. Thus, we conclude that a certain threshold of Ipl1/Aurora B kinase activity is essential to allow the repair of syntelic attachments.

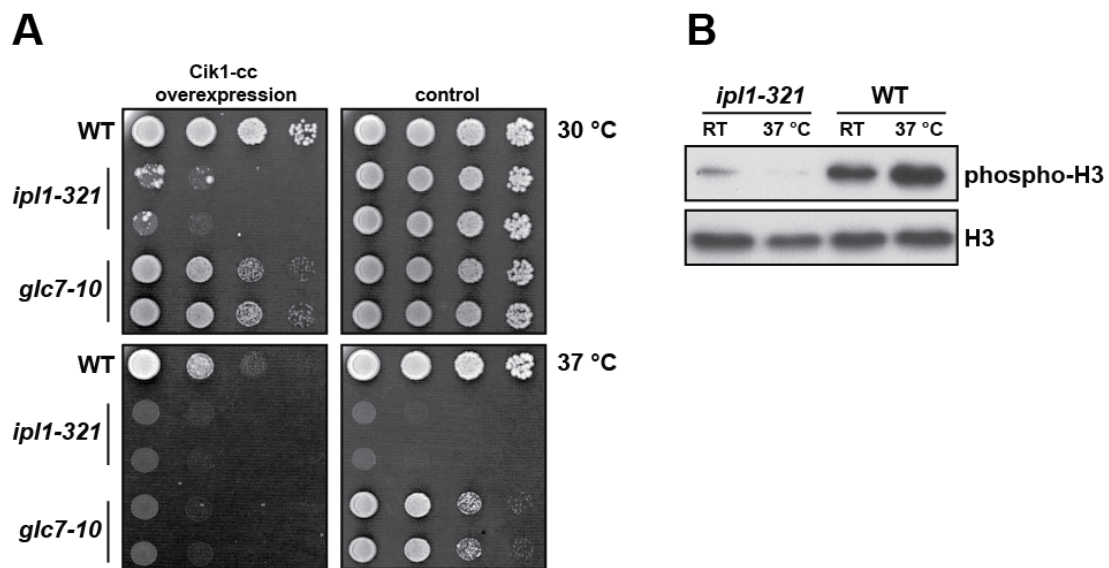


Figure 21. Reduced as well as increased levels of Ipl1/Aurora B phosphorylation interfere with the repair of syntelic attachments

(A) The sensitivity of wild type cells (WT) as well as of cells expressing temperature sensitive alleles of either the kinase Ipl1/Aurora B (*ipl1-321*) or the phosphatase PP1 (*glc7-10*) to Cik1-cc overexpression, which triggers the formation of syntelic attachments at high frequencies, was analyzed. Tenfold serial dilutions of yeast cultures were spotted on plates containing either 2% galactose to induce or 2% glucose to repress Cik1-cc expression (control) and incubated at the indicated temperatures (B) The phosphorylation of histone H3 on serine 10 in wild type (WT) and *ipl1-321* cells grown at room temperature (RT) or shifted to the restrictive temperature (37 °C) for 2.5 h was analyzed by immunoblotting using a phospho-epitope specific antibody (histone H3 was used as loading control).

Next, we asked whether Ipl1/Aurora B phosphorylation of kinetochore substrates has to be limited once all chromosomes become bioriented. Thus, we induced syntelic attachments by Cik1-cc overexpression in the temperature sensitive protein phosphatase 1 (PP1) mutant *glc7-10*. PP1 phosphatase counteracts Ipl1/Aurora B-dependent phosphorylation and impairment of its function leads to increased phosphorylation levels of various substrates (Andrews & Stark, 1999; Hsu *et al.*, 2000; Sassoone *et al.*, 1999). We found that *glc7-10* mutants can proliferate at the permissive temperature of 30 °C upon Cik1-cc overexpression (Figure 21A). However, the proliferation of *glc7-10* cells in the presence of syntelic attachments was completely abolished at 37 °C, although these mutants only displayed a minor growth defect compared to wild type cells in the absence of Cik1-cc

overexpression. Thus, both decreased and increased Ipl1/Aurora B-dependent phosphorylation results in the deficiency to repair syntelic attachments. In summary, these results highlight that phosphorylation of Ipl1/Aurora B substrates has to be precisely balanced in order to facilitate the repair of syntelic chromosome attachments and to establish chromosome biorientation.

3.5.2 Sgo1 maintains adequate levels of centromeric Ipl1/Aurora B in mitotic cells

In order to maintain balanced levels of Ipl1/Aurora B phosphorylation on kinetochore substrates, it is crucial to localize the CPC properly. Since *sgo1Δ* and *ipl1-321* mutants are comparably sensitive to Cik1-cc overexpression, we speculated that Sgo1 might contribute to the localization of Ipl1/Aurora B on centromeres, thereby influencing the phosphorylation of its substrates. In order to test this hypothesis, we determined the centromeric enrichment of Ipl1/Aurora B in wild type and *sgo1Δ* cells by ChIP-qPCR experiments. Consistently, we observed a reduction of Ipl1-FLAG levels on centromeric chromatin on three different chromosomes upon *SGO1* deletion in mitotic cells (Figure 22A). Notably, the absence of Sgo1 did not cause complete loss of Ipl1/Aurora B from these loci indicating that a second pathway ensures a basal level of Ipl1/Aurora B on centromeres in mitosis. In addition, we obtained similar results when analyzing the localization of Ipl1-GFP by fluorescence microscopy, which confirmed that Ipl1/Aurora B was less abundant on centromeres in *sgo1Δ* mutants, but not completely lost (data from K. Peplowska; Peplowska *et al.*, 2014).

We further analysed whether Rts1 is also important for the enrichment of Ipl1/Aurora B, similarly as it contributes to the localization of condensin to centromeres (Figure 18B). Thus, we repeated our ChIP analysis with *rts1Δ* mutants. In contrast to cells lacking Sgo1, we observed no reduction of Ipl1/Aurora B bound to centromeric chromatin in *rts1Δ* cells (Figure 22B). As Ipl1/Aurora B was equally enriched in wild type and *rts1Δ* cells, we conclude that Rts1 does not significantly contribute to CPC localization in budding yeast mitosis. Nevertheless, we found that the localization of Ipl1-GFP is more diffused in cells lacking Rts1 or expressing *sgo1* N51I compared to wild type cells (data from K. Peplowska; Peplowska *et al.*, 2014). This phenotype was similar, albeit less pronounced, than for cells lacking Sgo1.

To exclude that the decline of centromeric Ipl1/Aurora B enrichment observed in our ChIP experiments is caused by a reduction of total protein levels, we determined the steady state levels of FLAG-tagged Ipl1/Aurora B in wild type and *sgo1Δ/rts1Δ* cells. As we observed no major differences in the amounts of cellular Ipl1/Aurora B in wild type and mutant cells (Figure 22C), we conclude that Sgo1 contributes directly to the enrichment of Ipl1/Aurora B on centromeres. In contrast to condensin localization, Rts1 seems dispensable for Ipl1/Aurora B to become enriched on centromeres during mitosis.

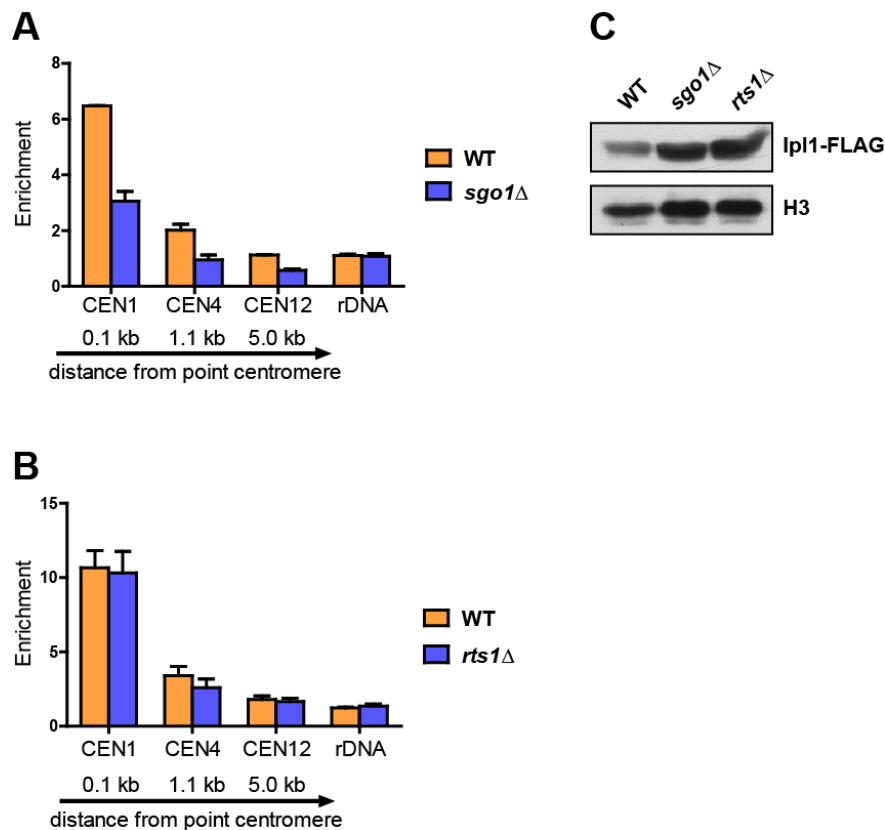


Figure 22. Sgo1, but not Rts1, is necessary for increased levels of the Ipl1/Aurora B kinase bound to centromeric chromatin in mitotic cells

(A) Enrichment of FLAG-tagged Ipl1/Aurora B on centromeric/pericentromeric DNA (0.1 kb away from CEN1, 1.1 kb away from CEN4 and 5.0 kb away from CEN12) and on rDNA (NTS1-2) in nocodazole-arrested wild type and *sgo1*Δ cells was determined by ChIP followed by qPCR. Enrichment was calculated from normalization to the levels of Ipl1-FLAG bound to an unspecific locus on the arm of chromosome 10 (*MDV1*). Error bars represent the standard error of the mean. (B) Enrichment of FLAG-tagged Ipl1 on centromeric/pericentromeric DNA and on rDNA in wild type and *rts1*Δ cells was determined by ChIP followed by qPCR. Experiments were performed as described in (A). Error bars represent the standard error of the mean. (C) The levels of FLAG-tagged Ipl1/Aurora B in exponentially growing wild type, *sgo1*Δ and *rts1*Δ cells were analyzed by Western blot analysis (histone H3 used as loading control).

3.5.3 Overexpression of CPC proteins partially rescues chromosome segregation defects in cells lacking Sgo1

The CPC members Sli15 and Bir1 have previously been shown to be high copy number suppressors of *sgo1*Δ mutants (Storchová *et al.*, 2011). Thus, we hypothesized that elevated levels of these proteins might increase the amount of Ipl1/Aurora B on centromeric chromatin, which partially bypasses the need for Sgo1. Accordingly, we found that the localization defect of Ipl1-GFP in *sgo1*Δ mutants was rescued to wild type levels upon ectopic expression of Sli15 or Bir1 using fluorescence microscopy (data from K. Peplowska; K. Peplowska *et al.*, 2014). Thus, we recapitulated previous experiments and tested whether ectopic expression of Sli15 rescues the sensitivity of *sgo1*Δ mutants towards microtubule poisons and towards overexpression of Cik1-cc. Notably, ectopic expression of Sli15 did not rescue the sensitivity of cells lacking Sgo1 to the induction of syntelic attachments (Cik1-

cc overexpression), whereas the sensitivity of these mutants towards nocodazole was indeed reduced (Figure 23; Storchová *et al.*, 2011). Based on these results, we speculate that Sgo1 has at least one other function besides localization of Ipl1/Aurora B, which is crucial for the repair of syntelic attachments.

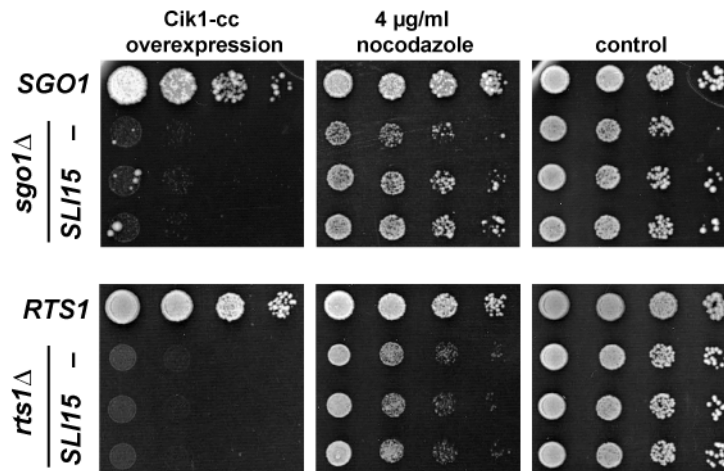


Figure 23. Overexpression of *SLI15* partially rescues the sensitivity of cells lacking Sgo1, but not Rts1, towards microtubule poisons

The effect of Sli15 overexpression on the sensitivity of *sgo1Δ* and *rts1Δ* cells to microtubule poisons (4 µg/ml nocodazole) or to the induction of syntelic attachments (Cik1-cc overexpression) was analyzed. The corresponding mutants were transformed with a high copy number plasmid containing *SLI15* (*SLI15*) or an empty plasmid (–) and tenfold serial dilutions were spotted on plates containing 2% galactose to induce Cik1-cc overexpression or 4 µg/ml nocodazole. Control plates without nocodazole contained 2% glucose as carbon source to repress transcription of *cik1-cc*.

Based on our ChIP analysis, centromeric enrichment of Ipl1/Aurora B in cells lacking Rts1 is not impaired (Figure 22B). Thus, we assumed that increasing the amount of Ipl1/Aurora B on centromeres should not improve the efficiency of *rts1Δ* mutants to repair syntelic attachments. Accordingly, we found that ectopic expression of Sli15 does not suppress the growth defect of *rts1Δ* mutants upon induction of syntelic attachments (Cik1-cc overexpression; Figure 23). In contrast to *sgo1Δ*, the sensitivity of *rts1Δ* cells towards nocodazole is also not rescued by *SLI15* overexpression. These experiments provide more evidence that Rts1 might be indeed dispensable for Ipl1/Aurora B enrichment on centromeres. Moreover, they imply that Sgo1 performs both Rts1-dependent as well as Rts1-independent functions at centromeric chromatin to facilitate the repair of syntelic attachments and the establishment of chromosome biorientation.

3.5.4 Overexpression of CPC proteins does not rescue the defective repair of syntelic attachments of condensin mutants

In fission yeast, Ipl1/Aurora B phosphorylates condensin thus facilitating its association with chromatin (Tada *et al.*, 2011). As *sgo1Δ* mutants lack both full enrichment of Ipl1/Aurora B and condensin on centromeric chromatin, we speculated that loss of condensin might be an indirect effect caused by reduced levels of Ipl1/Aurora B phosphorylation (Figure 18A; Figure 22A). To test this possibility we took advantage of the fact that overexpression of *SLI15* partially rescues *sgo1Δ* mutants, probably through ectopic enrichment of Ipl1/Aurora B on centromeres (Figure 23; Peplowska *et al.*, 2014). Thus, we analysed whether *SLI15* overexpression rescues temperature sensitive alleles of condensin (*smc2-8* and *ycg1-10*), which also fail to proliferate upon induction of syntelic attachments by Cik1-cc overexpression (Figure 19A).

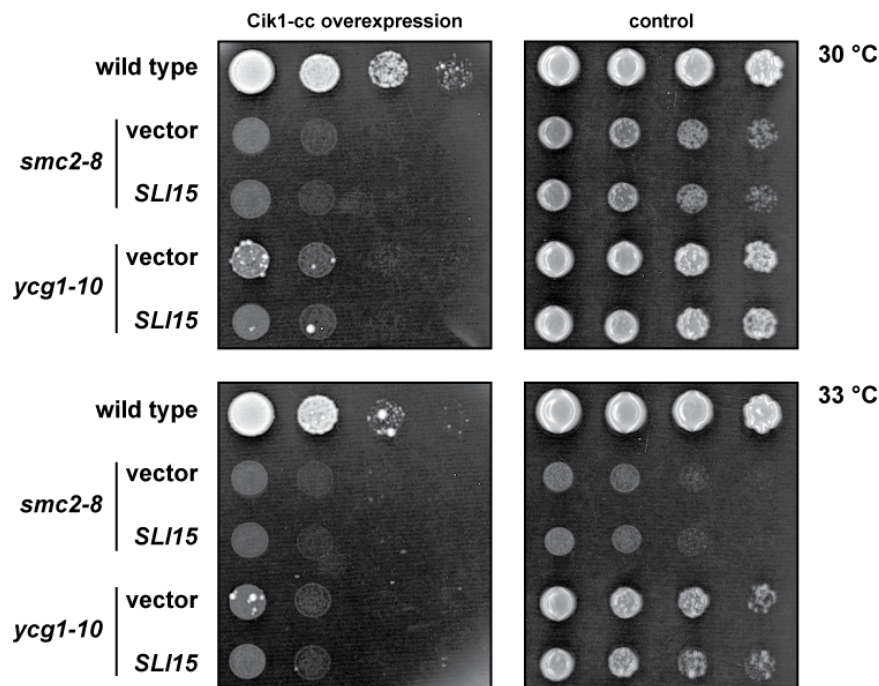


Figure 24. Overexpression of *SLI15* does not restore the capability to repair syntelic attachments in condensin mutants

The effect of *SLI15* overexpression on the sensitivity of the temperature sensitive condensin mutants *smc2-8* and *ycg1-10* to the induction of syntelic attachments (Cik1-cc overexpression) was analyzed. The corresponding mutants were transformed with a high copy number plasmid containing *SLI15* (*SLI15*) or an empty plasmid (vector), tenfold serial dilutions were spotted on plates containing 2% galactose to induce Cik1-cc overexpression and incubated at the indicated temperatures. Control plates contained 2% glucose as carbon source to repress transcription of *cik1-cc*.

We found that ectopic expression of *SLI15* does not improve the proliferation of *smc2-8* and *ycg1-10* mutants independently of the presence or absence of high levels of Cik1-cc (Figure 24). This finding suggests that elevated levels of Ipl1/Aurora B on centromeres do not compensate the loss of

functional condensin at centromeres even when Sgo1 is present. Accordingly, we found that centromeric localization of the condensin subunit Ycg1-GFP in *sgo1* Δ cells is not rescued by ectopic expression of *SLI15* or *BIR1* (data from K. Peplowska; Peplowska *et al.*, 2014). These data argue for a bifurcation of Sgo1's function in bringing Ipl1/Aurora B as well as condensin to centromeric chromatin to facilitate the repair of syntelic attachments.

4 Discussion

4.1 Cell cycle-dependent regulation of Sgo1 protein levels during mitosis

The cell cycle-dependent protein expression profile of Sgo1 in budding yeast resembles that of *bona fide* substrates of the APC/C, such as mitotic Clb2 and Pds1/securin (Figure 6A; Indjeian *et al.*, 2005). The APC/C determines ordered progression through mitosis by sequentially targeting diverse substrates for proteasomal degradation by ubiquitylation (reviewed in Peters, 2006). Accordingly, we were interested whether the degradation of Sgo1 at the end of mitosis is functionally important for mitotic cell division in budding yeast as well. Thus, we mapped elements on Sgo1 that are essential for its cell cycle-dependent degradation to interfere with its timely destruction.

We found a short stretch of amino acids located in the C-terminus of Sgo1, which is both necessary as well as sufficient for protein degradation during mitosis (Figure 7). Remarkably, this stretch of amino acids does not contain canonical degradation motifs, which are usually recognized by the APC/C for subsequent ubiquitylation (Song & Rape, 2011). Instead, a putative SUMO-interacting motif (SIM; amino acids 489 – 493: LLDIT) was predicted to be located within this region of Sgo1. Substituting leucine 489 and leucine 490 with alanine in this motif stabilized the protein levels of Sgo1 throughout the whole cell cycle (*sgo1* L489,490A; Figure 8). These findings argue that Sgo1 might interact with SUMOylated proteins in order to be efficiently recognized and ubiquitylated by the APC/C. In agreement with this hypothesis, it has been shown that the SUMOylation system contributes to the efficient turnover of the APC/C substrates Clb2 and Pds1/securin in budding yeast (Seufert *et al.*, 1995; Dieckhoff *et al.*, 2004). Another study investigating the role of the SUMO-targeted ubiquitin ligases (STUbLs) Slx5 and Slx8 further suggests that SUMOylation plays a role in the degradation of Sgo1 (van de Pasch *et al.*, 2013). The authors of this study found increased amounts of Rts1 localized to centromeres in cells lacking Slx5 or Slx8. As Sgo1 is essential for Rts1 localization, these increased amounts of Rts1 can be explained by the fact that Sgo1 might not be efficiently degraded in *slx5Δ/sl x8Δ* mutants (Figure 13; Verzijlbergen *et al.*, 2014). Accordingly, deletion of *SGO1* reduced the number of Rts1 foci localized to kinetochores in *slx5Δ* mutants (van de Pasch *et al.*, 2013). However, it remains to be tested whether this putative SIM indeed binds SUMO and/or SUMOylated proteins, which might allow recognition through the APC/C.

Recent work from Eshleman and Morgan provides an alternative explanation for the impaired degradation of mutant Sgo1 L489,490A, which does not necessarily involve the SUMO system (Figure 8). The authors showed in their study that budding yeast Sgo1 is ubiquitylated by the APC/C bound to its co-factors Cdc20 or Cdh1 *in vitro* (Eshleman & Morgan, 2014). Moreover, they identified a non-canonical D-Box, which is essential for the ubiquitylation and turnover of Sgo1 *in vivo*. This non-canonical D-Box is located adjacent to the putative SIM, which we identified in our analysis. Thus, it is possible that the substitution of leucine 489 and leucine 490 with alanine directly impairs the interaction between Sgo1's degradation motif and the APC/C. Hence, Sgo1 L489,490A might not be

efficiently recognized and ubiquitylated by the APC/C, because its non-canonical D-Box is altered. Future research should address whether Sgo1 L489,490A has a lower binding affinity for the APC/C than wild type Sgo1 to exclude the possibility that their interaction is bridged by SUMO and/or SUMOylated co-factors of the APC/C.

A moderately conserved equivalent of a non-canonical D-Box can be also found in human *HsSgo1* (Karamysheva *et al.*, 2009). Importantly, cell cycle-dependent degradation of *HsSgo1* also depends on this element, although canonical APC/C recognition motifs are required for its efficient turnover as well (Karamysheva *et al.*, 2009). Ectopic expression of a non-degradable version of *HsSgo1* fully rescues defects induced by *HsSgo1* siRNA indicating that its cell cycle dependent regulation is dispensable for its mitotic function in human somatic cells (Karamysheva *et al.*, 2009). Accordingly, we found that non-degradable Sgo1 is fully functional in the repair of syntelic attachments and rescues the sensitivity of *sgo1Δ* cells towards microtubule poisons in budding yeast (Figure 9). Consistent with these findings, Eshleman and Morgan showed that stabilization of Sgo1 by deletion of the non-canonical D-Box does not interfere with Sgo1's function in mitosis (Eshleman & Morgan, 2014). As non-degradable versions of human as well as budding yeast Sgo1 are fully functional during mitotic cell division, it seems that cell cycle-dependent regulation of Sgo1 proteins is dispensable at least in mitosis. Nevertheless, APC/C dependent degradation seems to be a common feature of Shugoshin proteins suggesting it is important for their functions beyond mitotic chromosome segregation.

Accordingly, it is intriguing to speculate that there is a strict requirement to completely degrade Sgo1 during meiotic cell division. Such a complete degradation of Sgo1 might not be as crucial for the faithful progression of mitosis, because the mode of action and the molecular targets of Sgo1 differ between both types of cell division. In budding yeast, Sgo1 protects meiosis-specific cohesin complexes and residual activity of this function would directly interfere with the physical separation of sister chromatids during anaphase II leading to the formation of aneuploid spores (Katis *et al.*, 2004; Kitajima *et al.*, 2004; Marston *et al.*, 2004). In contrast, we and others found that Sgo1 localizes condensin and the CPC to mitotic chromosomes (Figure 18, 22; Peplowska *et al.*, 2014; Verzijlbergen *et al.*, 2014), but does not affect mitotic cohesin complexes (Figure 17A; Indjeian *et al.*, 2005; Kiburz *et al.*, 2005; Peplowska *et al.*, 2014; Verzijlbergen *et al.*, 2014). Thus, residual Sgo1 activity during mitosis would not physically hinder the separation of sister chromatids and might be tolerated to a certain degree in budding yeast cells. To understand why Sgo1 is a target of APC/C-mediated degradation, future research should address whether the expression of non-degradable *sgo1* mutants affects the efficiency and fidelity of meiotic chromosome segregation.

4.2 Phosphorylation-dependent localization of Shugoshin proteins in mitosis

If the function of Sgo1 during mitosis is not terminated via its degradation, other means to regulate and cease Sgo1's function must exist. Recent work in budding yeast suggests that Sgo1 is removed from centromeres upon the establishment of chromosome biorientation (Nerusheva *et al.*, 2014). Thus, removal of Sgo1 from centromeres, rather than its direct degradation seems to be the major pathway to silence the function of Sgo1 on centromeres. This notion implies that the localization of Sgo1 to centromeres has to be dynamic and precisely regulated during different stages of mitosis. The association of Shugoshin proteins with centromeric chromatin is facilitated through binding of the conserved basic region to phosphorylated histone H2A in yeast and all higher eukaryotes studied so far (Kawashima *et al.*, 2010). We and others found that introduction of a single point mutation or complete removal of this region impairs Sgo1's function in the repair of syntelic attachments in budding yeast leading to increased sensitivity towards microtubule poisons (Figure 10B; Indjeian *et al.*, 2005; Kawashima *et al.*, 2010). Likewise, the deletion of Bub1's kinase domain, which phosphorylates H2A, abrogates the cell cycle arrest due to the loss of centromeric Sgo1 when sister chromatids are not under tension (Fernius & Hardwick, 2007). As the centromeric enrichment of Sgo1 relies on its interaction with phosphorylated histone H2A, weakening this interaction might lead to a spatial redistribution of Sgo1 molecules and therefore ceasing their activity.

Intriguingly, such a mechanism seems to regulate the function of *HsSgo1* in human cells during mitosis (Liu *et al.*, 2013a, 2013b). The phosphorylation of histone H2A on threonine 120 by *HsBub1* is the key determinant that concentrates *HsSgo1* around centromeric chromatin in prophase and prometaphase (Kawashima *et al.*, 2010). Notably, *HsSgo1* remains associated with chromosomes upon depletion of *HsBub1*, but relocates to chromosome axes (Kitajima *et al.*, 2005). This finding suggests the existence of a second interaction partner, which is capable to maintain the basal association of *HsSgo1* with chromosomes in the absence of phosphorylated histone H2A. This second chromosomal receptor is likely cohesin, as Cdk1-dependent phosphorylation of *HsSgo1* enables a physical interaction with this complex (Liu *et al.*, 2013a). This interaction is further important to preserve sister chromatid cohesion at centromeres, as *HsSgo1* recruits PP2A, which in turn dephosphorylates the cohesive factor sororin to maintain its association with cohesin (Liu *et al.*, 2013a).

Remarkably, cohesin binding seems to compete with the association of *HsSgo1* and phosphorylated histone H2A (Liu *et al.*, 2013b). Hence, the competition between these two different chromosomal receptors leads to a differentiation of *HsSgo1* molecules into two distinct pools. Gradual establishment of chromosome biorientation increases the association of *HsSgo1* with phosphorylated histone H2A indicating that the association with cohesin complexes is lost (Liu *et al.*, 2013b). Importantly, the association with histone H2A coincides with the removal of Cdk1 phosphorylation from *HsSgo1* suggesting that this modification correlates with the absence of tension between sister chromatids (Liu *et al.*, 2013b). After the release of associated *HsSgo1*-PP2A, centromeric cohesin complexes are

further removed from chromosomes in a WAPL-dependent mechanism (Liu *et al.*, 2013a). Taken together, these findings suggest a mechanism in which *HsSgo1* is first enriched around centromeric chromatin through binding to phosphorylated histone H2A. Upon phosphorylation by Cdk1, *HsSgo1* associates with cohesin complexes between tensionless sister chromatids to maintain the cohesive force between them. Once chromosome biorientation is achieved, *HsSgo1* itself becomes dephosphorylated and relocates back to phosphorylated histone H2A and leaves cohesin refractory to its removal by WAPL (Liu *et al.*, 2013b; Nishiyama *et al.*, 2010). This elaborate spatial distinction between two pools of *HsSgo1* might have evolved to ensure that *HsSgo1*'s protective function is limited to sister chromatids, which are not under tension.

Notably, mutant *HsSgo1* mimicking constitutive Cdk1 phosphorylation induces lagging chromosomes during anaphase in human cells (Liu *et al.*, 2013b). This phenotype is indicative of artificial and prolonged protection of sister-chromatid cohesion. Upon establishment of chromosome biorientation, phospho-mimicking *HsSgo1* accordingly fails to relocalize from inner centromeres, where it co-localizes with and protects cohesin complexes (Liu *et al.*, 2013b). According to the proposed mechanism, this finding implies that Cdk1 phosphorylation determines whether *HsSgo1* binds either cohesin or histone H2A (Liu *et al.*, 2013b). Therefore, Cdk1 phosphorylation must be removed by the activity of at least one phosphatase to allow the redistribution of *HsSgo1* molecules from cohesin to phosphorylated histone H2A, when chromosome biorientation is achieved. As Shugoshin proteins directly interact with PP2A (Kitajima *et al.*, 2006; Riedel *et al.*, 2006; Tang *et al.*, 2006), this phosphatase is a likely candidate to remove phosphate groups in order to regulate the spatial distribution of Shugoshin proteins. In agreement with such a function, depletion of PP2A abrogates the centromeric enrichment of *HsSgo1* in mitotic cells (Tang *et al.*, 2006). Notably, Tang and colleagues showed that co-depletion of the polo-like kinase 1 (Plk1) restores centromeric localization of *HsSgo1* in the absence of functional PP2A (Tang *et al.*, 2006). Thus, Plk1 contributes as third mitotic kinase to the precise spatial distribution of *HsSgo1* in human cells, in addition to Bub1 and Cdk1. Likewise, the removal of the *Drosophila* Shugoshin homolog MEI-S332 from centromeres at the metaphase to anaphase transition depends on its interaction with polo kinase (Clarke *et al.*, 2005). As polo or polo-like kinases have the same effect on Shugoshin proteins in two different organisms, this phosphorylation-dependent regulation might be an evolutionary conserved feature as well. Moreover, the involvement of polo-like kinases further emphasizes the complexity of the phosphorylation-based molecular network that precisely balances the localization of Shugoshin proteins. So far, most studies focused on the action of mitotic kinases and their effect on the localization of Shugoshin proteins. To complement these results, future research should investigate the exact role of PP2A and other phosphatases, such as PP1 during this process.

Remarkably, an opposing role for PP2A in the localization of Sgo1 was recently suggested in budding yeast (Nerusheva *et al.*, 2014). The authors of this study showed that the PP2A regulatory subunit Rts1 is required to remove Sgo1 efficiently from centromeres in a tension-dependent manner (Nerusheva *et al.*, 2014). Accordingly, the amounts of Sgo1 associated with centromeric chromatin are increased in *rts1* Δ cells (Nerusheva *et al.*, 2014). Likewise, the levels of a *sgo1* mutant, which fails to interact with Rts1/PP2A (*sgo1* 3A; Xu *et al.*, 2009), on centromeric chromatin are higher than that of

wild type Sgo1 (Nerusheva *et al.*, 2014). Thus, PP2A seems to affect the localization of Sgo1 in budding yeast as well as in human cells, but in an opposing manner. Despite this conflicting results, it is intriguing to speculate that PP2A generally removes phosphate groups from Sgo1 and its interaction partners in order to relocate Sgo1, when tension between sister chromatids is established. Accordingly, future research should address whether Sgo1 is a target of Cdk1 and/or polo-like kinase (Cdc5) phosphorylation in budding yeast as well. Additional experiments should further clarify the effect of PP2A activity on the phosphorylation levels of Sgo1 and how this correlates with the spatial distribution of Sgo1 molecules in budding yeast cells.

There is another observation from budding yeast that cannot be reconciled with the molecular mechanism, which has been proposed based on human proteins. Budding yeast Sgo1 neither affects the localization of cohesin complexes on centromeric chromatin (Kiburz *et al.*, 2005; Peplowska *et al.*, 2014; Verzijlbergen *et al.*, 2014) nor influences the cohesion of sister chromatids during mitosis (Indjeian *et al.*, 2005). These findings argue against the differentiation of distinct Sgo1 pools through binding of either cohesin or phosphorylated histone H2A in this organism. Spatial redistribution between two distinct subcellular receptor sites might nevertheless regulate and silence the function of Sgo1 in budding yeast mitosis. Such a second receptor site for Sgo1 might also explain the synthetic growth defect of *sgo1* T379D and *sgo1*ΔHB mutants upon ectopic expression of Mps1 (Figure 11B). In contrast to this synthetic growth defect, Mps1 overexpression is rather beneficial for cells lacking Sgo1 completely, where it rescues their sensitivity towards microtubule poisons (Figure 11A; Storchová *et al.*, 2011). The discrepancy between cells lacking Sgo1 and cells expressing mislocalized Sgo1 might be explained by the fact that the mutant proteins exclusively localize to and act at a second receptor site causing the synthetic growth defect, while they fail to interact with phosphorylated histone H2A. In addition, these results suggest that Mps1 directly acts on Sgo1, because disruption of the SAC by deletion of *MAD2* does not abolish this synthetic growth defect (Figure 11C). In agreement with this hypothesis, centromeric enrichment of Sgo1 indeed depends on the kinase activity of Mps1 in budding yeast (Storchová *et al.*, 2011). Alternatively, the loss of centromeric Sgo1 upon Mps1 inhibition can be explained by the absence of histone H2A phosphorylation, because Mps1 actively recruits Bub1 to kinetochores (London *et al.*, 2012). The exact molecular contributions of Mps1 phosphorylation on the spatial distribution of Sgo1 during mitosis remain to be determined by additional experiments.

Taken together, compelling evidence suggest that the localization of Shugoshin proteins in mitosis is very dynamic and precisely balanced through the action of several protein kinases and phosphatases. Considering the highly conserved nature of histone H2A phosphorylation by Bub1 (Kawashima *et al.*, 2010), it seems remarkable that the identity of additional kinases varies from one organism to the other. It remains to be tested whether there is one unifying and conserved mechanism for the phosphorylation-dependent localization of Shugoshin proteins, which involves the concerted action of Mps1, Bub1, Cdk1 and polo-like kinases. In addition, future research should address whether distinct pools of Sgo1, which might be determined by different interaction partners, exist in budding yeast and how they can be targeted through phosphorylation. The identification of such factors might also reveal how tension between sister chromatids can be translated into precisely targeted phosphorylation of Sgo1 in order to regulate its function during mitosis.

4.3 Sgo1 and PP2A function together in mitotic chromosome segregation

The best characterized function of Shugoshin proteins is the recruitment of the protein phosphatase 2A (PP2A), which in turn leads to the dephosphorylation and protection of centromeric cohesin during meiosis (Kitajima *et al.*, 2006; Riedel *et al.*, 2006). The N-terminal coiled-coil domain of Shugoshin proteins mediates the association with PP2A complexes through interactions with regulatory (B', Rts1) and catalytic (C, Pph21/Pph22) subunits (Xu *et al.*, 2009). In agreement with a previous study investigating the localization of PP2A subunits during cell cycle progression (Gentry & Hallberg, 2002), we found that Rts1 accumulates at centromeric chromatin in mitotic cells (Figure 13A). The enrichment of Rts1 on centromeres depends on the presence of Sgo1 and more specifically on the functional interaction with a conserved coiled-coil domain that can be interrupted by specific mutations (*e.g.* N51I; Figure 12; Figure 13A, C). Accordingly, we tested the functional relevance of this centromeric pool of PP2A complexes for mitotic chromosome segregation. Like *sgo1Δ* mutants, cells expressing *sgo1* N51I or lacking Rts1 are sensitive to microtubule poisons without having a major SAC defect (Figure 14; Xu *et al.*, 2009). Moreover, these mutants fail to repair incorrect chromosome attachments (Figure 15), suggesting that Sgo1 and Rts1 also collaborate to perform this function. We conclude that like in meiosis, Sgo1 localizes PP2A via its regulatory subunit Rts1 to centromeric chromatin to achieve chromosome biorientation. In mitosis, however, Sgo1 does not protect cohesin molecules from its premature cleavage or removal (Figure 17A; Indjeian *et al.*, 2005; Kiburz *et al.*, 2005; Peplowska *et al.*, 2014; Verzijlbergen *et al.*, 2014). Hence, the mechanism of PP2A recruitment is conserved between meiosis and mitosis in budding yeast, but the molecular targets of Sgo1 and PP2A differ between both types of cell division.

In addition to the result that Rts1 is essential upon induction of syntelic attachments (Figure 15), we performed two genetic experiments to raise more evidence for our hypothesis that Sgo1 and Rts1 collaborate during mitotic cell division. First, expression of a C-terminal truncation of Sgo1, which lacks the binding site for phosphorylated histone H2A and the degradation signal, reduces the sensitivity of *sgo1Δ* cells towards microtubule poisons (Figure 6C; Figure 16A). This partial rescue also depends on the binding of Rts1, as the introduction of the N51I point mutation abolishes this rescuing effect (Figure 16A). The disruption of Rts1 binding also abolishes the synthetic growth defect of cells expressing mislocalized Sgo1 (*sgo1* N51I,T379D) imposed through ectopic expression of Mps1 (Figure 16B). Although indirect, these genetic experiments further suggest that Sgo1 collaborates with PP2A and more specifically with Rts1 during mitosis in order to facilitate chromosome biorientation.

In contrast to our results that functional Rts1 at centromeres is necessary for the repair of syntelic attachments, a recent study suggests that it is dispensable to achieve chromosome biorientation in budding yeast (Verzijlbergen *et al.*, 2014). Cells lacking Rts1 segregate chromosomes with similar kinetics and fidelity as wild type cells, when the APC/C co-activator Cdc20 is depleted (Verzijlbergen *et al.*, 2014). Surprisingly, the expression of a Sgo1 mutant, which fails to interact with and localize Rts1 to centromeres (*sgo1* 3A; Xu *et al.*, 2009), interferes with correct chromosome segregation under the same experimental conditions (Verzijlbergen *et al.*, 2014). The authors explain this discrepancy by

an additional defect of the *sgo1* 3A allele besides disrupting the interaction with Rts1. In order to verify this conclusion, additional experiments characterizing the molecular defects that are caused by the *sgo1* 3A allele are necessary. In addition, a third study focusing on the role of Sgo1 and Rts1 in mitosis recently reported that artificial centromere targeting of Rts1 fully rescues chromosome missegregation caused by the deletion of *SGO1* (Eshleman & Morgan, 2014). Notably, centromere-tethered Rts1 rescues the missegregation phenotype of *sgo1* Δ cells indicating that it can act independently of Sgo1 once correctly localized (Eshleman & Morgan, 2014). These observations are in agreement with our results and emphasize that localizing Rts1 to centromeres is one of the main functions of Sgo1 in mitotic cell division, even though it might not be essential for correct chromosome segregation under unstressed conditions.

Taken together, compelling evidence shows that Sgo1 interacts with and localizes Rts1 to centromeres of mitotic chromosomes in budding yeast (Figure 13; Eshleman & Morgan, 2014; Peplowska *et al.*, 2014; Verzijlbergen *et al.*, 2014). The notion that Rts1 on the one hand regulates the centromeric localization of Sgo1 (as discussed before) and on the other acts downstream in the repair of syntelic attachments might help to reconcile the controversial results observed for *rts1* Δ cells. Future research should analyse in details whether there is indeed a reciprocal relationship between the localization of Sgo1 and PP2A, which is regulated via phosphorylation. Thus, additional experiments focusing on phosphatase deficient mutants of PP2A, chemical inhibition of PP2A and *rts1* mutants, which fail to form functional PP2A holoenzymes, are important to dissect the hierarchy of protein assembly at centromeric chromatin. In addition, such experiments will further yield important insights whether all defects observed in cells lacking Rts1 are caused by the absence of PP2A or whether Rts1 can act alone in the establishment of chromosome biorientation.

4.4 Sgo1-dependent enrichment of centromeric condensin allows the repair of incorrect chromosome attachments

Genome-wide binding studies revealed that condensin is enriched at centromeric chromatin, the rDNA locus and on genes bound by the RNA polymerase III transcription factor in budding yeast (TFIIIC; D'Ambrosio *et al.*, 2008a; Wang *et al.*, 2005). The centromeric localization of condensin is cell cycle regulated and can mainly be observed in mitotic cells (Bachelier-Bassi *et al.*, 2008). The enrichment of condensin complexes on centromeric chromatin, but not on rDNA, depends on the presence of functional Sgo1 (Figure 18; Peplowska *et al.*, 2014; Verzijlbergen *et al.*, 2014). Thus, the inability of *sgo1* Δ cells to repair incorrect chromosome attachments might be caused by the absence of condensin at centromeres. Cells lacking fully functional condensin due to the expression of temperature sensitive mutants of Smc2 or Ycg1 indeed fail to proliferate upon the induction of incorrect chromosome attachments at high frequencies (Figure 19A). Potentially, this defect can be explained by the inability of cells to detect the absence of tension between sister chromatids that are incorrectly attached to the mitotic spindle. In order to measure the changes in tension between sister

chromatids, outward directed forces imposed by the mitotic spindle on chromosomes that are counteracted by cohesin have to be precisely balanced. This notion led to the proposal of a mitotic spring, which consists of centromeric chromatin, cohesin as well as condensin and integrates all forces applied to mitotic chromosomes in budding yeast (Stephens *et al.*, 2011). Altering the physical properties of this mitotic spring might render cells unable to detect small changes of tension between a pair of sister chromatids. Thus, the capability of cells to discriminate correct and incorrect chromosome attachments might be impaired through the loss of factors contributing to this mitotic spring. Accordingly, we found that loss of centromeric condensin (*e. g.* in cells lacking Sgo1 and Rts1) leads to increased stretching of pericentric chromatin, which can be also observed in cells lacking functional condensin (*e. g.* in temperature sensitive condensin mutants; Figure 20; Stephens *et al.*, 2011). Thus, we speculate that Sgo1 and to a minor extent Rts1/PP2A maintain the centromeric enrichment of condensin in order to form a functional mitotic spring, which allows cells to detect incorrect, tensionless chromosome attachments. In agreement with our hypothesis, Sgo1 is essential to mediate changes in the geometry of the inner kinetochore in response to altered tension between sister chromatids (Haase *et al.*, 2012). Future research should address whether the activity of the centromeric pool of condensin translates tension generated by the mitotic spindle into shape changes of the inner kinetochore and whether the only role of Sgo1 in this process is to ensure timely localization of condensin.

Several findings in other species support the hypothesis that condensin acts on centromeric chromatin to maintain it susceptible to respond to microtubule-generated forces (Gerlich *et al.*, 2006; Ribeiro *et al.*, 2009; Samoshkin *et al.*, 2009; Uchida *et al.*, 2009). Depletion of condensin I subunits in human cells leads to a marked increase in the interkinetochore distance of mitotic chromosomes (*i. e.* centromere stretching; Gerlich *et al.*, 2006). Importantly, this increased stretching of centromeres cannot be observed in cells treated with nocodazole, thus suggesting that microtubule-generated forces underlie this defect (Gerlich *et al.*, 2006). Moreover, depletion of condensin I uncouples the movement of individual sister centromeres, further indicating that centromeric chromatin in human cells shows a spring-like behaviour as well (Gerlich *et al.*, 2006). Likewise, centromere stretching can be also observed in chicken cells upon transcriptional repression of the condensin subunit *SMC2*, hinting at a common role for condensin on centromeres (Ribeiro *et al.*, 2009). Thus, it might be a conserved feature of eukaryotic chromosomes that condensin maintains centromeric chromatin in an elastic state, which allows it to act as a molecular spring. Remarkably, impairing condensin in chicken cells further activates the SAC to delay mitotic progression, thereby linking the compaction of centromeric chromatin to the repair of incorrect chromosome attachments and subsequent checkpoint activation (Ribeiro *et al.*, 2009). Analogously, human cells depleted of condensin I also degrade mitotic cyclin B with delayed kinetics (Uchida *et al.*, 2009). The activation of the SAC is likely triggered by the suppression of (intra-)kinetochore stretching, which is usually induced by the opposing forces of the mitotic spindle and stiff (or spring-like) centromeric chromatin under unperturbed conditions (Uchida *et al.*, 2009). These findings suggest a general mechanism in which condensin I maintains centromeric chromatin in a stiff conformation to counteract the forces of the mitotic spindle, thereby leading to stretched kinetochores, which in turn can dampen SAC signalling (Uchida *et al.*, 2009).

Taken together, condensin seems to be a conserved factor contributing to the structural integrity of centromeric chromatin in eukaryotes. The structural integrity of these regions is important to adequately respond to forces applied to kinetochores and might enable cells to sense tension on bioriented chromosomes. Future research should address how condensin mechanistically acts on chromatin to maintain stiff centromeric structures. It will further be important to understand how this function of condensin is limited to centromeres in early stages of mitosis. As condensin also performs other functions in chromosome segregation for example during later stages of mitosis, its sequential action has to be precisely regulated (e. g. D'Ambrosio *et al.*, 2008b; St-Pierre *et al.*, 2009).

Restricting the action of condensin spatially might be achieved via its localization through Sgo1 in budding yeast (Figure 18; Peplowska *et al.*, 2014; Verzijlbergen *et al.*, 2014). Given the common role of condensin at centromeres in eukaryotes, the question remains whether its localization to these regions is also conserved. In other fungi, such as fission yeast or *Candida albicans*, the centromeric enrichment of condensin is mediated via members of the monopolin complex (Burrack *et al.*, 2013; Tada *et al.*, 2011). This complex also mediates the association of condensin with the rDNA locus in budding yeast (Johzuka & Horiuchi, 2009). However, the deletion of the monopolin subunits *CSM1* or *LRS4* does not affect the proliferation of cells upon induction of syntelic attachments at 30 °C indicating that condensin is properly localized to and functional at centromeres in these cells (Figure 19B). Thus, it is rather unlikely that the monopolin complex facilitates centromeric enrichment of condensin in budding yeast. Nevertheless, the enrichment of condensin at pericentric chromatin is slightly reduced in *lrs4Δ* cells indicating that monopolin might contribute to but is not essential for centromere association (Snider *et al.*, 2014). Interestingly, *lrs4Δ*, but not *csm1Δ*, cells show a mild growth defect upon induction of syntelic attachments at lower temperature suggesting that at least Lrs4 might play a minor role in centromeric condensin localization (Figure 19B). Hence, future research should focus on a quantitative analysis of condensin enrichment at centromeres in various monopolin mutants of different fungi to evaluate the contribution of the monopolin complex. In addition, it should be analysed whether Shugoshin proteins contribute to condensin localization in other species. It is tempting to speculate that Shugoshin proteins act in a conserved pathway affecting the localization and function of complexes regulating the structural maintenance of mitotic chromosomes. Thus, future experiments should address whether Shugoshin proteins regulate cohesin and condensin complexes to maintain the structural integrity of centromeric chromatin as part of a conserved mechanism in eukaryotes, which allows the detection of incorrect chromosome attachments. Another important aspect of such a putative mechanism, which should be addressed, is whether all functions of Shugoshin proteins are mediated by or depend on PP2A and its enzymatic activity.

4.5 Sgo1 regulates Ipl1/Aurora B levels at centromeres

In addition to its role in localizing condensin, Sgo1 also contributes to the maintenance of full centromeric enrichment of the CPC effector kinase Ipl1/Aurora B in budding yeast (Figure 22; Peplowska *et al.*, 2014; Verzijlbergen *et al.*, 2014). Again this function seems to be conserved among

Shugoshin proteins, because the localization of Ipl1/Aurora B also depends on the interaction of CPC proteins with *SpSgo2* and *HsSgo1/HsSgo2* in fission yeast and human cells, respectively (Tsukahara *et al.*, 2010). However, the mechanistic aspects of how proper levels of Ipl1/Aurora B at centromeres are achieved in these organisms seems to differ from budding yeast (Kelley *et al.*, 2010; Tsukahara *et al.*, 2010; Wang *et al.*, 2010; Yamagishi *et al.*, 2010). So far the common feature of this pathway seems to be the interaction of Shugoshin proteins with one or more members of the CPC other than Ipl1/Aurora B that is enabled through phosphorylation by the kinase Cdk1 (Tsukahara *et al.*, 2010). Such an interaction still has to be verified in budding yeast, but overexpression of the CPC members Sli15/Incenp or Bir1/Survivin can partially rescue some phenotypes of cells lacking Sgo1 (Figure 23; Storchova *et al.*, 2011). Indeed, the localization of Ipl1/Aurora B at centromeres is restored to levels similar to wild type cells under these conditions (Peplowska *et al.*, 2014). Nevertheless, these increased amounts of centromeric Ipl1/Aurora B are not sufficient to restore the capability of *sgo1Δ* or *rts1Δ* cells to repair syntelic attachments (Figure 23). Consistently, the centromeric localization of condensin complexes is not restored under these conditions (Peplowska *et al.*, 2014). These findings emphasize that fully functional repair of syntelic attachments in budding yeast relies on both correct localization of Ipl1/Aurora B and a centromeric pool of condensin molecules.

More importantly, these data argue against a linear pathway in which Sgo1 localizes Ipl1/Aurora B to centromeres, which in turn facilitates the loading of condensin, as it has been suggested for fission yeast (Tada *et al.*, 2011). Phosphorylation of the condensin subunit *SpCnd2* by Ipl1/Aurora B contributes to the association of condensin with centromeres as well as chromosome arms in fission yeast (Tada *et al.*, 2011). Likewise, the association of condensin I with chromosomes is also regulated by Ipl1/Aurora B in human cells (Lipp *et al.*, 2007; Takemoto *et al.*, 2007). As Sli15/Incenp overexpression does not restore the localization of condensin at centromeres (Peplowska *et al.*, 2014), condensin loading onto chromosomes seems to be regulated by other means than Ipl1/Aurora B phosphorylation as it is in human cells and fission yeast. Likewise, Sli15/Incenp overexpression is not sufficient to restore the capability of temperature sensitive condensin mutants to repair incorrect attachments further supporting this notion (Figure 24). However, additional experiments are necessary to verify this hypothesis. Future research should address how the overexpression of CPC members can restore Ipl1/Aurora B localization in *sgo1Δ* cells and whether the phosphorylation of its substrates at the kinetochore is affected.

This phosphorylation of kinetochore components, such as Dam1, is of special interest, because it facilitates the correction of incorrect chromosome attachments (Cheeseman *et al.*, 2002). Remarkably, the expression of a truncated version of Sli15/Incenp, which clusters the CPC together with Ipl1/Aurora B on microtubules, seems to fully rescue the defects of *sgo1Δ* cells (Campbell & Desai, 2013). This result suggests that the crucial function of Sgo1 in the repair of syntelic attachments is to regulate Ipl1/Aurora B localization and thereby, affecting its kinase activity. How clustering CPC complexes on microtubules can bypass the need for condensin to maintain the structural integrity of centromeres remains to be determined. One possibility to explain these conflicting results might be that centromeric condensin contributes to the localization or activation of Ipl1/Aurora B. CPC proteins indeed fail to localize properly to kinetochores in condensin mutants in budding yeast (Li *et al.*, 2011).

This data predicts again a linear pathway in which condensin acts upstream of Ipl1/Aurora B and the CPC. According to this model, overexpression of Sli15/Incenp should allow the repair of syntelic attachments in cells lacking Sgo1 as it restores Ipl1/Aurora B localization. However, *sgo1Δ* cells are still sensitive to overexpression of Cik1-cc under this condition arguing against this sequential mechanism (Figure 23). In order to reconcile these conflicting results, future experiments should quantitatively analyse the phosphorylation of Ipl1/Aurora B substrates that are relevant for chromosome biorientation. These experiments will be important to determine whether the activity of Ipl1/Aurora B is comparable in cells expressing truncated Sli15/Incenp or overexpressing wild type Sli15/Incenp.

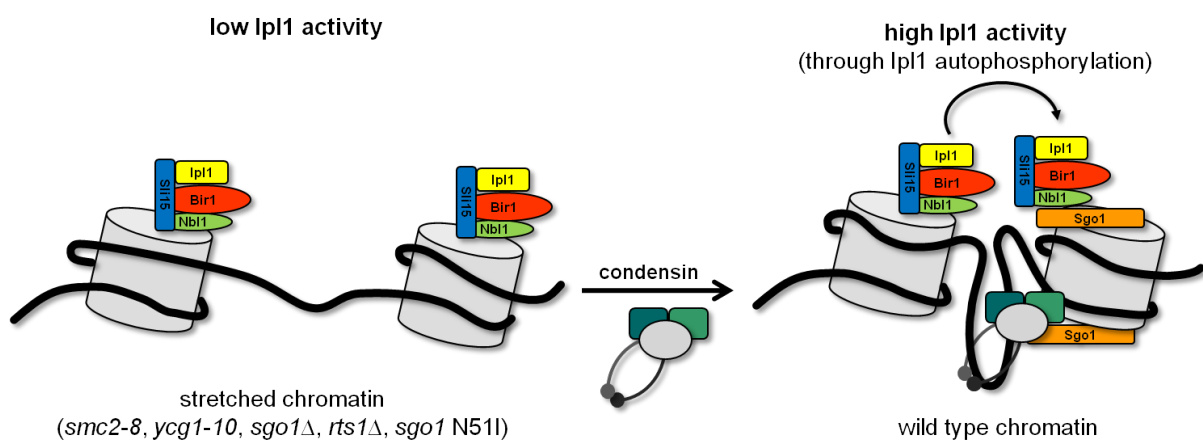


Figure 25. Condensin might influence overall Ipl1 kinase activity by facilitating spatial proximity of individual CPC complexes

Schematic figure of how condensin activity might contribute to the regulation of Ipl1/Aurora B phosphorylation. The activity of centromeric condensin maintains stiff chromatin structures in wild type cells during mitosis. Within these structures individual CPC complexes are in spatial proximity and thus, capable to phosphorylate each other leading to an increase in overall kinase activity (right side). The loss of centromeric condensin (e. g. in *sgo1Δ*, *rts1Δ* and *sgo1 N51I* mutants) or general impairment of condensin (e. g. in *smc2-8* and *ycg1-10* mutants) leads to defective chromatin structures around centromeres. Individual CPC complexes might not be capable to reach and phosphorylate each other within this stretched chromatin (left side). Thus, phosphorylation of Ipl1/Aurora B substrates, which is important for the turnover of incorrect chromosome attachments, might be reduced under such conditions.

These experiments will also allow us to validate whether condensin acts indirectly on Ipl1/Aurora B. Condensin might be needed to bring individual CPC complexes in close proximity, because it compacts centromeric chromatin (Figure 20; Stephens *et al.*, 2011). The spatial proximity of CPC complexes might in turn facilitate the autophosphorylation of Ipl1/Aurora B, thereby increasing its overall kinase activity within cells (Figure 25; reviewed in Ruchaud *et al.*, 2007; Carmena *et al.*, 2012). Such a model is in agreement with the notion that Ipl1/Aurora B forms a phosphorylation gradient expanding from centromeres in metaphase (Liu *et al.*, 2009). Thus, interfering with the compaction of centromeric chromatin might alter the dimension of this gradient leading to imbalanced phosphorylation of proteins regulating the kinetochore-microtubule attachments. It is possible that clustering CPC complexes on microtubules through expression of truncated Sli15/Incenp (Campbell & Desai, 2013) bypasses the need for centromeric compaction, because in such cells the

phosphorylation gradient has the right dimensions to reach its functional substrates and operates at levels comparable to wild type cells.

The function of Shugoshin proteins remains only partially understood, despite extensive research in the past decade. Members of this conserved protein family ensure sister chromatid cohesion during meiosis in most eukaryotic organisms studied so far. Shugoshin proteins further contribute to the fidelity of mitotic chromosome segregation in many eukaryotic species. However, their precise role during mitosis is less understood and seems not to be as conserved between species as their meiotic function. Using budding yeast as a model organism, we have shown that Sgo1 acts as a binding platform facilitating the localization of the PP2A subunit Rts1, condensin as well as Ipl1/Aurora B to centromeres during mitotic cell division. Accordingly, we think that Sgo1's role is to maintain these proteins (and their associated complexes) localized to centromeres to allow the repair incorrect chromosome attachments until biorientation is achieved.

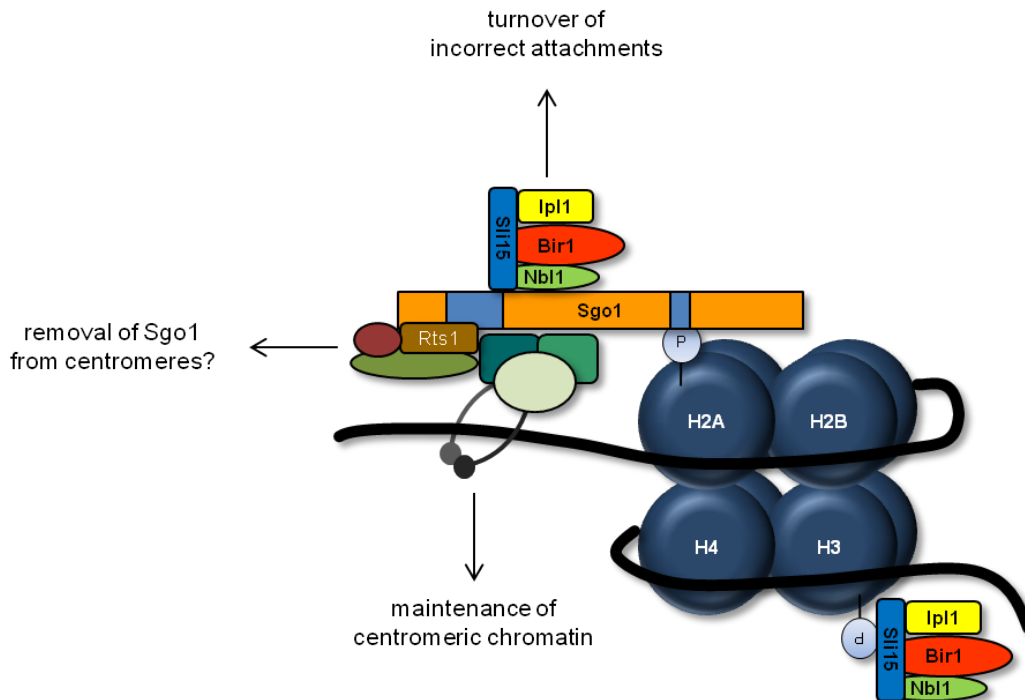


Figure 26. Sgo1 facilitates faithful chromosome segregation through the concurrent maintenance of centromeric pools of condensin, Ipl1/Aurora B and PP2A during mitotic cell division in budding yeast

Based on our analysis, we speculate that Sgo1 contributes in at least two ways to facilitate the repair of incorrect attachments on the molecular level. First, it maintains a pool of condensin complexes to provide the structural integrity of centromeric chromatin, which allows the detection of tension between sister chromatids. Sgo1 likely performs this function in collaboration with PP2A through binding to its regulatory subunit Rts1. In addition, Sgo1 localizes Ipl1/Aurora B to centromeric nucleosomes to release incorrect chromosome attachments, which are characterized by the absence of tension

between their sister chromatids. Based on our results, we propose that Sgo1 performs these functions rather in parallel than in a sequential order (Figure 26). We conclude furthermore that Sgo1's cell cycle-dependent degradation, which is initiated through ubiquitylation by the APC/C (Eshleman & Morgan, 2014), is dispensable to ensure faithful chromosome segregation during mitotic cell division. In contrast, its dynamic localization, which is controlled through the coordinated action of several mitotic kinases and phosphatases, is essential for the precise segregation of chromosomes in budding yeast.

5 Material and methods

5.1 Material

5.1.1 Chemicals, consumables, equipment and commercially available kits

Chemicals and consumables were purchased from the following companies and applied as received (if not stated otherwise):

5 PRIME, Inc. (Gaithersburg, USA), Acros Organics (Geel, Belgium), Agilent Technologies (La Jolla, USA), ALEXIS Biochemicals (Lörrach, Germany), Applichem (Darmstadt, Germany), Applied Biosciences (Darmstadt, Germany), Beckman Coulter (Krefeld, Germany), Becton Dickinson (Heidelberg, Germany), Bio-Rad Laboratories (Munich, Germany), Enzo Life Sciences (Lörrach, Germany), Fermentas (St. Leon-Rot, Germany), GE Healthcare (Munich, Germany), GeneTex (Irvine, USA), Gilson (Bad Camberg, Germany), Invitrogen (Karlsruhe, Germany), Merck Biosciences (Darmstadt, Germany), Millipore (Molsheim, France), Mobitec (Göttingen, Germany), NEB (Frankfurt, Germany), Nunc (Wiesbaden, Germany), PerkinElmer (Rodgau, Germany), QIAGEN (Hilden, Germany), R&D Systems (Minneapolis, USA), Roche (Mannheim, Germany), Roth (Karlsruhe, Germany), Santa Cruz Biotechnology, Inc. (Dallas, USA), Sarstedt (Nürmbrecht, Germany), SERVA Electrophoresis (Heidelberg, Germany), Sigma-Aldrich (Taufkirchen, Germany), Stratagene (Amsterdam, The Netherlands).

Following equipment was used to perform the experiments of this study:

Axio Observer Z1 inverted microscope (Carl Zeiss MicroImaging, Jena, Germany), Beckman Avanti J25 centrifuge, J-10, J-16.250 and J-25.50 rotors (Beckman Coulter, Krefeld, Germany), Bioruptor UCD-200 (Diagenode sa, Liege, Belgium), Certomat BS1 incubation shaker (B. Braun Biotech, Melsungen, Germany), CoolSnap HQ camera (Roper Scientific, Canada), CSU-X1 spinning disk confocal head (Yokogawa, Herrsching, Germany), EmulsiFlex-C3 homogeniser (AVESTIN, Mannheim, Germany), Electrophoresis Power Supply EPS 301 (GE Healthcare Biosciences, USA), Eppendorf centrifuge 5417C, 5415R, Thermomixer Comfort (Eppendorf, Hamburg, Germany), Forma 900 freezer, Heraeus Function line incubator (Thermo Fisher Scientific, Bonn, Germany), Infors HT incubation shaker (Infors, Switzerland), LaserStack Launch (Intelligent Imaging Innovations, USA), MS-2000 stage (Applied Scientific Instrumentation, USA), LightCycler 480 (Roche Diagnostics GmbH, Mannheim, Germany), MUPID ONE electrophoresis unit (Advance Co., Japan), Nanodrop ND-1000 spectrophotometer (PEQLAB, Erlangen, Germany), Rotina 420R centrifuge (Hettich, Tuttlingen, Germany), SmartSpec 3000 spectrophotometer, C1000 thermal cycler, Mini-PROTEAN II electrophoresis system (Bio-Rad Laboratories, Munich, Germany), Vortex Genie 2, Disruptor Genie, Roto-Shake Genie (Scientific industries, USA), X-ray film processor MI-5 (Medical Index, Bad Rappenau, Germany).

If not stated otherwise, following commercially available kits were used for the purification of plasmids and DNA fragments:

AccuPrep® Plasmid Mini Extraction kit (Bioneer, Republic of Korea), Amersham ECL Prime™ kit (GE Healthcare Biosciences, USA), QIAquick® Gel Extraction kit, QIAquick® PCR Purification kit, QIAprep® Spin Miniprep kit (all QIAGEN, Hilden, Germany).

5.1.2 Enzymes

Calf intestine alkaline phosphatase (CIP, 10 U/μl), λ-phosphatase (400 U/μl), restriction endonucleases (ApaI (50 U/μl), AvrII (4 U/μl), BamHI (20 U/μl), ClaI (10 U/μl), DpnI (20 U/μl), EcoRI (20 U/μl), HindIII (20 U/μl), KpnI (10 U/μl), Nhe (10 U/μl), SacII (20 U/μl), SmaI (20 U/μl), SphI (10 U/μl), StuI (10 U/μl), XhoI (20 U/μl)), T4 DNA ligase (400 U/μl) (all NEB, Frankfurt, Germany), *Ex Taq*™ DNA polymerase (5 U/μl) (TaKaRa Bio Inc., Japan), Fast Digest restriction endonucleases (BamHI, EcoRI, HindIII, *XhoI*), *Pfu* DNA polymerase (2.5 U/μl) (all Fermentas, St. Leon-Rot, Germany), *PfuTurbo* DNA polymerase (Agilent Technologies, La Jolla, USA), Proteinase K (Sigma-Aldrich, Taufkirchen, Germany).

5.1.3 Oligonucleotides

All oligonucleotides used in this study were produced by Eurofins MWG Operon (Ebersberg, Germany).

Table 2. Complete list of oligonucleotides, which were used for quantitative real-time PCR (qPCR), cloning, site-directed mutagenesis, sequencing, amplification of DNA fragments for genomic integration and colony PCR. Lower case letters indicate the overhang containing the respective restriction site.

Nr.	Primer	Sequence	Purpose
1	CEN1_for	AGCACTAGGCGGTGGACCTTAT	qPCR: CEN1
2	CEN1_rev	AAAACACCCGAGGCAGCAGA	qPCR: CEN1
3	CEN4_3_for	AATTGGTCTCGAAATAGAAATTGGGCCT	qPCR: CEN4
4	CEN4_3_rev	TTAGACCATTCTATAACAACCTCAGCTATGT	qPCR: CEN4
5	SFI1_for	GACGCTAATGCATATTGATAATGTTTCATTT	qPCR: CEN12
6	SFI1_rev	CTTTCTCTAAATTTCTTCAGCACCATTTTT	qPCR: CEN12
7	NTS1_2_for	AGTTTCTAGGGAATGATGATGGCAA	qPCR: rDNA
8	NTS1_2_rev	TCCGGTTTTGTTCTCTTCCCTCCAT	qPCR: rDNA
9	control_for	GCGTGCCTGGTCACAGGTTTCATACGAC	qPCR: control
10	control_rev	TCATACGGCCCAAATATTTACGTCCC	qPCR: control
11	5'-TAP-AvrII	cgccctaggGGTCGACGGATCCCC	cloning: plasmid Nr. 3
12	3'-TAP-HindIII	cccaagcttTCACTGATGATTGCGGT	cloning: plasmid Nr. 3, 4

13	5'- <i>P_{SGO1}</i> -SacII	tccccgcggAATGATTTAGTTTCCC	cloning: plasmid 4
14	3'- <i>P_{SGO1}</i> -SmaI	cgccccgggGGTCAAACAATAACCCCTC	cloning: plasmid 4
15	5'- <i>sgo1</i> ΔC-SmaI	cgccccgggATGATAGAACTGAAGAAAAAGG	cloning: plasmid 4
16	3'- <i>sgo1</i> ΔC-XhoI	cgcctcgagTTTTTTGGTGCGATATGTT	cloning: plasmid 4
17	5'-TAP-XhoI	ccgctcgagGGTCGACGGATCCCC	cloning: plasmid 4, 12
18	5'- <i>sgoB</i> -AvrII	cgccctaggATAGAACTGAAGAAAAAGGT	cloning: plasmid 5
19	3'- <i>sgoB</i> -AvrII	gcgcctaggTCTTCTAGTTCTCGTAAATG	cloning: plasmid 5
20	5'- <i>sgoC</i> -AvrII	cgccctaggTCAGAAAACTTGTGGATGC	cloning: plasmid 6, 8
21	3'- <i>sgoC</i> -AvrII	gcgcctaggAAGTAAAGGCGACGATTTTT	cloning: plasmid 6
22	5'- <i>sgoD</i> -AvrII	cgccctaggGACATTACAAATAAATCGGA	cloning: plasmid 7
23	3'- <i>sgoD</i> -AvrII	gcgcctaggTTTTTTGGTGCGATATGTTT	cloning: plasmid 7, 8
24	5'- <i>P_{ADH1}</i> -SacII	gcgccgcggGAGCTCGCCGGGATCGAAGA	cloning: plasmid 9
25	3'- <i>P_{ADH1}</i> -SmaI	gcgccgggTCCGGGGGGGATCCACTAGT	cloning: plasmid 9
26	5'- <i>P_{GAL1}</i> -SacII	tccccgcggTGGAACCTTCAGTAATACG	cloning: plasmid 12, 15, 16, 22
27	3'- <i>P_{GAL1}</i> -BamHI	cgggatccCGTATAGTTTTTTCTCCTTGAC	cloning: plasmid 12, 15, 16, 22
28	5'- <i>cik1-cc</i> -ClaI	cgcctcgatATGATTGAAAGGGTTAAGAACAA	cloning: plasmid 12
29	3'- <i>cik1-cc</i> -XhoI	gcgctcgagTTCCTGTTGAACCTTTTCTA	cloning: plasmid 12
30	3'-TAP-KpnI	ccgggtaccTCACTGATGATTGCGGT	cloning: plasmid 12
31	5'-GST-EcoRI	cgcaagcttATGTCCCCTATACTAGGTT	cloning: plasmid 15
32	3'-GST-HindIII	cgcaagcttAGATCCACGCGGAACCAGA	cloning: plasmid 15
33	5'- <i>MPS1</i> -HindIII	cgcaagcttATGTCAACAACTCATTCC	cloning: plasmid 15
34	3'- <i>MPS1</i> -XhoI	gccctcgagCTAAATTTTGTAACTGCAA	cloning: plasmid 15
35	5'-myc ₉ -EcoRI	cgcaagcttATGTCCGGTTCTGCTGCTA	cloning: plasmid 16
36	3'-myc ₉ -HindIII	gcgaagcttGCTAGTGGATCCGTTCAAG	cloning: plasmid 16
37	5'-eGFP-XhoI	gcgctcgagGGAGCAGGTGCTGGTGCTGG	cloning: plasmid 22
38	3'-eGFP-ApaI	cgcgggcccTACTTGTACAGCTCGTCCA	cloning: plasmid 22
39	<i>sgo1</i> - L489,490A-for	GCCCTAAAAAATCGTCGCCTGCAGCTGACATT ACAAATAAATCGGA	mutagenesis: plasmid 10, 11
40	<i>sgo1</i> - L489,490A-rev	TCCGATTTATTTGTAATGTCAGCTGCAGGCGA CGATTTTTTAG	mutagenesis: plasmid 10, 11
41	<i>sgo1</i> ΔHB-for	TATCATTTACGAGAACTAGAAGATCAGAAAAA CTTGTGGATGCTAC	mutagenesis: plasmid 14
42	<i>sgo1</i> ΔHB-rev	GTAGCATCCACAAGTTTTTCTGATCTTCTAGTT CTCGTAAATGATA	mutagenesis: plasmid 14
43	<i>sgo1</i> -N51I-for	GTCGTATTCGAGGCAAatcTCCCTGCTGGCCA AGGAT	mutagenesis: plasmid 20, 21
44	<i>sgo1</i> -N51I-rev	CTTGGCCAGCAGGGAgaTTGCCTCGAATACG ACTGT	mutagenesis: plasmid 20, 21
45	seq1-SGO1	CACACGCATATATATGTTT	sequencing: SGO1

46	seq2-SGO1	CAGAATCACACGAGTC	sequencing: SGO1
47	seq3-SGO1	GTCGTCTCAAAGGATTATGG	sequencing: SGO1
48	seq- <i>P_{GAL1}</i>	AAAAGTATCAACAAAAAATT	sequencing
49	seq2-MPS1	TGAGGATTCTCACCAAAC	sequencing
50	seq3-MPS1	ATTTTACCATCGACCTGC	sequencing
51	seq4-MPS1	TGGGACTCCAAATTATAT	sequencing
52	seq-pET-21b	CCCTCTAGAAATAATTTTGT	sequencing
53	seq-TAP-rev	AGACGGCTATGAAATTCT	sequencing
54	<i>mad2Δ</i> _for	TCGTACAAGAGTATTGAAAACCACTTCAAAGG GGCCAATAGCACATTTAagattgtactgagagtgcac	PCR: gene deletion
55	<i>mad2Δ</i> _rev	GAGATTTTTTTGGACTTCCGTCTTTTTTTTTTTT TTTGACTTGAATTCTActgtgcggtatttcacaccg	PCR: gene deletion
56	<i>rts1Δ</i> _for	ACTTATTAAGATCAATAGGCACGTGCTATTTTC GAACATCCACTTTCAATagattgtactgagagtgcag	PCR: gene deletion
57	<i>rts1Δ</i> _rev	GGCATGCCCTAAACTTCCTCACTTCTTCGAGC TTGTAATGAATTGCTGTTctgtgcggtatttcacaccg	PCR: gene deletion
58	<i>PDS1</i> -C-for	TGTACAGCGAAGAAGGCCTCGATCCTGAAGA ACTAGAGGACTTAGTTACTcgtacgctgcaggtcgac	PCR: epitope tagging
59	<i>PDS1</i> -C-rev	ATCTGTATATACGTGTATATATGTTGTGTGTAT GTGAATGAGCAGTGGATatcgtatgaattcgagctcg	PCR: epitope tagging
60	<i>RTS1</i> -C-for	ATAACACATTAAATGAAGAGAACGAAAATGAT TGTGACAGCGAGATACAGcgtacgctgcaggtcgac	PCR: epitope tagging
61	<i>RTS1</i> -C-rev	GGCATGCCCTAAACTTCCTCACTTCTTCGAGC TTGTAATGAATTGCTGTTatcgtatgaattcgagctcg	PCR: epitope tagging
62	<i>MCD1</i> -C-for	ATATTAAAATAGACGCCAAACCTGCACTATTT GAAAGGTTTATCAATGCTcgtacgctgcaggtcgac	PCR: epitope tagging
63	<i>MCD1</i> -C-rev	TGCATCAGCTTATTGGGTCCACCAAGAAATCC CCTCGGCGTAAGTAGGTTatcgtatgaattcgagctcg	PCR: epitope tagging
64	<i>SMC2</i> -C-for	GGGTCTTCAGGACGAGATTTCAAGATGGTAC CTCCGTAGTTAGTATAATGcgtacgctgcaggtcgac	PCR: epitope tagging
65	<i>SMC2</i> -C-rev	TTGAAATATGATTACATTACAATATTTATTTGTC TTATGAAAATAACCAatcgtatgaattcgagctcg	PCR: epitope tagging
66	<i>IPL1</i> -C-for	TGCATCCTTGATACTAAGAAACAAGCCCTTT TGGGAAAATAAGCGGTTAcgtacgctgcaggtcgac	PCR: epitope tagging
67	<i>IPL1</i> -C-rev	TGCGGGAGTGATTAATAGTGCCCTTCAAACGA TTCTGTCATACTTTAATTatcgtatgaattcgagctcg	PCR: epitope tagging
68	<i>sgo1Δ</i> C-C-for	CTAATTCTCATCCAAAGACCAAAATTAAGCATT CCATGAAGCCGCCTAGGcgtacgctgcaggtcgac	PCR: epitope tagging
69	TAP-C-rev	TTTTTCCATCTTCTCTTCATGGATTAATTAAC CCGGGGATCCGTCGACCatcgtatgaattcgagctcg	PCR: epitope tagging
70	<i>MAD2</i> -800up	CTTGTCAAGACTTTTATTAG	colony PCR

71	<i>MAD2</i> -300down	TTGGTCAAAATTTGTGAGGC	colony PCR
72	<i>RTS1</i> -800up	CACGACTTGACTGTGAGGAA	colony PCR
73	<i>RTS1</i> -300down	AAGAAAAACGAAGATATATTTTGAGA	colony PCR

5.1.4 Plasmids

Table 3. Complete list of plasmids generated for expression of recombinant proteins in *E. coli* and shuttle vectors for yeast transformation.

Nr.	Plasmid	Description	Source
1	pRS405- <i>P_{SGO1}</i> - <i>SGO1</i> -TAP	yeast integrative (YI) plasmid for the expression of TAP-tagged Sgo1	K. Peplowska
2	pRS406- <i>P_{SGO1}</i> - <i>sgo1</i> ΔC-TAP	YI plasmid for the expression of C-terminally truncated Sgo1ΔC-TAP (amino acids 1–340)	this study
3	pRS405- <i>P_{SGO1}</i> - <i>sgo1</i> ΔC-TAP	YI plasmid for the expression of C-terminally truncated Sgo1ΔC-TAP (amino acids 1–340)	this study
4	RS406- <i>P_{SGO1}</i> - <i>sgo1</i> ΔN-TAP	YI plasmid for the expression of N-terminally truncated Sgo1ΔC-TAP (amino acids 341–590)	this study
5	pRS405- <i>P_{SGO1}</i> - <i>sgo1</i> ΔC+B-TAP	YI plasmid for the expression of a TAP-tagged Sgo1 fragment (amino acids 1–370)	this study
6	pRS405- <i>P_{SGO1}</i> - <i>sgo1</i> ΔC+C-TAP	YI plasmid for the expression of a TAP-tagged Sgo1 fragment (amino acids 1–340 + 391–490)	this study
7	pRS405- <i>P_{SGO1}</i> - <i>sgo1</i> ΔC+D-TAP	YI plasmid for the expression of a TAP-tagged Sgo1 fragment (amino acids 1–340 + 491–590)	this study
8	pRS405- <i>P_{SGO1}</i> - <i>sgo1</i> ΔC+CD-TAP	YI plasmid for the expression of a TAP-tagged Sgo1 fragment (amino acids 1–340 + 391–590)	this study
9	pRS316- <i>P_{ADH1}</i> - <i>sgo1</i> ΔN-TAP	yeast centromeric (YC) plasmid for the overexpression of a TAP-tagged Sgo1 fragment (amino acids 341–590)	this study
10	pRS316- <i>P_{ADH1}</i> - <i>sgo1</i> ΔN L489,490A-TAP	YC plasmid for the overexpression of a non-degradable, TAP-tagged Sgo1 fragment (amino acids 341–590)	this study
11	pRS405- <i>P_{SGO1}</i> - <i>sgo1</i> L489,490A-TAP	YI plasmid for the expression of a non-degradable, TAP-tagged Sgo1 mutant	this study

12	pRS406- <i>P_{GAL1}-cik1-cc-TAP</i>	YI plasmid for the inducible overexpression of the TAP-tagged coiled-coil domain of Cik1 (amino acids 81–360)	this study
13	pRS405- <i>P_{SGO1}-sgo1</i> T379D-TAP	YI plasmid for the expression of a mislocalized, TAP-tagged Sgo1 mutant	K. Peplowska
14	pRS405- <i>P_{SGO1}-sgo1ΔHB-</i> TAP	YI plasmid for the expression of a mislocalized, TAP-tagged Sgo1 mutant (internal deletion of amino acids 371–390)	this study
15	pRS406- <i>P_{GAL1}-GST-MPS1</i>	YI plasmid for the inducible overexpression of GST-tagged Mps1	this study
16	pRS406- <i>P_{GAL1}-myc₉-MPS1</i>	YI plasmid for the inducible overexpression of myc-tagged Mps1	this study
17	pET-21b- <i>sgo1ΔC</i>	bacterial expression plasmid for the heterologous expression of a His ₆ -tagged Sgo1 fragment (amino acids 1–340) in <i>E. coli</i>	K. Peplowska
18	pET-21b- <i>sgo1ΔC</i> N51I	bacterial expression plasmid for the expression of a His ₆ -tagged, mutant Sgo1 fragment (amino acids 1–340) in <i>E. coli</i>	K. Peplowska
19	pRS405- <i>P_{SGO1}-sgo1</i> N51I- TAP	YI plasmid for the expression of a TAP-tagged Sgo1 mutant defective in PP2A binding	K. Peplowska
20	pRS405- <i>P_{SGO1}-sgo1ΔC</i> N51I-TAP	YI plasmid for the expression of a TAP-tagged Sgo1 fragment defective in PP2A binding (amino acids 1–340)	this study
21	pRS405- <i>P_{SGO1}-sgo1</i> N51I,T379D-TAP	YI plasmid for the expression of a mislocalized, TAP-tagged Sgo1 mutant defective in PP2A binding	this study
22	pRS403- <i>P_{GAL1}-cik1-cc-</i> eGFP	YI plasmid for the inducible overexpression of the eGFP-tagged coiled-coil domain of Cik1 (amino acids 81–360)	this study
23	pRS425- <i>SLI15</i>	yeast episomal (YE) plasmid for constitutive overexpression of Sli15	Storchová <i>et al.</i> , 2011
24	pRS403	empty YI plasmid used for cloning	Sikorski & Hieter, 1989
25	pRS405	empty YI plasmid used for cloning	Sikorski & Hieter, 1989
26	pRS406	empty YI plasmid used for cloning	Sikorski & Hieter, 1989
27	pRS316	empty YC plasmid used for cloning	Sikorski & Hieter, 1989

28	pRS425	empty YE plasmid used for cloning	Christianson <i>et al.</i> , 1992
29	pYM13	template plasmid for genomic tagging of yeast proteins with TAP	Janke <i>et al.</i> , 2004
30	pYM15	template plasmid for genomic tagging of yeast proteins with HA ₆	Janke <i>et al.</i> , 2004
31	pYM21	template plasmid for genomic tagging of yeast proteins with myc ₉	Janke <i>et al.</i> , 2004
32	pYM28	template plasmid for genomic tagging of yeast proteins with eGFP	Janke <i>et al.</i> , 2004
33	pBF83	modified template plasmid for genomic tagging of yeast proteins with 3xFLAG	gift from B. Pfander
34	pET-21b	empty bacterial expression plasmid	Millipore

5.1.5 Bacterial strains and culture conditions

Bacteria were cultivated at 37 °C either in liquid lysogeny broth (LB) media (1.0% (w/v) tryptone, 0.5% (w/v) NaCl, 0.5% yeast extract) with constant shaking or on LB agar plates (1.5% (w/v) agar) in LB media). LB media were supplemented with 50 µg/ml ampicillin in order to select for transformed bacteria cells. Bacteria cells grown on LB selection media were usually stored for up to 14 days at 4 °C. For long-term storage at –80 °C, bacteria cells containing the desired plasmid were grown to stationary phase in liquid cultures and glycerol was added to a final concentration of 15% (v/v).

Table 4. Summary of *Escherichia coli* strains used as host organism for amplification as well as long-term storage of plasmid DNA (XL1-Blue) and protein expression (BL21(DE3)).

<i>E. coli</i> strain	Genotype	Source
XL1-Blue	<i>recA1 endA1 gyrA96 thi-1 hsdR17 supE44 relA1 lac</i> [F' <i>proAB lacIqZDM15 Tn10</i> (Tet ^r)]	Stratagene
BL21(DE3)	B F [–] <i>ompT hsdS</i> (rB [–] mB [–]) <i>dcm</i> ⁺ Tet ^r <i>gal</i> λ (DE3) <i>endA</i> Hte	Stratagene

5.1.6 Yeast strains and culture conditions

Yeast cells were cultured either in full-medium (YP) or synthetic complete (SC) medium. Full-medium contained 1% yeast extract, 2% bactopectone and 2% of glucose, galactose or raffinose as carbon source (YPD/YPG/YPR). Synthetic complete media contained 0.67% yeast nitrogen base, 0.02%

complete synthetic mix (including all essential amino acids and uracil as well as adenine except the respective ones used as auxotrophy marker) and 2% glucose, galactose or raffinose (SDC/SGC/SRC). YP or SC selection plates were prepared by the addition of agar to a final concentration of 2% to the corresponding media before autoclaving. Yeast strains containing the drug resistance marker genes *kanMX4*, *hphNT1* or *natNT2* were selected on YPD plates supplemented with 200 mg/l geniticine disulfate (G418), 500 mg/l hygromycin B (Hph) and 100 mg/l nourseothricin (NAT), respectively. When necessary, 5'-Fluoroorectic acid was added to a final concentration of 0.1% (w/v).

Yeast strains streaked on selection plates were stored up to 14 days at 4 °C. Freshly grown yeast cells were frozen in 15% (v/v) glycerol solutions for long-term storage at –80 °C. Single yeast colonies from selection plates were used to inoculate liquid yeast cultures for experiments. Liquid yeast cultures and agar plates were usually incubated at 30 °C, except strains lacking Sgo1 or expressing *sgo1* mutants, which were incubated at room temperature to reduce the frequency of chromosome loss (Indjeian *et al.*, 2005). For experiments, yeast cells were usually grown to mid-log phase and the density of the corresponding cultures was determined photometrically (OD₆₀₀ ranging from 0.6 to 1.5).

All yeast strains used in this study are listed in Table 5 and derived from the genetic background of W303 (*leu2-3, 112 trp1-1 can1-100 ura3-1 ade2-1 his3-11,15*) or BY4741 (*his3Δ1 leu2Δ0 met15Δ0 ura3Δ0*).

Table 5. Summary of the relevant genotypes of all yeast strains used or generated in this study. Numbers in brackets denote the corresponding plasmid used for yeast transformation (see Table 3).

Strain	Background	Relevant genotype	Source	Figure
YZ1254	W303	<i>MATa sgo1::hphNT1</i> pRS405- <i>LEU2-P_{SGO1}</i> - SGO1-TAP (Nr. 1) pRS406- <i>URA3-P_{SGO1}</i> - <i>sgo1ΔC</i> -TAP (Nr. 2)	this study	6A
YZ1239	W303	<i>MATa sgo1::hphNT1</i> pRS405- <i>LEU2-P_{SGO1}</i> - <i>sgo1ΔC</i> -TAP (Nr. 3) <i>sgo1ΔC</i> -eGFP:: <i>HIS3MX6</i>	this study	6B
152	W303	<i>MATa sgo1::hphNT1</i> pRS405- <i>LEU2-P_{SGO1}</i> - SGO1-TAP (Nr. 1) SGO1-eGFP- <i>HIS3MX6</i> SPC29-RFP- <i>kanMX4</i>	K. Peplowska	6B; 10A
YZ1262	W303	<i>MATa sgo1::hphNT1</i> pRS405- <i>LEU2-P_{SGO1}</i> - SGO1-TAP (Nr. 1) pRS406- <i>URA3-P_{SGO1}</i> - <i>sgo1ΔN</i> -TAP (Nr. 4)	this study	6C
145	W303	<i>MATa sgo1::hphNT1</i> pRS405- <i>LEU2-P_{SGO1}</i> - <i>sgo1ΔC</i> -TAP (Nr. 3)	this study	7B
YZ1345	W303	<i>MATa sgo1::hphNT1</i> pRS405- <i>LEU2-P_{SGO1}</i> - <i>sgo1ΔC</i> +B-TAP (Nr. 5)	this study	7B
YZ1346	W303	<i>MATa sgo1::hphNT1</i> pRS405- <i>LEU2-P_{SGO1}</i> - <i>sgo1ΔC</i> +C-TAP (Nr. 6)	this study	7B

YZ1347	W303	<i>MATa sgo1::hphNT1</i> pRS405- <i>LEU2-P_{SGO1}</i> - <i>sgo1</i> ΔC+D-TAP (Nr. 7)	this study	7B
YZ1348	W303	<i>MATa sgo1::hphNT1</i> pRS405- <i>LEU2-P_{SGO1}</i> - <i>sgo1</i> ΔC+CD-TAP (Nr. 8)	this study	7B
YZ1339	W303	<i>MATa</i> pRS416- <i>URA3-P_{ADH1}</i> - <i>sgo1</i> ΔN-TAP (Nr. 9)	this study	8A
YZ1366	W303	<i>MATa</i> pRS416- <i>URA3-P_{ADH1}</i> - <i>sgo1</i> ΔN L489,490A-TAP (Nr. 10)	this study	8A
189	W303	<i>MATa sgo1::hphNT1</i> pRS405- <i>LEU2-P_{SGO1}</i> - <i>SGO1</i> -TAP (Nr. 1) <i>PDS1-myc₉::HIS3MX6</i>	K. Peplowska	8B
YZ1510	W303	<i>MATa sgo1::hphNT1</i> pRS405- <i>LEU2-P_{SGO1}</i> - <i>sgo1</i> L489,490A-TAP (Nr. 11) <i>PDS1-myc₉::HIS3MX6</i>	this study	8B
YZ1507	W303	<i>MATa</i> pRS406- <i>URA3-P_{GAL1}</i> - <i>cik1</i> -cc-TAP (Nr. 12)	this study	9A; 21A; 24
YZ1360	W303	<i>MATa sgo1::hphNT1</i> pRS406- <i>URA3-P_{GAL1}</i> - <i>cik1</i> -cc-TAP (Nr. 12)	this study	9A; 15A; 19A, B
YZ1410	W303	<i>MATa sgo1::hphNT1</i> pRS405- <i>LEU2-P_{SGO1}</i> - <i>sgo1</i> L489,490A-TAP (Nr. 11) pRS406- <i>URA3-P_{GAL1}</i> - <i>cik1</i> -cc-TAP (Nr. 12)	this study	9A, B
YZ1359	W303	<i>MATa sgo1::hphNT1</i> pRS405- <i>LEU2-P_{SGO1}</i> - <i>SGO1</i> -TAP (Nr. 1) pRS406- <i>URA3-P_{GAL1}</i> - <i>cik1</i> -cc-TAP (Nr. 12)	this study	9B; 15A; 19A, B; 23
151	W303	<i>MATa sgo1::hphNT1</i> pRS405- <i>LEU2-P_{SGO1}</i> - <i>sgo1</i> T379D-TAP (Nr. 13) <i>sgo1</i> T379D-eGFP- <i>HIS3MX6</i> <i>SPC29-RFP-kanMX4</i>	K. Peplowska	10A
116	W303	<i>MATa sgo1::hphNT1</i> pRS405- <i>LEU2-P_{SGO1}</i> - <i>SGO1</i> -TAP (Nr. 1)	K. Peplowska	10B; 11A, B; 14A; 16A
69	W303	<i>MATa sgo1::hphNT1</i>	K. Peplowska	10B; 11A; 14A, 16A
118	W303	<i>MATa sgo1::hphNT1</i> pRS405- <i>LEU2-P_{SGO1}</i> - <i>sgo1</i> T379D-TAP (Nr. 13)	K. Peplowska	10B; 11A
YZ1327	W303	<i>MATa sgo1::hphNT1</i> pRS405- <i>LEU2-P_{SGO1}</i> - <i>sgo1</i> ΔHB-TAP (Nr. 14)	this study	10B
YZ1271	W303	<i>MATa sgo1::hphNT1</i> pRS405- <i>LEU2-P_{SGO1}</i> - <i>SGO1</i> -TAP (Nr. 1) pRS406- <i>URA3-P_{GAL1}</i> - <i>GST-MPS1</i> (Nr. 15)	this study	11A–C; 16B
YZ1272	W303	<i>MATa sgo1::hphNT1</i> pRS406- <i>URA3-P_{GAL1}</i> - <i>GST-MPS1</i> (Nr. 15)	this study	11A, B; 16B
YZ1274	W303	<i>MATa sgo1::hphNT1</i> pRS405- <i>LEU2-P_{SGO1}</i> - <i>sgo1</i> T379D-TAP (Nr. 13) pRS406- <i>URA3-P_{GAL1}</i> - <i>GST-MPS1</i> (Nr. 15)	this study	11A–C; 16B

YZ1328	W303	<i>MATa sgo1::hphNT1</i> pRS405- <i>LEU2-P_{SGO1}</i> - <i>sgo1</i> ΔHB-TAP (Nr. 14) pRS406- <i>URA3-P_{GAL1}</i> - <i>myc₉-MPS1</i> (Nr. 16)	this study	11B; 16B
YZ1335	W303	<i>MATa sgo1::hphNT1</i> pRS405- <i>LEU2-P_{SGO1}</i> - <i>sgo1</i> ΔC-TAP (Nr. 3) pRS406- <i>URA3-P_{GAL1}</i> - <i>myc₉-MPS1</i> (Nr. 16)	this study	11B
YZ1287	W303	<i>MATa sgo1::hphNT1</i> pRS405- <i>LEU2-P_{SGO1}</i> - <i>SGO1</i> -TAP (Nr. 1) pRS406- <i>URA3-P_{GAL1}</i> - <i>GST-MPS1</i> (Nr. 15) <i>mad2::kanMX4</i>	this study	11C
YZ1281	W303	<i>MATa sgo1::hphNT1</i> pRS405- <i>LEU2-P_{SGO1}</i> - <i>sgo1</i> T379D-TAP (Nr. 13) pRS406- <i>URA3-P_{GAL1}</i> - <i>GST-MPS1</i> (Nr. 15) <i>mad2::kanMX4</i>	this study	11C
284	W303	<i>MATa sgo1::hphNT1</i> <i>pPPH22::natNT2-pADH1-HA₃ TPD3-myc₉::HIS3MX6</i> <i>RTS1</i> -TAP:: <i>TRP1</i>	K. Peplowska	12
YZ1471	W303	<i>MATa RTS1</i> -FLAG:: <i>natNT2</i>	this study	13A, B
YZ1472	W303	<i>MATa sgo1::hphNT1</i> <i>RTS1</i> -FLAG:: <i>natNT2</i>	this study	13A, B
343	W303	<i>MATa sgo1::hphNT1</i> <i>RTS1</i> -eGFP- <i>HIS3MX6</i> pRS405- <i>LEU2-P_{SGO1}</i> - <i>SGO1</i> -TAP- <i>LEU2</i> (Nr. 1) <i>SPC29</i> -RFP- <i>natNT2</i>	K. Peplowska	13C
344	W303	<i>MATa sgo1::hphNT1</i> <i>RTS1</i> -eGFP:: <i>HIS3MX6</i> pRS405- <i>LEU2-P_{SGO1}</i> - <i>sgo1</i> N51I-TAP <i>SPC29</i> -RFP- <i>natNT2</i>	K. Peplowska	13C
174	W303	<i>MATa sgo1::hphNT1</i> pRS405- <i>LEU2-P_{SGO1}</i> - <i>sgo1</i> N51I-TAP (Nr. 19)	K. Peplowska	14A
YZ1298	W303	<i>MATa rts1::kanMX4</i>	this study	14A
YZ1383	W303	<i>MATa sgo1::hphNT1</i> pRS405- <i>LEU2-P_{SGO1}</i> - <i>SGO1</i> -TAP (Nr. 1) pRS406- <i>URA3-P_{GAL1}</i> - <i>cik1-cc</i> -TAP (Nr. 12) <i>PDS1</i> -HA6:: <i>HIS3MX6</i>	this study	14B; 15B
YZ1385	W303	<i>MATa rts1::kanMX4</i> pRS406- <i>URA3-P_{GAL1}</i> - <i>cik1-cc</i> -TAP (Nr. 12) <i>PDS1</i> -HA6:: <i>HIS3MX6</i>	this study	14B; 15B
YZ1361	W303	<i>MATa rts1::kanMX4</i> pRS406- <i>URA3-P_{GAL1}</i> - <i>cik1-cc</i> -TAP (Nr. 12)	this study	15A; 19A
YZ1364	W303	<i>MATa sgo1::hphNT1</i> pRS405- <i>LEU2-P_{SGO1}</i> - <i>sgo1</i> N51I-TAP (Nr. 19) pRS406- <i>URA3-P_{GAL1}</i> - <i>cik1-cc</i> -TAP (Nr. 12)	this study	15A
145	W303	<i>MATa sgo1::hphNT1</i> pRS405- <i>LEU2-P_{SGO1}</i> - <i>sgo1</i> ΔC-TAP (Nr. 3)	this study	16A
YZ1259	W303	<i>MATa sgo1::hphNT1</i> pRS405- <i>LEU2-P_{SGO1}</i> - <i>sgo1</i> ΔC N51I-TAP (Nr. 20)	this study	16A

YZ1273	W303	<i>MATa sgo1::hphNT1</i> pRS405- <i>LEU2-P_{SGO1}-sgo1</i> N51I-TAP (Nr. 19) pRS406- <i>URA3-P_{GAL1}-GST-MPS1</i> (Nr. 15)	this study	16B
YZ1314	W303	<i>MATa sgo1::hphNT1</i> pRS405- <i>LEU2-P_{SGO1}-sgo1</i> N51I, T379D-TAP (Nr. 21) pRS406- <i>URA3-P_{GAL1}-GST-MPS1</i> (Nr. 15)	K. Peplowska	16B
YZ1473	W303	<i>MATa MCD1-FLAG::natNT2</i>	this study	17A, B
YZ1474	W303	<i>MATa sgo1::hphNT1 MCD1-FLAG::natNT2</i>	this study	17A, B
YZ1442	W303	<i>MATa SMC2-FLAG::natNT2</i>	this study	18A, B, C
YZ1443	W303	<i>MATa sgo1::hphNT1 SMC2-FLAG::natNT2</i>	this study	18A, C
YZ1488	W303	<i>MATa rts1::kanMX4 SMC2-FLAG::natNT2</i>	this study	18B, C
YZ1414	W303	<i>MATa brn1-539-HA₃ ycg1-488-HA₃ ycs4-543-MYC₁₃ cdc15-2</i> pRS403- <i>HIS3-P_{GAL1}-cik1-cc-eGFP</i> (Nr. 22)	this study	19A
YZ1418	W303	<i>MATa smc2-8</i> pRS406- <i>URA3-P_{GAL1}-cik1-cc-TAP</i> (Nr. 12)	this study	19A
YZ1419	W303	<i>MATa ycg1-10</i> pRS406- <i>URA3-P_{GAL1}-cik1-cc-TAP</i> (Nr. 12)	this study	19A
YZ1423	BY4741	<i>MATa csm1::kanMX4</i> pRS406- <i>URA3-P_{GAL1}-cik1-cc-TAP</i> (Nr. 12)	this study	19B
YZ1424	BY4741	<i>MATa lrs4::kanMX4</i> pRS406- <i>URA3-P_{GAL1}-cik1-cc-TAP</i> (Nr. 12)	this study	19B
YZ1222	BY4741	<i>MATa his3::TetR-GFP-HIS3 CENIV::TetO-URA3 sgo1::hphNT1</i> pRS405- <i>LEU2-P_{SGO1}-SGO1-TAP-LEU2</i> (Nr. 1) <i>SPC29-RFP::kanMX4</i>	Z. Storchova	20
YZ1226	BY4741	<i>MATa his3::TetR-GFP-HIS3 CENIV::TetO-URA3 sgo1::hphNT1 SPC29-RFP::kanMX4</i>	Z. Storchova	20
YZ1227	BY4741	<i>MATa his3::TetR-GFP-HIS3 CENIV::TetO-URA3 sgo1::hphNT1</i> pRS405- <i>LEU2-P_{SGO1}-sgo1</i> N51I-TAP (Nr. 19) <i>SPC29-RFP::kanMX</i>	Z. Storchova	20
386	BY4741	<i>MATa his3::TetR-GFP-HIS3 CENIV::TetO-URA3 rts1::natNT2 SPC29-RFP::kanMX</i>	K. Peplowska	20
YZ1511	W303	<i>MATa ipl1-321</i> pRS406- <i>URA3-P_{GAL1}-cik1-cc-TAP</i> (Nr. 12)	this study	21A
YZ1512	W303	<i>MATa glc7-10</i> pRS406- <i>URA3-P_{GAL1}-cik1-cc-TAP</i> (Nr. 12)	this study	21A
YZ169	W303	<i>MATa ipl1-321</i>	S. Biggins	21B
W303	W303	<i>MATa</i>		21B
YZ1444	W303	<i>MATa IPL1-FLAG::natNT2</i>	this study	22A–C
YZ1453	W303	<i>MATa sgo1::hphNT1 IPL1-FLAG::natNT2</i>	this study	22A, C
YZ1489	W303	<i>MATa rts1::kanMX4 IPL1-FLAG::natNT2</i>	this study	22B, C

YZ1425	W303	<i>MATa sgo1::hphNT1</i> pRS406- <i>URA3-P_{GAL1}-cik1-cc-TAP</i> (Nr. 12) [2μ, <i>LEU2</i> , <i>SLI15</i>] (Nr. 23)	this study	23
YZ1476	W303	<i>MATa sgo1::hphNT1</i> pRS406- <i>URA3-P_{GAL1}-cik1-cc-TAP</i> (Nr. 12) [2μ, <i>LEU2</i>]	this study	23
YZ1475	W303	<i>MATa rts1::kanMX4</i> pRS406- <i>URA3-P_{GAL1}-cik1-cc-TAP</i> (Nr. 12) [2μ, <i>LEU2</i> , <i>SLI15</i>] (Nr. 23)	this study	23
YZ1477	W303	<i>MATa rts1::kanMX4</i> pRS406- <i>URA3-P_{GAL1}-cik1-cc-TAP</i> (Nr. 12) [2μ, <i>LEU2</i>]	this study	23
YZ1433	W303	<i>MATa smc2-8</i> pRS406- <i>URA3-P_{GAL1}-cik1-cc-TAP</i> (Nr. 12) [2μ, <i>LEU2</i> , <i>SLI15</i>] (Nr. 23)	this study	24
YZ1432	W303	<i>MATa smc2-8</i> pRS406- <i>URA3-P_{GAL1}-cik1-cc-TAP</i> (Nr. 12) [2μ, <i>LEU2</i>]	this study	24
YZ1435	W303	<i>MATa ycg1-10</i> pRS406- <i>URA3-P_{GAL1}-cik1-cc-TAP</i> (Nr. 12) [2μ, <i>LEU2</i> , <i>SLI15</i>] (Nr. 23)	this study	24
YZ1434	W303	<i>MATa ycg1-10</i> pRS406- <i>URA3-P_{GAL1}-cik1-cc-TAP</i> (Nr. 12) [2μ, <i>LEU2</i>]	this study	24

5.1.7 Antibodies

Table 6: Summary of applied antibodies, their sources and used dilutions.

	Source	Dilution	Company
<i>Primary antibodies</i>			
anti-GST (GTX70195)	mouse	1:5000	GeneTex
anti-Pgk1	mouse	1:1000	Invitrogen
anti-H3 (pAB)	rabbit	1:5000	Active Motif
anti-phosphorylated H3 (serine 10)	mouse	1:1000	Millipore
anti-Cdc20 (sc-6730)	goat	1:500	Santa Cruz Biotechnology
anti-Clb2 (sc-9071)	rabbit	1:500	Santa Cruz Biotechnology
anti-FLAG (M2)	mouse	1:1000	Sigma-Aldrich
anti-HA (sc-805)	rabbit	1:2000	Santa Cruz Biotechnology
anti-myc (sc-40)	mouse	1:2000	Santa Cruz Biotechnology

Material and methods

Secondary antibodies

anti-mouse IgG-HRP	goat	1:20000	R&D Systems
anti-rabbit IgG-HRP	goat	1:20000	R&D Systems
anti-goat IgG-HRP	chicken	1:20000	R&D Systems

HRP-conjugated antibodies

PAP #1291	rabbit	1:2000	Sigma-Aldrich
-----------	--------	--------	---------------

5.2 Molecular biology methods

5.2.1 Polymerase chain reaction (PCR)

Selective amplification of DNA sequences for cloning was performed using polymerase chain reaction (PCR) according to standard laboratory procedures (Sambrook *et al.*, 1989). Standard PCRs were performed using either 5 U of *Ex Taq* (TaKaRa; 2 mM MgCl₂, 350 µM of each dNTP, 1 µM of each primer) or 2.5 U of *Pfu* DNA polymerase (Fermentas; 2 mM MgSO₄, 350 µM of each dNTP, 1 µM of each primer) in a total volume of 50 µl. All polymerases were applied in their manufacturer's buffer. In general, the thermocycler setup, which is stated in Table 7 was used and the duration of the elongation step was adjusted to the size of the amplified fragment.

DNA fragments for targeted gene deletion or epitope-tagging via homologous recombination were also amplified by PCR according to previously published protocols (Janke *et al.*, 2004; Knop *et al.*, 1999; Taxis & Knop, 2006). In general, 50 µl reactions with 5 U of *Ex Taq* (TaKaRa; 2 mM MgCl₂, 350 µM of each dNTP, 1 µM of each primer) and Primers Nr. 54–69 (see Table 2) were assembled and PCR was performed according to an optimized thermocycler setup for different selection markers (Janke *et al.*, 2004). PCR products were purified using the QIAquick® PCR Purification kit (QUIAGEN, Hilden, Germany) and subsequently transformed into competent budding yeast cells (see 5.2.8).

PCR was additionally used to verify the targeted disruption of *MAD2* and *RTS1* through the replacement of the corresponding open reading frame with the *kanMX4* resistance marker gene ("Colony PCR"). To this end, a small amount of freshly grown yeast cells from individual colonies was transferred to a PCR-tube and boiled for 1 min in a microwave. The cells were resuspended in 25 µl of PCR reaction mixture supplemented with 2.5 U of *Ex Taq* (TaKaRa; 2 mM MgCl₂, 350 µM of each dNTP, 1 µM of each primer) and primers Nr. 70–73. Colony PCR was performed using the thermocycler setup, which is summarized in Table 7, and the size of the resulting DNA fragments was analyzed by agarose gel electrophoresis (see 5.2.6).

Table 7. General thermocycler setup used for the amplification of DNA fragments

PCR step	Duration and temperature
Initial denaturing	2 min @ 95 °C
Denaturing step	1 min @ 95 °C
Annealing step	1 min @ 48 °C
Elongation step	1 min per 500 bp @ 72 °C (<i>Pfu</i>) or 1 min per 1000 bp @ 72 °C (<i>Ex Taq</i>)
Number of cycles	35
Final pol. step	10 min @ 72 °C

5.2.2 PCR-based introduction of point mutations

Individual point mutations or small internal deletions (60 bp in *sgo1*ΔHB; plasmid Nr. 14) were introduced by PCR-based strategy according to the Stratagene QuikChange™ Site-Directed Mutagenesis Kit (Agilent Technologies, La Jolla, USA). Template plasmids, which have been purified from *E. coli* cells, were amplified with self-complementary primers containing the desired point mutations (primers Nr. 39–44; see Table 2). Mutagenic PCR (2 mM MgSO₄, 250 μM of each dNTP, 0.25 μM of each primer) was performed in 25 μl reactions containing 1.25 U of *PfuTurbo* DNA polymerase (Agilent Technologies, La Jolla, USA) and the corresponding buffer according to the thermocycler setup, which is summarized in Table 8. The complete reaction was treated for 1 h at 37 °C with 20 U of the restriction endonuclease DpnI (NEB, Frankfurt, Germany), which selectively degrades the methylated template plasmid. 1 μl of this reaction was transformed into chemically competent *E. coli* cells (50 μl; see 5.2.7). Introduction of the corresponding point mutations or internal deletion of base pairs was verified by sequencing.

Table 8. Thermocycler setup used for the introduction of specific point mutations by PCR-based site-directed mutagenesis

PCR step	Duration and temperature
Initial denaturing	3 min @ 95 °C
Denaturing step	30 sec @ 95 °C
Annealing step	1 min @ 55 °C
Elongation step	1 min per 500 bp @ 68 °C
Number of cycles	19

5.2.3 Restriction hydrolysis

DNA molecules were cleaved with commercially available restriction endonucleases (see 5.1.2 Enzymes). In this study, restriction hydrolysis was performed either in preparative or analytical manner. For preparative purposes approximately 3 μg of extracted plasmid DNA or 10 μl of PCR product were digested using 10 U of conventional (NEB, Frankfurt, Germany) or 5 U of Fast Digest (Fermentas, St. Leon-Rot, Germany) restriction enzymes in a total volume of 20 μl. Restriction hydrolysis was performed in the corresponding buffer and the reactions were incubated for 2 h at 37 °C. Reactions with *Apal* or *SmaI* were first incubated for 1.5 h at 25 °C before the second enzyme was added. Subsequently, these reactions were incubated for additional 1.5 h at 37 °C. The insertion of the DNA molecules encoding additional fragments of *Sgo1* into plasmid Nr. 3 (pRS405-*P_{SGO1}*-*sgo1*ΔC-TAP) was performed by creating only one cut at the 3'-end of *sgo1*ΔC using *AvrII* (NEB, Frankfurt, Germany). In order to prevent restricted plasmid Nr. 3 from recircularization without the

corresponding inserts, it was treated for additional 30 min at 37 °C with 10 U of calf intestine alkaline phosphatase (CIP, NEB) to remove the phosphate groups at the free 5'-end. Thereby, the nucleophilic attack of the 3'-hydroxyl group to the α -phosphate group of the 5'-end is inhibited. The products of preparative restriction digest were subjected to electrophoretic separation on 1% agarose gels and the desired fragments were purified using the QIAquick® Gel Extraction kit according to the manufacturer's instructions.

In order to control the proper insertion of a cloned fragment into the desired plasmid analytical restriction hydrolysis was performed. To this end, 5 μ l of purified vector were digested with 5 U of conventional (NEB, Frankfurt, Germany) or 2.5 U of Fast Digest (Fermentas, St. Leon-Rot, Germany) restriction enzymes in a total volume of 10 μ l supplemented with the respective manufacturer's buffer. The same endonucleases, which were used for the initial cloning step, were applied and the size of the resulting fragments was analyzed by DNA agarose electrophoresis.

5.2.4 Ligation

The enzyme T4 DNA ligase was used to catalyze the formation of the phosphodiester bond between the hydroxyl group of the 3'- and the free α -phosphate group of the 5'-restriction site. Only free ends, which are either blunt or complementary to each other, can be connected through the formation of a covalent bond, which is catalyzed by the T4 DNA ligase. Ligation reactions were assembled with approx. 10 ng of digested vector and an excess of the corresponding insert in a molar ratio of 1:10. DNA fragments purified from agarose gels were incubated with 400 U of T4 DNA ligase (50 mM Tris/HCl pH 7.5, 10 mM MgCl₂, 1 mM ATP, 10 mM DTT) in a total volume of 20 μ l for 1 h at RT. The concentration of DNA fragments after restriction hydrolysis and extraction from agarose gels for ligation reactions was assessed according to the fluorescence intensity of the ethidium bromide stained band after electrophoresis (MassRuler DNA Ladder Mix, #SM0403, Fermentas, St. Leon-Rot, Germany). The complete ligation reaction was used for transformation into competent *E. coli* cells (see 5.2.8 Transformation of chemical competent *E. coli* cells).

5.2.5 Sequencing

Purified plasmids were sequenced by the Microchemistry Core Facility of the Max Planck Institute of Biochemistry using an ABI 3730 sequencer with the corresponding BigDye® Terminator v3.1 cycle sequencing kit. The resulting sequences were aligned to the sequences of corresponding wild type genes, obtained from the *Saccharomyces* Genome Database (<http://www.yeastgenome.org/>). The alignments of nucleotide sequences were performed using the BLAST (Basic Local Alignment Search Tool) tool (<http://www.ncbi.nlm.nih.gov/>).

5.2.6 DNA agarose electrophoresis

All DNA samples were subjected to electrophoretic separation on 1% (w/v) agarose gels in TAE buffer (40 mM Tris/HCl pH 8.0, 20 mM acetic acid, 2 mM EDTA). DNA agarose electrophoresis was performed with direct current at a constant voltage of 100 V for at least 30 min. Samples were loaded in TAE buffer supplemented with 10% (w/v) glycerol, 0.005% bromophenol blue and 0.005% xylene cyanol FF. Different DNA molecules are separated according to their size and conformation, which correlates to their velocity of migration through the network of polymerized agarose. In order to visualize the DNA fragments, agarose gels were prepared containing 0.01% (w/v) ethidium bromide as fluorescent dye, which intercalates into DNA. This intercalation shifts the wavelength for the maximal fluorescence of ethidium bromide and therefore, DNA-ethidium bromide adducts can be detected under UV light ($\lambda = 366$ nm). DNA markers of the GeneRuler (#SM0311) and MassRuler (#SM0403) series, respectively (all Fermentas, St. Leon-Rot, Germany) were used as molecular weight standards.

5.2.7 Purification of plasmid DNA from *E. coli*

To amplify plasmid DNA, 5 ml of liquid LB medium (supplemented with 50 μ g/ml ampicillin) were inoculated with cells from individual *E. coli* colonies in a sterile capped glass tube and incubated for at least 16 h at 37 °C. Cells were collected by centrifugation (2 min, 5000 g, RT) and plasmid DNA was extracted using the *AccuPrep*® Plasmid Mini Extraction kit (Bioneer, Republic of Korea) according to its instructions. Plasmid DNA was eluted in 50 μ l sterile, deionized water instead of the provided elution buffer.

5.2.8 Transformation of chemical competent *E. coli* cells

Bacteria in ice cold solutions containing calcium chloride show typically higher rates for DNA uptake compared to untreated cells and are therefore called chemical competent or CaCl₂-competent cells. The calcium cations supposedly compensate the negative charge of the DNA backbone, allowing approximation to charged phospholipids of the *E. coli* cell envelope (Hanahan, 1983). Aliquoted (100, 200 μ l) cell suspensions of the strains XL1-blue and BL21(DE) were stored at -80 °C after calcium chloride treatment. These aliquots were thawed on ice and 50 μ l of the suspension were transformed using approximately 100 ng of plasmid DNA or 20 μ l of ligation reactions. The mixtures were incubated for 20 min on ice. After a 1 min heat shock at 42°C the suspension was incubated for additional 2 min on ice, so that the cells can take up the plasmids. 1 ml LB-media was added and the transformed cells were recovered for 45 min at 37 °C. Subsequently, these cells were collected by centrifugation (2 min, 5000 g, RT), resuspended in 100 μ l sterile water and plated on selection plates containing ampicillin and grown overnight at 37 °C.

5.2.9 Transformation of *S. cerevisiae*

All yeast transformations were performed using a modified version of the standard lithium acetate/polyethylene glycol (LiAc/PEG) protocol. 20 ml of a liquid yeast culture were grown overnight to an optical density (OD₆₀₀) of approx. 0.5–0.8 and harvested by centrifugation (2 min, 3500 g, RT). The cells were washed with 25 ml of sterile, deionized H₂O and the resulting pellet was resuspended in 1 ml 0.1 M lithium acetate solution. Cells were pelleted by centrifugation (2 min, 3500 g, RT) and subsequently resuspended in 250 µl of 0.1 M LiAc. 50 µl of this cell suspension were used for each transformation reaction and mixed with either 1 µg of purified plasmid (yeast centromeric or episomal plasmids: pRS316 and pRS425), 2 µg of linearized vector (yeast integrative plasmids: pRS403, pRS405 and pRS406) or 2 µg of a PCR product for integration via homologous recombination. After addition of 240 µl of 50% PEG4000, 36 µl of 1 M LiAc and 5 µl of single stranded (ssDNA) from salmon testis (10 mg/ml, Invitrogen), the reactions were thoroughly mixed and incubated for 30 min at 30 °C under gentle shaking. In order to increase the transformation efficiency, each reaction was supplemented with 36 µl DMSO and subject to a 10 min heat-shock at 42 °C. Subsequently, the cells were harvested by centrifugation (2 min, 3500 g) and the supernatant was completely removed. The pellet was resuspended in 120 µl of sterile, deionized water and plated on corresponding selection media.

The integration of plasmids encoding wild type or mutant versions of Sgo1 (plasmids Nr. 1–8, 11, 13, 14, 19–21) was targeted into the endogenous *SGO1* promoter (in-between *YOR072W* and *YOR073W*) through linearization using the restriction enzyme SphI (NEB, Frankfurt, Germany). Plasmids derived from pRS406 (plasmids Nr. 12, 15, 16) were integrated into the *URA3* locus (*YEL021W*) after linearization using StuI (NEB, Frankfurt, Germany). Plasmid Nr. 22 (derived from pRS403) was integrated into the *HIS3* locus (*YOR202W*) after restriction hydrolysis using NheI (NEB, Frankfurt, Germany).

5.2.9 Extraction of genomic DNA from *S. cerevisiae*

Genomic DNA from budding yeast cells was prepared by phenol/chloroform extraction and subsequent ethanol precipitation. A small amount of yeast cells (freshly grown on agar plates) was transferred to a 1.5 ml reaction tube and resuspended in 200 µl lysis buffer (10 mM Tris/HCl pH 8, 100 mM NaCl, 1 mM EDTA, 2% Triton X-100, 1% SDS). 200 µl of a phenol/chloroform/iso-amylalcohol mixture (Roti® Phenol/C/I, Roth, Karlsruhe, Germany) were added and the mixture was thoroughly mixed. To lyse the yeast cells, approximately 0.3 g of acid washed glass beads (425–600 µm; Sigma-Aldrich) were added and the sample was vortexed for 3 min at maximum speed. Subsequently, 200 µl TE buffer (10 mM Tris/HCl pH 8, 1 mM EDTA) were added and the mixture was vortexed for additional 3 min at maximum speed. Organic and aqueous phase were separated by centrifugation (10 min, 16100 g, RT) and the aqueous phase was transferred to a fresh microcentrifuge tube. To precipitate

DNA from the aqueous phase, 700 µl of pure ethanol were added and the mixture was incubated for 30 min at RT. Genomic DNA was pelleted by centrifugation (10 min, 16100 g, RT), the supernatant was removed and the resulting DNA was washed once with 500 µl of pre-cooled 70% ethanol. After drying, the pellet was resuspended in 50 µl of sterile, deionized water. Genomic DNA extracted by this method was used as template for PCR to either amplify yeast genes for cloning or to verify the correct integration of DNA fragments by homologous recombination.

5.2.10 Sensitivity of yeast mutants towards microtubule poisons and protein overexpression

To analyze the effect of specific mutations on chromosome segregation, the growth of corresponding mutant strains was compared either in the presence of microtubule poisons (benomyl or nocodazole) or upon induction of syntelic attachments by galactose-inducible overexpression of Cik1-cc (Jin *et al.*, 2012). To this end mutant and wild type yeast cells were grown overnight in YP or SC medium containing 2% glucose, diluted to an OD₆₀₀ of 0.3 and tenfold serial dilutions were spotted on YPD/YPG plates or on SC plates containing indicated concentrations of benomyl and nocodazole, respectively. If not stated otherwise, plates were incubated for 2–5 days at 25 °C or 30 °C. Likewise, yeast cells containing a plasmid to overexpress Mps1 under control of the *GAL1* promoter (Nr. 15 or 16) were spotted on plates containing benomyl and 2% galactose to test whether high levels of Mps1 can rescue the chromosome segregation defect of *sgo1* mutants. In addition, the effect of Sli15 overexpression from a high copy number plasmid (yeast episomal plasmid Nr. 23) on mutants with chromosome segregation defects was analyzed. To maintain high levels of the episomal plasmid in these mutants, cells were spotted on YP/SC plates or on plates containing nocodazole without leucine to avoid the loss of copies of plasmid Nr. 23.

5.2.11 Induction of cell cycle arrest and synchronization of *S. cerevisiae* cultures

Haploid *MATa* yeast cells were arrested in G1 through addition of the mating pheromone α -factor (Core Facility, Max Planck Institute of Biochemistry, Martinsried, Germany) to a final concentration of 20 µM. As α -factor becomes degraded over time, the pheromone was added twice at different time points to ensure stringent cell cycle arrest. Liquid cultures of exponentially growing yeast cells in YP or SC complete medium (OD₆₀₀ ranging from 0.6 to 1.5) were supplemented with α -factor to a final concentration of 10 µM and incubated at RT, 25 °C or 30 °C under constant shaking. After 1.5 h incubation, a second aliquot of α -factor was added to reach a final concentration of 20 µM. Subsequently, cultures were incubated for additional 1.5 h at the corresponding temperature.

To arrest yeast cells in mitosis, liquid cultures of exponentially growing yeast cells in YP or SC complete medium (OD₆₀₀ ranging from 0.6 to 1.5) were supplemented with nocodazole (5 mg/ml in DMSO; Santa Cruz Biotechnology, Inc., Dallas, USA) to a final concentration of 20 µg/ml. For

complete depolymerisation of microtubules, the cultures were incubated for 3 h at RT, 25 °C or 30 °C under constant shaking.

The frequency of either large budded (mitotic) or unbudded (G1) cells in the corresponding yeast cultures was determined by light microscopy (ECLIPSE E400, Nikon) to confirm the cell cycle arrest. Cells were released from cell cycle arrest by washout of α -factor or nocodazole. To this end, cells were collected by centrifugation (2 min, 3500 g, RT), the supernatant was removed and the pellet was washed twice with 25 ml of sterile, deionized water. Subsequently, the pellet was resuspended in either YP or SC medium and samples (equivalent to one OD₆₀₀ unit of cells) for cell cycle experiments were withdrawn at indicated timepoints. These samples were snap-frozen in liquid nitrogen and processed according to 5.3.1 after the timecourse was completed.

5.3 Protein biochemistry techniques

5.3.1 TCA precipitation of cellular proteins

The level of endogenous (Cdc20, Clb2, histone H3, Pgk1) and epitope-tagged proteins (eGFP, GST, HA, FLAG, myc) in yeast cells was analyzed via immunoblotting after precipitation of the proteins using trichloroacetic acid (TCA). To this end, cells equivalent to one OD₆₀₀ unit were harvested by centrifugation (2 min, 3500 g) and resuspended in 500 μ l sterile, deionized H₂O. The cells were incubated for 10 min on ice after 100 μ l of alkaline lysis buffer (1.85 M NaOH, 7.5% (v/v) β -mercaptoethanol, 10 mM PMSF) were added. After lysis the cellular proteins were precipitated by addition of TCA to a final concentration of 25% (w/v). The reactions were incubated for 10 min on ice for complete precipitation. Subsequently, the precipitate was collected by centrifugation (10 min, 16100 g, 4 °C) and the supernatant was discarded. The protein-pellet was washed with 1 ml of pre-cooled acetone. To remove residual acetone, the samples were dried completely at 65 °C. The proteins were resuspended in 50 μ l of SDS-sample buffer (62.5 mM Tris/HCl pH 6.8, 2% (w/v) SDS, 10% (v/v) glycerol, 5% (v/v) β -mercaptoethanol, 0.002% (w/v) bromophenol blue) and denatured by boiling for 5 min at 95 °C. Subsequently, the samples were subjected to SDS-PAGE and immunoblotting as described in 5.3.2 and 5.3.3.

5.3.2 SDS-PAGE

Protein samples from yeast cells were separated by discontinuous sodium dodecylsulfate polyacrylamide gel electrophoresis (SDS-PAGE) as previously described (Laemmli, 1970). The denaturing reagent SDS binds to the proteins with its hydrophobic tail and compensates their native charge. Thus, the net charge of a protein correlates with its size in SDS-sample buffer (62.5 mM Tris/HCl pH 6.8, 2% (w/v) SDS, 10% (v/v) glycerol, 5% (v/v) β -mercaptoethanol, 0.002% (w/v)

bromophenole blue). The samples were loaded on polyacrylamide gels (7.5%, 10% or 12.5% separation gel, 5% stacking gel) and electrophoresis was conducted in running buffer (25 mM Tris/HCl, 200 mM glycine, 0.1% (w/v) SDS) at a constant voltage of 200 V for 1 h. PrecisionPlus All Blue protein marker (# 161-0373, Bio-Rad Laboratories) was used as a molecular weight standard. After electrophoresis proteins were either transferred to membranes for immunoblotting or stained for 45–60 min with Coomassie Brilliant Blue (0.25% Coomassie Brilliant Blue R250, 50% (v/v) methanol, 10% (v/v) acetic acid) at room temperature. To remove background of the protein dye, gels were washed with destaining solution (40% methanol, 10% acetic acid) for 2 h.

5.3.3 Immunoblotting

Proteins from polyacrylamide gels were transferred to polyvinylidene difluoride (PVDF) membranes (Roche Diagnostics) using the Mini-PROTEAN wet transfer system (Bio-Rad Laboratories). The blotting unit was assembled in pre-cooled transfer buffer (25 mM Tris/HCl, 1.44% (w/v) glycerol, 20% (v/v) methanol) and transfer was conducted for 70 min at a voltage of 100 V with a direct current of 350 mA. For increased transfer efficiency PVDF membranes were activated in methanol for 2 min and washed with transfer buffer.

In order to inhibit unspecific protein-protein interactions, all membranes were blocked for at least 45 min with 5% skim milk powder in Tris-buffered saline (TBS; 25 mM Tris/HCl pH 7.4, 75 mM NaCl) supplemented with 0.1% (w/v) polyoxyethylene sorbitan monolaurate (Tween). Subsequently, membranes were incubated with primary antibodies (see Table 6) diluted in 5% milk TBS-T either for 2 h at room temperature or overnight at 4 °C under constant shaking. To remove unspecific-bound proteins from membranes, they were washed three times for 10 min with TBS-T under gentle shaking. Secondary antibodies conjugated to horseradish peroxidase (see Table 6) were diluted in 5% milk TBS-T and membranes were incubated with this solution for 2 h at room temperature. Membranes were repeatedly washed for 10 min with TBS-T to remove proteins, which bound due to unspecific protein-protein interactions. Membrane-bound proteins of interest were detected via the enzymatic activity of the horseradish peroxidase conjugated to the corresponding secondary or to the PAP antibody. The ECLprime™ kit (Amersham/GE Healthcare, Little Chalfont, UK) was used for the detection of the resulting luminescence on ECL hyperfilms with variable exposure times (GE Healthcare, Little Chalfont, UK) according to the instruction manual.

5.3.4 *in vitro* binding analysis of Sgo1 and purified PP2A complexes

PP2A complexes containing TAP-tagged Rts1 were purified from yeast strain 284 via affinity chromatography using calmodulin sepharose beads (GE Healthcare, Munich, Germany). In brief, yeast cells were harvested by centrifugation, resuspended in lysis buffer (10 mM Hepes, 200 mM KCl,

1 mM MgCl₂, 1 mM DTT, 1 mM PMSF, 0.5% Triton X-100, supplemented with Roche Protease Inhibitor Mix) and glass bead lysis was performed. The fraction of soluble proteins was separated from cell debris by centrifugation (45 min, 100000 g, 4 °C) and incubated with calmodulin sepharose beads to immunoprecipitate PP2A complexes. Bead-bound proteins were washed with high salt lysis buffer (10 mM Hepes, 600 mM KCl, 1 mM MgCl₂, 1 mM DTT, 1 mM PMSF, 0.5% Triton X-100, supplemented with Roche Protease Inhibitor Mix) and subsequently eluted through the addition of ethylene glycol tetraacetic acid (EGTA) to a final concentration of 5 mM. Equal amounts of purified PP2A complexes were incubated with wild type or mutant (N51I), His₆-tagged Sgo1ΔC fragments and Ni²⁺-NTA-Agarose beads (QIAGEN, Hilden, Germany) for 2 h in pulldown buffer (50 mM Tris/HCl, 300 mM NaCl, 10 mM imidazole, 1 mM PMSF supplemented with Roche protease inhibitor mix). Sgo1ΔC fragments had been expressed from plasmids Nr. 17 and 18 in *E. coli* BL21 (DE3) cells and purified via Ni²⁺-NTA affinity chromatography. Bead-bound Sgo1ΔC fragments were separated from soluble proteins by centrifugation and repeatedly washed with pulldown buffer. Purified proteins were eluted by boiling in SDS sample buffer and subjected to SDS-PAGE followed by immunoblotting to detect co-purified PP2A subunits (experiments were performed by K. Peplowska).

5.4 Chromatin immunoprecipitation (ChIP) followed by quantitative PCR

Chromatin immunoprecipitation (ChIP) experiments were performed using a modified procedure based on a previously published protocol (Kalocsay *et al.*, 2009). Exponentially growing yeast cells were diluted to an optical density (OD₆₀₀) of 0.3 in 100 ml of fresh YPD and incubated for 2 h under constant shaking at room temperature (130 rpm, RT). Each culture was supplemented with 20 μl/ml nocodazole to depolymerize all microtubules and incubated for additional 3 h (130 rpm, RT) to arrest cells in mitosis. The induction of the mitotic arrest was confirmed by analyzing the morphology of yeast cells using light microscopy (ECLIPSE E400, Nikon). DNA and proteins in mitotic cells were cross-linked through addition of formaldehyde to a final concentration of 1% and incubation for 16 min (130 rpm, RT). The cross-linking reaction was terminated through addition of autoclaved 2.5 M glycine solution to a final concentration of 375 mM and incubation for 25 min under constant shaking (130 rpm, RT). Cells equivalent to 50 units of OD₆₀₀ were withdrawn from each culture and pelleted by centrifugation (5 min, 3500 g, 4 °C). Subsequently, the cell pellet was resuspended in 25 ml of pre-cooled phosphate-buffered saline (PBS; 137 mM NaCl, 2.7 mM KCl, 10 mM Na₂HPO₄, 1.8 mM KH₂PO₄), pelleted by centrifugation (5 min, 3500 g, 4 °C) and washed once with 1 ml of PBS. Cells were harvested by centrifugation (5 min, 3500 g, 4 °C), the supernatant was removed and cells were snap-frozen in liquid nitrogen for storage at –80 °C.

The resulting cell pellet was resuspended in 800 μl FA lysis buffer (50 mM HEPES, 150 mM NaCl, 1 mM EDTA, 1% Triton X-100, 0.1 % Deoxycholic acid, 0.1 % SDS) supplemented with protease inhibitors (1 mg/ml Pefabloc SC (Roche) and EDTA-free complete protease inhibitor mix (Roche)) and zirconia beads (0.5 mm, BioSpec Inc., Bartlesville, USA) were added. Subsequently, yeast cells were lysed in seven runs (3 min each with a frequency of 30 Hz) using a bead beater (MM301, Retsch

GmbH, Haan) with 3 min cooling intervals after each run. To separate cell lysate and zirconia beads, the reaction tubes were pierced with a small needle and the lysate was collected in a 15 ml falcon by centrifugation (1 min, 100 g, 4 °C). After the cell lysate was transferred to a fresh 2 ml reaction tube, the chromatin fraction was separated from soluble proteins by centrifugation (15 min, 16100 g, 4 °C). The resulting chromatin pellet was resuspended in 1 ml of FA lysis buffer (50 mM HEPES, 150 mM NaCl, 1 mM EDTA, 1% Triton X-100, 0.1 % Deoxycholic acid, 0.1 % SDS) supplemented with protease inhibitors (1 mg/ml Pefabloc SC (Roche) and EDTA-free complete protease inhibitor mix (Roche)) and transferred to 15 ml Sumilon tubes (Sumitomo Bakelite Co., Japan). The purified chromatin was sheared by water bath sonification to an average fragment size of 250–500 bp with 40 cycles of 30 sec sonification followed by a 30 sec break using the Bioruptor UCD-200 system (Diagenode sa, Liege, Belgium). The soluble chromatin fragments were separated from cell debris and intact cells by centrifugation (35 min, 6150 g, 4 °C) and used as input material for the immunoprecipitation (20 µl were withdrawn as “input” sample for qPCR analysis).

800 µl of this soluble chromatin fraction were incubated with 40 µl of anti-FLAG antibody coupled to super-paramagnetic beads (mouse monoclonal antibody M2, product #M8823, Sigma) for 2 h at room temperature with head-over-tail rotation. Bead-bound protein-DNA adducts were collected using a magnetic rack and washed three times with 400 µl FA lysis buffer (50 mM HEPES, 150 mM NaCl, 1 mM EDTA, 1% Triton X-100, 0.1 % Deoxycholic acid, 0.1 % SDS). Additionally, the immunoprecipitated material was washed twice with 400 µl high salt buffer (50 mM HEPES, 500 mM NaCl, 1 mM EDTA, 1% Triton X-100, 0.1 % Deoxycholic acid, 0.1 % SDS) and once with 400 µl ChIP washing buffer (10 mM Tris/HCl pH 8, 250 mM LiCl, 1 mM EDTA, 0.5% NP-40, 0.5% Deoxycholic acid). After a final washing step with 400 µl TE (10 mM Tris/HCl pH 8, 1 mM EDTA), the beads were resuspended in 110 µl ChIP elution buffer (50 mM Tris/HCl pH 7.5, 1 mM EDTA, 1% SDS). To elute the bound protein-DNA adducts from the antibody-coated beads, the suspension was incubated for 10 min at 65 °C under gentle shaking (1000 rpm). Finally, the beads were collected with a magnetic rack at the bottom of the reaction tube and 100 µl of the supernatant containing the cross-linked material was transferred to a fresh tube (“ChIP” sample). Input as well as ChIP samples were treated for 2 h with Proteinase K (1 mg/ml) at 42 °C to digest immunoprecipitated proteins and further incubated for 6 h at 65 °C to revert residual protein-DNA cross-links.

Co-precipitated DNA fragments were purified via phenol-chloroform extraction followed by ethanol precipitation. To this end, 200 µl of a phenol/chloroform/iso-amylalcohol mixture (Roti® Phenol/C/I, Roth, Karlsruhe, Germany) were thoroughly mixed with ChIP as well as input samples and transferred to phase lock gel tubes (5 PRIME, Inc., Gaithersburg, USA). Organic and aqueous phases were separated by centrifugation (5 min, 16100 g, RT) and the aqueous phase was transferred to a new phase lock gel tube. Subsequently, 500 µl of the phenol/chloroform/iso-amylalcohol mixture were added to the aqueous phase, mixed thoroughly and organic and aqueous phases were again separated by centrifugation (5 min, 16100 g, RT). Purified DNA fragments were precipitated from the aqueous phase by addition of 1 ml ethanol and incubation for 1 h at –20 °C. The precipitated DNA was collected by centrifugation (30 sec, 16100 g, RT), the pellet was washed once with 70% ethanol and resuspended in 50 µl elution buffer (from the QIAGEN PCR purification kit).

In order to evaluate the enrichment of DNA co-precipitated with FLAG-tagged proteins, quantitative real-time PCR (RT-qPCR) was performed using the LightCycler LC480 system in combination with the LightCycler 480 SYBR Green I Master hot-start reaction mix (Roche Diagnostics GmbH, Mannheim, Germany) according to the protocol, which is summarized in Table 9. PCR reactions (0.6 μ M of each primer) containing either 2 μ l of ChIP samples or 2 μ l of input samples (1:10 dilution) were assembled as technical triplicates in 384-well LightCycler plates using the CAS-1200 robot system (Corbett Lifesciences/QuiaGen, Hilden, Germany).

For each used primer pair (see Table 2), a standard curve was generated based on a dilution series from one of the input samples (1:5, 1:50, 1:500 and 1:5000). This standard curve was used for the quantification of the amount of co-purified DNA fragments in ChIP and input samples (second derivative maximum of the PCR amplification curves). To validate the obtained quantification, the specificity of the PCR reaction was monitored by melting curve analysis of each amplified DNA fragment. The ratio of DNA-ChIP sample to DNA-input sample was calculated for centromeric/pericentromeric regions (0.1 kb away from CEN1 (primers Nr. 1 and 2), 1.1 kb away from CEN4 (primers Nr. 3 and 4) and 5 kb away from CEN12 (primers Nr. 5 and 6)) and for the rDNA locus (NTS1-2; primers Nr. 7 and 8). The relative enrichment was calculated by normalization to the ChIP/Input ratio for a control locus on the arm of chromosome 10 (*MDV1/YJL112W*; primers Nr. 9 and 10).

Table 9. Setup of the LightCycler LC480 system to amplify co-purified DNA fragments for quantitative real-time PCR analysis

PCR step	Duration and temperature
Initial denaturing	10 min @ 95 °C
Denaturing step	10 sec @ 95 °C
Annealing step	10 sec @ 55 °C
Elongation step	16 sec @ 72 °C
Number of cycles	45
melting curve analysis	

5.5 Fluorescence microscopy to visualize GFP/RFP-tagged proteins

Images of cells expressing proteins tagged with GFP or RFP were obtained using a fully automated Zeiss inverted microscope (AxioObserver Z1) equipped with a MS-2000 stage (Applied Scientific Instrumentation, USA), a CSU-X1 spinning disk confocal head (Yokogawa, Herrsching), a LaserStack Launch with selectable laser lines (Intelligent Imaging Innovations, USA) and an X-CITE Fluorescent Illumination System. Images were captured using a CoolSnap HQ camera (Roper Scientific, Canada) under the control of the Slidebook software (Intelligent Imaging Innovations, USA). All fluorescence

signals were imaged with a 63x oil objective. A total of 10 z-stacks were collected and each optical section was 0.4 μm thick. Projected images were used for display.

6 References

- Alexandru, G., Uhlmann, F., Mechtler, K., Poupart, M. A., & Nasmyth, K (2001). Phosphorylation of the cohesin subunit Scc1 by Polo/Cdc5 kinase regulates sister chromatid separation in yeast. *Cell* **105**, 459–472.
- Andrews, P. D., & Stark, M. J (2000). Type 1 protein phosphatase is required for maintenance of cell wall integrity, morphogenesis and cell cycle progression in *Saccharomyces cerevisiae*. *J Cell Sci.* **113**, 507–520.
- Bachellier-Bassi, S., Gadai, O., Bourout, G., & Nehrbass, U (2008). Cell cycle-dependent kinetochore localization of condensin complex in *Saccharomyces cerevisiae*. *J Struct Biol.* **162**, 248–259.
- Ben-Shahar, T. R., Heeger, S., Lehane, C., East, P., Flynn, H., Skehel, M., & Uhlmann, F (2008). Eco1-Dependent Cohesin Acetylation During Establishment of Sister Chromatid Cohesion. *Science* **321**, 563–566.
- Biggins, S., Severin, F. F., Bhalla, N., Sassoon, I., Hyman, A. A., & Murray, A. W (1999). The conserved protein kinase Ipl1 regulates microtubule binding to kinetochores in budding yeast. *Genes Dev.* **13**, 532–544.
- Bishop, J. D., & Schumacher, J. M (2002). Phosphorylation of the carboxyl terminus of inner centromere protein (INCENP) by the Aurora B Kinase stimulates Aurora B kinase activity. *J Biol Chem.* **277**, 27577–27580.
- Bouck, D. C., Joglekar, A. P., & Bloom, K. S (2008). Design features of a mitotic spindle: balancing tension and compression at a single microtubule kinetochore interface in budding yeast. *Annu Rev Genet.* **42**, 335–359.
- Buonomo, S. B., Clyne, R. K., Fuchs, J., Loidl, J., Uhlmann, F., & Nasmyth, K (2000). Disjunction of homologous chromosomes in meiosis I depends on proteolytic cleavage of the meiotic cohesin Rec8 by separin. *Cell* **103**, 387–398.
- Burrack, L. S., Applen Clancey, S. E., Chacón, J. M., Gardner, M. K., & Berman, J (2013). Monopolin recruits condensin to organize centromere DNA and repetitive DNA sequences. *Mol Biol Cell.* **24**, 2807–2819.
- Burton, J. L., & Solomon, M. J (2007). Mad3p, a pseudosubstrate inhibitor of APC^{Cdc20} in the spindle assembly checkpoint. *Genes Dev.* **21**, 655–667.

- Campbell, C. S., & Desai, A (2013). Tension sensing by Aurora B kinase is independent of survivin-based centromere localization. *Nature* **497**, 118–121.
- Carmena, M., Wheelock, M., Funabiki, H., & Earnshaw, W. C (2012). The chromosomal passenger complex (CPC): from easy rider to the godfather of mitosis. *Nat Rev Mol Cell Biol.* **13**, 789–803.
- Chao, W. C. H., Kulkarni, K., Zhang, Z., Kong, E. H., & Barford, D (2012). Structure of the mitotic checkpoint complex. *Nature* **484**, 208–213.
- Chan, Y. W., Jeyapakash, A. A., Nigg, E. A., & Santamaria, A (2012). Aurora B controls kinetochore-microtubule attachments by inhibiting Ska complex-KMN network interaction. *J Cell Biol.* **196**, 563–571.
- Cheeseman, I. M., Anderson, S., Jwa, M., Green, E. M., Kang, J.-S., Yates, J. R. 3rd, Chan, C. S., Drubin, D. G., & Barnes, G (2002). Phospho-regulation of kinetochore-microtubule attachments by the Aurora kinase Ipl1p. *Cell* **111**, 163–172.
- Cheeseman, I. M (2014). The kinetochore. *Cold Spring Harb Perspect Biol.* **6**, a015826.
- Christianson, T. W., Sikorski, R. S., Dante, M., Shero, J. H., & Hieter, P (1992). Multifunctional yeast high-copy-number shuttle vectors. *Gene* **110**, 119–122.
- Cimini, D., Howell, B., Maddox, P., Khodjakov, A., Degrossi, F., & Salmon, E. D (2001). Merotelic kinetochore orientation is a major mechanism of aneuploidy in mitotic mammalian tissue cells. *J Cell Biol.* **153**, 517–527.
- Ciosk, R., Zachariae, W., Michaelis, C., Shevchenko, A., Mann, M., & Nasmyth, K (1998). An ESP1/PDS1 Complex Regulates Loss of Sister Chromatid Cohesion at the Metaphase to Anaphase Transition in Yeast. *Cell* **93**, 1067–1076.
- Ciosk, R., Shirayama, M., Shevchenko, A., Tanaka, T., Toth, A., & Nasmyth, K (2000). Cohesin's Binding to Chromosomes Depends on a Separate Complex Consisting of Scc2 and Scc4 Proteins. *Mol Cell* **5**, 243–254.
- Clarke, A. S., Tang, T. T., Ooi, D. L., & Orr-Weaver, T. L (2005). POLO kinase regulates the Drosophila centromere cohesion protein MEI-S332. *Dev Cell* **8**, 53–64.
- Cohen-Fix, O., Peters, J. M., Kirschner, M. W., & Koshland, D (1996). Anaphase initiation in *Saccharomyces cerevisiae* is controlled by the APC-dependent degradation of the anaphase inhibitor Pds1p. *Genes Dev.* **10**, 3081–3093.

- D'Ambrosio, C., Schmidt, C. K., Katou, Y., Kelly, G., Itoh, T., Shirahige, K., & Uhlmann, F (2008a). Identification of cis-acting sites for condensin loading onto budding yeast chromosomes. *Genes Dev.* **22**, 2215–2227.
- D'Ambrosio, C., Kelly, G., Shirahige, K., & Uhlmann, F (2008b). Condensin-dependent rDNA decatenation introduces a temporal pattern to chromosome segregation. *Curr Biol.* **18**, 1084–1089.
- De Antoni, A., Pearson, C. G., Cimini, D., Canman, J. C., Sala, V., Nezi, L., Mapelli, M., Sironi, L., Faretta, M., Salmon, E. D., & Musacchio, A (2005). The Mad1/Mad2 complex as a template for Mad2 activation in the spindle assembly checkpoint. *Curr Biol.* **15**, 214–225.
- DeLuca, J. G., Gall, W. E., Ciferri, C., Cimini, D., Musacchio, A., & Salmon, E. D (2006). Kinetochore microtubule dynamics and attachment stability are regulated by Hec1. *Cell* **127**, 969–982.
- Dieckhoff, P., Bolte, M., Sancak, Y., Braus, G. H., & Irniger, S (2004). Smt3/SUMO and Ubc9 are required for efficient APC/C-mediated proteolysis in budding yeast. *Mol Microbiol.* **51**, 1375–1387.
- Dinkel, H., Van Roey, K., Michael, S., Davey, N. E., Weatheritt, R. J., Born, D., Speck, T., Krüger, D., Grebnev, G., Kuban, M., Strumillo, M., Uyar, B., Budd, A., Altenberg, B., Seiler, M., Chemes, L. B., Glavina, J., Sánchez, I. E., Diella, F., & Gibson, T. J (2014). The eukaryotic linear motif resource ELM: 10 years and counting. *Nucleic Acids Res.* **42**, D259–266.
- Eshleman, H. D., & Morgan, D. O (2014). Sgo1 recruits PP2A to chromosomes to ensure sister chromatid bi-orientation during mitosis. *J Cell Sci.* **127**, 4974–4983.
- Fernius, J., & Hardwick, K. G (2007). Bub1 kinase targets Sgo1 to ensure efficient chromosome biorientation in budding yeast mitosis. *PLoS Genet.* **3**, e213.
- Fuller, B. G., Lampson, M. A., Foley, E. A., Rosasco-Nitcher, S., Le, K. V., Tobelmann, P., Brautigan, D. L., Stukenberg, P. T., & Kapoor, T. M (2008). Midzone activation of aurora B in anaphase produces an intracellular phosphorylation gradient. *Nature* **453**, 1132–1136.
- Gentry, M. S., & Hallberg, R. L (2002). Localization of *Saccharomyces cerevisiae* protein phosphatase 2A subunits throughout mitotic cell cycle. *Mol Biol Cell* **13**, 3477–3492.
- Gerlich, D., Hirota, T., Koch, B., Peters, J. M., & Ellenberg, J (2006). Condensin I stabilizes chromosomes mechanically through a dynamic interaction in live cells. *Curr Biol.* **16**, 333–344.
- Gillett, E. S., Espelin, C. W., & Sorger, P. K (2004). Spindle checkpoint proteins and chromosome-microtubule attachment in budding yeast. *J Cell Biol.* **164**, 535–546.

- Gruber, S., Haering, C. H., & Nasmyth, K (2003). Chromosomal cohesin forms a ring. *Cell* **112**, 765–777.
- Gutiérrez-Caballero, C., Cebollero, L. R., & Pendás, A. M (2012). Shugoshins: from protectors of cohesion to versatile adaptors at the centromere. *Trends Genet.* **28**, 351–360.
- Haase, J., Stephens, A., Verdaasdonk, J., Yeh, E., & Bloom, K (2012). Bub1 kinase and Sgo1 modulate pericentric chromatin in response to altered microtubule dynamics. *Curr Biol.* **22**, 471–481.
- Haering, C. H., Löwe, J., Hochwagen, A., & Nasmyth, K (2002). Molecular Architecture of SMC Proteins and the Yeast Cohesin Complex. *Mol Cell* **9**, 773–788.
- Hanahan, D (1983). Studies on transformation of *Escherichia coli* with plasmids. *Journal of Molecular Biology* **166**, 557–580.
- Hara, K., Zheng, G., Qu, Q., Liu, H., Ouyang, Z., Chen, Z., Tomchick, D. R., & Yu, H (2014). Structure of cohesin subcomplex pinpoints direct shugoshin-Wapl antagonism in centromeric cohesion. *Nat Struct Mol Biol.* **21**, 864–870.
- Hardwick, K. G., Weiss, E., Luca, F. C., Winey, M., & Murray, A. W (1996). Activation of the budding yeast spindle assembly checkpoint without mitotic spindle disruption. *Science* **273**, 953–956.
- Hardwick, K. G., Johnston, R. C., Smith, D. L., & Murray, A. W (2000). MAD3 encodes a novel component of the spindle checkpoint which interacts with Bub3p, Cdc20p, and Mad2p. *J Cell Biol.* **148**, 871–882.
- Hauf, S (2013). The spindle assembly checkpoint: progress and persistent puzzles. *Biochem Soc Trans.* **41**, 1755–1760.
- He, X., Asthana, S., & Sorger, P. K (2000). Transient sister chromatid separation and elastic deformation of chromosomes during mitosis in budding yeast. *Cell* **101**, 763–775.
- Hendzel, M. J., Wei, Y., Mancini, M. A., Van Hooser, A., Ranalli, T., Brinkley, B. R., Bazett-Jones, D. P., & Allis, C. D (1997). Mitosis-specific phosphorylation of histone H3 initiates primarily within pericentromeric heterochromatin during G2 and spreads in an ordered fashion coincident with mitotic chromosome condensation. *Chromosoma* **106**, 348–360.
- Herzog, F., Primorac, I., Dube, P., Lenart, P., Sander, B., Mechtler, K., Stark, H., & Peters, J. M (2009). Structure of the anaphase-promoting complex/cyclosome interacting with a mitotic checkpoint complex. *Science* **323**, 1–5.

- Hirano, T., & Mitchison, T. J (1994). A heterodimeric coiled-coil protein required for mitotic chromosome condensation in vitro. *Cell* **79**, 449–458.
- Hirano, T (2012). Condensins: universal organizers of chromosomes with diverse functions. *Genes Dev.* **26**, 1659–1678.
- Honda, R., Körner, R., & Nigg, E. A (2003). Exploring the functional interactions between Aurora B, INCENP, and survivin in mitosis. *Mol Biol Cell* **14**, 3325–3341.
- Hoyt, M. A., Totis, L., & Roberts, B. T (1991). *S. cerevisiae* genes required for cell cycle arrest in response to loss of microtubule function. *Cell* **66**, 507–517.
- Hsu, J. Y., Sun, Z. W., Li, X., Reuben, M., Tatchell, K., Bishop, D. K., Grushcow, J. M., Brame, C. J., Caldwell, J. A., Hunt, D. F., Lin, R., Smith, M. M., & Allis, C. D (2000). Mitotic phosphorylation of histone H3 is governed by Ipl1/aurora kinase and Glc7/PP1 phosphatase in budding yeast and nematodes. *Cell* **102**, 279–291.
- Huang, H., Feng, J., Famulski, J., Rattner, J. B., Liu, S. T., Kao, G. D., Muschel, R., Chan, G. K., & Yen, T. J (2007). Tripin/hSgo2 recruits MCAK to the inner centromere to correct defective kinetochore attachments. *J Cell Biol.* **177**, 413–424.
- Hwang, L. H., Lau, L. F., Smith, D. L., Mistrot, C. A., Hardwick, K. G., Hwang, E. S., Amon, A., & Murray, A. W (1998). Budding yeast Cdc20: a target of the spindle checkpoint. *Science* **279**, 1041–1044.
- Indjeian, V. B., Stern, B. M., & Murray, A. W (2005). The centromeric protein Sgo1 is required to sense lack of tension on mitotic chromosomes. *Science* **307**, 130–133.
- Indjeian, V. B., & Murray, A. W (2007). Budding yeast mitotic chromosomes have an intrinsic bias to biorient on the spindle. *Curr Biol.* **17**, 1837–1846.
- Ishiguro, T., Tanaka, K., Sakuno, T., & Watanabe, Y (2010). Shugoshin-PP2A counteracts casein-kinase-1-dependent cleavage of Rec8 by separase. *Nat Cell Biol.* **12**, 500–506.
- Ivanov, D., & Nasmyth, K (2005). A topological interaction between cohesin rings and a circular minichromosome. *Cell* **122**, 849–860.
- Janke, C., Ortíz, J., Tanaka, T. U., Lechner, J., & Schiebel, E (2002). Four new subunits of the Dam1-Duo1 complex reveal novel functions in sister kinetochore biorientation. *EMBO J.* **21**, 181–193.

- Janke, C., Magiera, M. M., Rathfelder, N., Taxis, C., Reber, S., Maekawa, H., Moreno-Borchart, A., Doenges, G., Schwob, E., Schiebel, E., & Knop, M (2004). A versatile toolbox for PCR-based tagging of yeast genes: new fluorescent proteins, more markers and promoter substitution cassettes. *Yeast* **21**, 947–962.
- Jeyaprakash, A. A., Klein, U. R., Lindner, D., Ebert, J., Nigg, E. A., & Conti, E (2007). Structure of a Survivin-Borealin-INCENP core complex reveals how chromosomal passengers travel together. *Cell* **131**, 271–285.
- Jin, F., Liu, H., Li, P., Yu, H. G., & Wang, Y (2012). Loss of function of the Cik1/Kar3 motor complex results in chromosomes with syntelic attachment that are sensed by the tension checkpoint. *PLoS Genet.* **8**, e1002492.
- Johzuka, K., & Horiuchi, T (2009). The cis element and factors required for condensin recruitment to chromosomes. *Mol Cell* **34**, 26–35.
- Kalocsay, M., Hiller, N. J., & Jentsch, S (2009). Chromosome-wide Rad51 spreading and SUMO-H2A.Z-dependent chromosome fixation in response to a persistent DNA double-strand break. *Mol Cell* **33**, 335–343.
- Karamysheva, Z., Diaz-Martinez, L. A., Crow, S. E., Li, B., & Yu, H (2009). Multiple anaphase-promoting complex/cyclosome degrons mediate the degradation of human Sgo1. *J Biol Chem.* **284**, 1772–1780.
- Katis, V. L., Galova, M., Rabitsch, K. P., Gregan, J., & Nasmyth, K (2004). Maintenance of cohesin at centromeres after meiosis I in budding yeast requires a kinetochore-associated protein related to MEI-S332. *Curr Biol.* **14**, 560–572.
- Katis, V. L., Lipp, J. J., Imre, R., Bogdanova, A., Okaz, E., Habermann, B., Mechtler, K., Nasmyth, K., & Zachariae, W (2010). Rec8 phosphorylation by casein kinase 1 and Cdc7-Dbf4 kinase regulates cohesin cleavage by separase during meiosis. *Dev Cell* **18**, 397–409.
- Kawashima, S. A., Tsukahara, T., Langeegger, M., Hauf, S., Kitajima, T. S., & Watanabe, Y (2007). Shugoshin enables tension-generating attachment of kinetochores by loading Aurora to centromeres. *Genes Dev.* **21**, 420–435.
- Kawashima, S. A., Yamagishi, Y., Honda, T., Ishiguro, K., & Watanabe, Y (2010). Phosphorylation of H2A by Bub1 prevents chromosomal instability through localizing shugoshin. *Science* **327**, 172–177.
- Kelly, A. E., Ghenoiiu, C., Xue, J. Z., Zierhut, C., Kimura, H., & Funabiki, H (2010). Survivin reads phosphorylated histone H3 threonine 3 to activate the mitotic kinase Aurora B. *Science* **330**, 235–239.

- Kerrebrock, A. W., Miyazaki, W. Y., Birnby, D., & Orr-Weaver, T. L (1992). The *Drosophila* mei-S332 gene promotes sister-chromatid cohesion in meiosis following kinetochore differentiation. *Genetics* **130**, 827–841.
- Kerrebrock, A. W., Moore, D. P., Wu, J. S., & Orr-Weaver, T. L (1995). Mei-S332, a *Drosophila* protein required for sister-chromatid cohesion, can localize to meiotic centromere regions. *Cell* **83**, 247–256.
- Kiburz, B. M., Reynolds, D. B., Megee, P. C., Marston, A. L., Lee, B. H., Lee, T. I., Levine, S. S., Young, R. A., & Amon, A (2005). The core centromere and Sgo1 establish a 50-kb cohesin-protected domain around centromeres during meiosis I. *Genes Dev.* **19**, 3017–3030.
- Kitajima, T. S., Miyazaki, Y., Yamamoto, M., & Watanabe, Y (2003). Rec8 cleavage by separase is required for meiotic nuclear divisions in fission yeast. *EMBO J.* **22**, 5643–5653.
- Kitajima, T. S., Kawashima, S. A., & Watanabe, Y (2004). The conserved kinetochore protein shugoshin protects centromeric cohesion during meiosis. *Nature* **427**, 510–517.
- Kitajima, T. S., Hauf, S., Ohsugi, M., Yamamoto, T., & Watanabe, Y (2005). Human Bub1 defines the persistent cohesion site along the mitotic chromosome by affecting Shugoshin localization. *Curr Biol.* **15**, 353–359.
- Kitajima, T. S., Sakuno, T., Ishiguro, K., Iemura, S., Natsume, T., Kawashima, S. A., & Watanabe, Y (2006). Shugoshin collaborates with protein phosphatase 2A to protect cohesin. *Nature* **441**, 46–52.
- Klein, F., Mahr, P., Galova, M., Buonomo, S. B., Michaelis, C., Nairz, K., & Nasmyth, K (1999). A central role for cohesins in sister chromatid cohesion, formation of axial elements, and recombination during yeast meiosis. *Cell* **98**, 91–103.
- Knop, M., Siegers, K., Pereira, G., Zachariae, W., Winsor, B., Nasmyth, K., & Schiebel, E (1999). Epitope tagging of yeast genes using a PCR-based strategy: more tags and improved practical routines. *Yeast* **15**, 963–972.
- Kotwaliwale, C. V., Frei, S. B., Stern, B. M., & Biggins, S (2007). A pathway containing the Ipl1/aurora protein kinase and the spindle midzone protein Ase1 regulates yeast spindle assembly. *Dev Cell* **13**, 433–445.
- Laemmli, U. K (1970). Cleavage of Structural Proteins during the Assembly of the Head of Bacteriophage T4. *Nature* **227**, 680–685.
- Lampert, F., Hornung, P., & Westermann, S (2010). The Dam1 complex confers microtubule plus end-tracking activity to the Ndc80 kinetochore complex. *J Cell Biol.* **189**, 641–649.

- Lampert, F., & Westermann, S (2011). A blueprint for kinetochores - new insights into the molecular mechanics of cell division. *Nat Rev Mol Cell Biol.* **12**, 407–412.
- Lara-Gonzalez, P., Westhorpe, F. G., & Taylor, S. S (2012). The spindle assembly checkpoint. *Curr Biol.* **22**, 966–980.
- Li, R., & Murray, A. W (1991). Feedback control of mitosis in budding yeast. *Cell* **66**, 519–531.
- Li, Z., Vizeacoumar, F. J., Bahr, S., Li, J., Warringer, J., Vizeacoumar, F. S., Min, R., Vandersluis, B., Bellay, J., Devit, M., Fleming, J. A., Stephens, A., Haase, J., Lin, Z. Y., Baryshnikova, A., Lu, H., Yan, Z., Jin, K., Barker, S., Datti, A., Giaever, G., Nislow, C., Bulawa, C., Myers, C. L., Costanzo, M., Gingras, A. C., Zhang, Z., Blomberg, A., Bloom, K., Andrews, B., & Boone, C (2011). Systematic exploration of essential yeast gene function with temperature-sensitive mutants. *Nat Biotechnol.* **29**, 361–367.
- Lipp, J. J., Hirota, T., Poser, I., & Peters, J. M (2007). Aurora B controls the association of condensin I but not condensin II with mitotic chromosomes. *J Cell Sci.* **120**, 1245–1255.
- Liu, D., Vader, G., Vromans, M. J., Lampson, M. A., & Lens, S. M (2009). Sensing chromosome bi-orientation by spatial separation of aurora B kinase from kinetochore substrates. *Science* **323**, 1350–1353.
- Liu, H., Rankin, S., & Yu, H (2013a). Phosphorylation-enabled binding of SGO1-PP2A to cohesin protects sororin and centromeric cohesion during mitosis. *Nat Cell Biol.* **15**, 40–49.
- Liu, H., Jia, L., & Yu, H (2013b). Phospho-H2A and cohesin specify distinct tension-regulated Sgo1 pools at kinetochores and inner centromeres. *Curr Biol.* **23**, 1927–1933.
- Liu, S. T., Rattner, J. B., Jablonski, S. A., & Yen, T. J (2006). Mapping the assembly pathways that specify formation of the trilaminar kinetochore plates in human cells. *J Cell Biol.* **175**, 41–53.
- London, N., Ceto, S., Ranish, J. A., & Biggins, S (2012). Phosphoregulation of Spc105 by Mps1 and PP1 regulates Bub1 localization to kinetochores. *Curr Biol.* **22**, 900–906.
- London, N., & Biggins, S (2014). Mad1 kinetochore recruitment by Mps1-mediated phosphorylation of Bub1 signals the spindle checkpoint. *Genes Dev.* **28**, 140–152.
- Makrantonis, V., & Stark, M. J (2009). Efficient chromosome biorientation and the tension checkpoint in *Saccharomyces cerevisiae* both require Bir1. *Mol Cell Biol.* **29**, 4552–4562.

- Marston, A. L., Tham, W. H., Shah, H., & Amon, A (2004). A genome-wide screen identifies genes required for centromeric cohesion. *Science* **303**, 1367–1370.
- Marston, A. L (2014). Chromosome segregation in budding yeast: sister chromatid cohesion and related mechanisms. *Genetics* **196**, 31–63.
- McGuinness, B. E., Hirota, T., Kudo, N. R., Peters, J. M., & Nasmyth, K (2005). Shugoshin prevents dissociation of cohesin from centromeres during mitosis in vertebrate cells. *PLoS Biol.* **3**, e86.
- Melby, T. E., Ciampaglio, C. N., Briscoe, G., & Erickson, H. P (1998). The symmetrical structure of structural maintenance of chromosomes (SMC) and MukB proteins: long, antiparallel coiled coils, folded at a flexible hinge. *J Cell Biol.* **142**, 1595–1604.
- Meluh, P. B., Yang, P., Glowczewski, L., Koshland, D., & Smith, M. M (1998). Cse4p is a component of the core centromere of *Saccharomyces cerevisiae*. *Cell* **94**, 607–613.
- Miranda, J. J., De Wulf, P., Sorger, P. K., & Harrison, S. C (2005). The yeast DASH complex forms closed rings on microtubules. *Nat Struct Mol Biol.* **12**, 138–143.
- Moldovan, G., Pfander, B., & Jentsch, S (2006). PCNA controls establishment of sister chromatid cohesion during S phase. *Mol Cell* **23**, 723–732.
- Murayama, Y., & Uhlmann, F (2014). Biochemical reconstitution of topological DNA binding by the cohesin ring. *Nature* **505**, 367–371.
- Musacchio, A., & Salmon, E. D (2007). The spindle-assembly checkpoint in space and time. *Nat Rev Mol Cell Biol.* **8**, 379–393.
- Nasmyth, K., & Haering, C. H (2005). The structure and function of SMC and kleisin complexes. *Annu Rev Biochem.* **74**, 595–648.
- Nasmyth, K., & Haering, C. H (2009). Cohesin: Its Roles and Mechanisms. *Annu Rev Genet.* **43**, 525–558.
- Nerusheva, O. O., Galander, S., Fernius, J., Kelly, D., & Marston A. L (2014). Tension-dependent removal of pericentromeric shugoshin is an indicator of sister chromosome biorientation. *Genes Dev.* **28**, 1291–1309.
- Nishiyama, T., Ladurner, R., Schmitz, J., Kreidl, E., Schleiffer, A., Bhaskara, V., Bando, M., Shirahige, K., Hyman, A. A., Mechtler, K., & Peters JM (2010). Sororin mediates sister chromatid cohesion by antagonizing Wapl. *Cell* **143**, 737–749.

Ocampo-Hafalla, M. T., & Uhlmann, F (2011). Cohesin loading and sliding. *J Cell Sci.* **124**, 685–691.

Palmer, D. K., O'Day, K., Wener, M. H., Andrews, B. S., & Margolis, R. L (1987). A 17-kD centromere protein (CENP-A) copurifies with nucleosome core particles and with histones. *J Cell Biol.* **104**, 805–815

Palmer, D. K., O'Day, K., Trong, H. L., Charbonneau, H., & Margolis, R. L (1991). Purification of the centromere-specific protein CENP-A and demonstration that it is a distinctive histone. *Proc Natl Acad Sci USA* **88**, 3734–3738.

Parisi, S., McKay, M. J., Molnar, M., Thompson, M. A., van der Spek, P. J., van Drunen-Schoenmaker, E., Kanaar, R., Lehmann, E., Hoeijmakers, J. H., & Kohli, J (1999). Rec8p, a meiotic recombination and sister chromatid cohesion phosphoprotein of the Rad21p family conserved from fission yeast to humans. *Mol Cell Biol.* **19**, 3515–3528

Peplowska, K., Wallek, A. U., & Storchová, Z (2014). Sgo1 regulates both condensin and Ipl1/Aurora B to promote chromosome biorientation. *PLoS Genet.* **10**, e1004411.

Peters, J. M (2006). The anaphase promoting complex/cyclosome: a machine designed to destroy. *Nat Rev Mol Cell Biol.* **7**, 644–656.

Primorac, I., & Musacchio, A (2013). Panta rhei: the APC/C at steady state. *J Cell Biol.* **201**, 177–189.

Renshaw, M. J., Ward, J. J., Kanemaki, M., Natsume, K., Nédélec, F. J., & Tanaka, T. U (2010). Condensins promote chromosome recoiling during early anaphase to complete sister chromatid separation. *Dev Cell* **19**, 232–244.

Ribeiro, S. A., Gatlin, J. C., Dong, Y., Joglekar, A., Cameron, L., Hudson, D. F., Farr, C. J., McEwen, B. F., Salmon, E. D., Earnshaw, W. C., & Vagnarelli, P (2009). Condensin regulates the stiffness of vertebrate centromeres. *Mol Biol Cell* **20**, 2371–2380.

Riedel, C. G., Katis, V. L., Katou, Y., Mori, S., Itoh, T., Helmhart, W., Gálová, M., Petronczki, M., Gregan, J., Cetin, B., Mudrak, I., Ogris, E., Mechtler, K., Pelletier, L., Buchholz, F., Shirahige, K., & Nasmyth, K (2006). Protein phosphatase 2A protects centromeric sister chromatid cohesion during meiosis I. *Nature* **441**, 53–61.

Rowland, B. D., Roig, M. B., Nishino, T., Kurze, A., Uluocak, P., Mishra, A., Beckouët, F., Underwood, P., Metson, J., Imre, R., Mechtler, K., Katis, V. L., & Nasmyth, K (2009). Building sister chromatid cohesion: smc3 acetylation counteracts an antiestablishment activity. *Mol Cell* **33**, 763–774.

- Ruchaud, S., Carmena, M., & Earnshaw, W. C (2007). Chromosomal passengers: conducting cell division. *Nat Rev Mol Cell Biol.* **8**, 798–812.
- Salic, A., Waters, J. C., & Mitchison, T. J (2004). Vertebrate shugoshin links sister centromere cohesion and kinetochore microtubule stability in mitosis. *Cell* **118**, 567–578.
- Sambrook, J., Fritsch, E. F., & Maniatis, T (1989). Molecular Cloning. Vol 2. (Cold Spring Harbor, N.Y., Cold Spring Harbor Laboratory Press, 1989).
- Samoshkin, A., Arnaoutov, A., Jansen, L. E., Ouspenski, I., Dye, L., Karpova, T., McNally, J., Dasso, M., Cleveland, D. W., & Strunnikov, A (2009). Human condensin function is essential for centromeric chromatin assembly and proper sister kinetochore orientation. *PLoS One* **4**, e6831.
- Sassoon, I., Severin, F. F., Andrews, P. D., Taba, M. R., Kaplan, K. B., Ashford, A. J., Stark, M. J, Sorger, P. K., & Hyman, A. A (1999). Regulation of *Saccharomyces cerevisiae* kinetochores by the type 1 phosphatase Glc7p. *Genes Dev.* **13**, 545–555.
- Schmidt, C. K., Brookes, N., & Uhlmann, F (2009). Conserved features of cohesin binding along fission yeast chromosomes. *Genome Biol.* **10**, R52.
- Schmitz, J., Watrin, E., Lénárt, P., Mechtler, K., & Peters, J. M (2007). Sororin is required for stable binding of cohesin to chromatin and for sister chromatid cohesion in interphase. *Curr Biol.* **17**, 630–636.
- Seufert, W., Futcher, B., & Jentsch, S (1995). Role of a ubiquitin-conjugating enzyme in degradation of S- and M-phase cyclins. *Nature* **373**, 78–81.
- Shang, C., Hazbun, T. R., Cheeseman, I. M., Aranda, J., Fields, S., Drubin, D. G., & Barnes, G (2003). Kinetochore protein interactions and their regulation by the Aurora kinase Ipl1p. *Mol Biol Cell* **14**, 3342–3355.
- Shepperd, L. A., Meadows, J. C., Sochaj, A. M., Lancaster, T. C., Zou, J., Buttrick, G. J., Rappsilber, J., Hardwick, K. G., & Millar, J. B (2012). Phosphodependent recruitment of Bub1 and Bub3 to Spc7/KNL1 by Mph1 kinase maintains the spindle checkpoint. *Curr Biol.* **22**, 891–899.
- Shi, Y (2009). Serine/threonine phosphatases: mechanism through structure. *Cell* **139**, 468–484.
- Sikorski, R. S., & Hieter, P (1989). A system of shuttle vectors and yeast host strains designed for efficient manipulation of DNA in *Saccharomyces cerevisiae*. *Genetics* **122**, 19–27.

- Simonetta, M., Manzoni, R., Mosca, R., Mapelli, M., Massimiliano, L., Vink, M., Novak, B., Musacchio, A., & Ciliberto, A (2009). The influence of catalysis on mad2 activation dynamics. *PLoS Biol.* **7**, e10.
- Snider, C. E., Stephens, A. D., Kirkland, J. G., Hamdani, O., Kamakaka, R. T., & Bloom, K (2014). Dyskerin, tRNA genes, and condensin tether pericentric chromatin to the spindle axis in mitosis. *J Cell Biol.* **207**, 189–199.
- Song, L., & Rape, M (2011). Substrate-specific regulation of ubiquitination by the anaphase-promoting complex. *Cell Cycle* **10**, 52–56.
- Stephens, A. D., Haase, J., Vicci, L., Taylor, R. M. 2nd, & Bloom, K (2011). Cohesin, condensin, and the intramolecular centromere loop together generate the mitotic chromatin spring. *J Cell Biol.* **193**, 1167–1180.
- Stoler, S., Keith, K. C., Curnick, K. E., & Fitzgerald-Hayes, M (1995). A mutation in CSE4, an essential gene encoding a novel chromatin-associated protein in yeast, causes chromosome nondisjunction and cell cycle arrest at mitosis. *Genes Dev.* **9**, 573–586.
- Storchová, Z., Becker, J. S., Talarek, N., Kögelsberger, S., & Pellman, D (2011). Bub1, Sgo1, and Mps1 mediate a distinct pathway for chromosome biorientation in budding yeast. *Mol Biol Cell* **22**, 1473–1485.
- St-Pierre, J., Douziech, M., Bazile, F., Pascariu, M., Bonneil, E., Sauvé, V., Ratsima, H., & D'Amours, D (2009). Polo kinase regulates mitotic chromosome condensation by hyperactivation of condensin DNA supercoiling activity. *Mol Cell* **34**, 416–426.
- Sumara, I., Vorlaufer, E., Stukenberg, P. T., Kelm, O., Redemann, N., Nigg, E. A., & Peters, J. M (2002). The dissociation of cohesin from chromosomes in prophase is regulated by Polo-like kinase. *Mol Cell* **9**, 515–525.
- Tada, K., Susumu, H., Sakuno, T., & Watanabe, Y (2011). Condensin association with histone H2A shapes mitotic chromosomes. *Nature* **474**, 477–483.
- Takemoto, A., Murayama, A., Katano, M., Urano, T., Furukawa, K., Yokoyama, S., Yanagisawa, J., Hanaoka, F., & Kimura, K (2007). Analysis of the role of Aurora B on the chromosomal targeting of condensin I. *Nucleic Acids Res.* **35**, 2403–2412.
- Tanaka, T. U., Rachidi, N., Janke, C., Pereira, G., Galova, M., Schiebel, E., Stark, M. J., & Nasmyth, K (2002). Evidence that the Ipl1-Sli15 (Aurora kinase-INCENP) complex promotes chromosome bi-orientation by altering kinetochore-spindle pole connections. *Cell* **108**, 317–329.

- Tang, T. T., Bickel, S. E., Young, L. M., & Orr-Weaver, T. L (1998). Maintenance of sister-chromatid cohesion at the centromere by the *Drosophila* MEI-S332 protein. *Genes Dev.* **12**, 3843–3856.
- Tang, Z., Shu, H., Qi, W., Mahmood, N. A., Mumby, M. C., & Yu, H (2006). PP2A is required for centromeric localization of Sgo1 and proper chromosome segregation. *Dev Cell* **10**, 575–585.
- Tanno, Y., Kitajima, T. S., Honda, T., Ando, Y., Ishiguro, K., & Watanabe, Y (2010). Phosphorylation of mammalian Sgo2 by Aurora B recruits PP2A and MCAK to centromeres. *Genes Dev.* **24**, 2169–2179.
- Taxis, C., & Knop, M (2006). System of centromeric, episomal, and integrative vectors based on drug resistance markers for *Saccharomyces cerevisiae*. *Biotechniques* **40**, 73–78.
- Thadani, R., Uhlmann, F., & Heeger, S (2012). Condensin, chromatin crossbarring and chromosome condensation. *Curr Biol.* **22**, 1012–1021.
- Tien, J. F., Umbreit, N. T., Gestaut, D. R., Franck, A. D., Cooper, J., Wordeman, L., Gonen, T., Asbury, C. L., & Davis, T. N (2010). Cooperation of the Dam1 and Ndc80 kinetochore complexes enhances microtubule coupling and is regulated by aurora B. *J Cell Biol.* **189**, 713–723.
- Tsukahara, T., Tanno, Y., & Watanabe, Y (2010). Phosphorylation of the CPC by Cdk1 promotes chromosome bi-orientation. *Nature* **467**, 719–723.
- Uchida, K. S., Takagaki, K., Kumada, K., Hirayama, Y., Noda, T., & Hirota, T (2009). Kinetochore stretching inactivates the spindle assembly checkpoint. *J Cell Biol.* **184**, 383–390.
- Uhlmann, F., & Nasmyth, K (1998). Cohesion between sister chromatids must be established during DNA replication. *Curr Biol.* **8**, 1095–1102.
- Uhlmann, F., Lottspeich, F., & Nasmyth, K (1999). Sister-chromatid separation at anaphase onset is promoted by cleavage of the cohesin subunit Scc1. *Nature* **400**, 37–42.
- Uhlmann, F., Wernic, D., Poupart, M. A., Koonin, E. V., & Nasmyth, K (2000). Cleavage of cohesin by the CD clan protease separin triggers anaphase in yeast. *Cell* **103**, 375–386.
- Unal, E., Heidinger-Pauli, J. M., Kim, W., Guacci, V., Onn, I., Gygi, S. P., & Koshland, D. E (2008). A molecular determinant for the establishment of sister chromatid cohesion. *Science* **321**, 566–569.
- van de Pasch, L. A., Miles, A. J., Nijenhuis, W., Brabers, N. A., van Leenen, D., Lijnzaad, P., Brown, M. K., Ouellet, J., Barral, Y., Kops, G. J., & Holstege, F. C (2013). Centromere binding and a conserved role in chromosome stability for SUMO-dependent ubiquitin ligases. *PLoS One* **8**, e65628.

- Verzijlbergen, K. F., Nerusheva, O. O., Kelly, D., Kerr, A., Clift, D., de Lima Alves, F., Rappsilber, J., & Marston, A. L (2014). Shugoshin biases chromosomes for biorientation through condensin recruitment to the pericentromere. *Elife* **3**, e01374.
- Vleugel, M., Hoogendoorn, E., Snel, B., & Kops, G. J (2012). Evolution and function of the mitotic checkpoint. *Dev Cell* **23**, 239–250.
- Waizenegger, I. C., Hauf, S., Meinke, A., & Peters, J. M (2000). Two distinct pathways remove mammalian cohesin from chromosome arms in prophase and from centromeres in anaphase. *Cell* **103**, 399–410.
- Wang, B. D., Eyre, D., Basrai, M., Lichten, M., & Strunnikov, A (2005). Condensin binding at distinct and specific chromosomal sites in the *Saccharomyces cerevisiae* genome. *Mol Cell Biol.* **25**, 7216–7225.
- Wang, F., Dai, J., Daum, J. R., Niedzialkowska, E., Banerjee, B., Stukenberg, P. T., Gorbisky, G. J., & Higgins, J. M (2010). Histone H3 Thr-3 phosphorylation by Haspin positions Aurora B at centromeres in mitosis. *Science* **330**, 231–235.
- Watanabe, Y., & Nurse, P (1999). Cohesin Rec8 is required for reductional chromosome segregation at meiosis. *Nature* **400**, 461–464.
- Weiss, E., & Winey, M (1996). The *Saccharomyces cerevisiae* spindle pole body duplication gene MPS1 is part of a mitotic checkpoint. *J Cell Biol.* **132**, 111–123.
- Welburn, J. P., Grishchuk, E. L., Backer, C. B., Wilson-Kubalek, E. M., Yates, J. R. 3rd, & Cheeseman, I. M (2009). The human kinetochore Ska1 complex facilitates microtubule depolymerization-coupled motility. *Dev Cell* **16**, 374–385.
- Welburn, J. P., Vleugel, M., Liu, D., Yates, J. R. 3rd, Lampson, M. A., Fukagawa, T., & Cheeseman, I. M (2010). Aurora B phosphorylates spatially distinct targets to differentially regulate the kinetochore-microtubule interface. *Mol Cell* **38**, 383–392.
- Westermann, S., Avila-Sakar, A., Wang, H. W., Niederstrasser, H., Wong, J., Drubin, D. G., Nogales, E., & Barnes, G (2005). Formation of a dynamic kinetochore- microtubule interface through assembly of the Dam1 ring complex. *Mol Cell* **17**, 277–290.
- Westermann, S., Wang, H. W., Avila-Sakar, A., Drubin, D. G., Nogales, E., & Barnes, G (2006). The Dam1 kinetochore ring complex moves processively on depolymerizing microtubule ends. *Nature* **440**, 565–569.

- Wieland, G., Orthaus, S., Ohndorf, S., Diekmann, S., & Hemmerich, P (2004). Functional complementation of human centromere protein A (CENP-A) by Cse4p from *Saccharomyces cerevisiae*. *Mol Cell Biol.* **24**, 6620–6630.
- Winey, M., Mamay, C. L., O'Toole, E. T., Mastronarde, D. N., Giddings, T. H. Jr, McDonald, K. L., & McIntosh, J. R (1995). Three-dimensional ultrastructural analysis of the *Saccharomyces cerevisiae* mitotic spindle. *J Cell Biol.* **129**, 1601–1615.
- Wordeman, L., Wagenbach, M., & von Dassow, G (2007). MCAK facilitates chromosome movement by promoting kinetochore microtubule turnover. *J Cell Biol.* **179**, 869–879.
- Xiong, B., & Gerton, J. L (2010). Regulators of the cohesin network. *Annu Rev Biochem.* **79**, 131–153.
- Xu, Z., Cetin, B., Anger, M., Cho, U. S., Helmhart, W., Nasmyth, K., & Xu, W (2009). Structure and function of the PP2A-shugoshin interaction. *Mol Cell* **35**, 426–441.
- Yamagishi, Y., Sakuno, T., Shimura, M., & Watanabe, Y (2008). Heterochromatin links to centromeric protection by recruiting shugoshin. *Nature* **455**, 251–255.
- Yamagishi, Y., Honda, T., Tanno, Y., & Watanabe, Y (2010). Two histone marks establish the inner centromere and chromosome bi-orientation. *Science* **330**, 239–243.
- Yamagishi, Y., Yang, C., Tanno, Y., & Watanabe, Y (2012). MPS1/Mph1 phosphorylates the kinetochore protein KNL1/Spc7 to recruit SAC components. *Nat Cell Biol.* **14**, 746–752.
- Yamagishi, Y., Sakuno, T., Goto, Y., & Watanabe, Y (2014). Kinetochore composition and its function: lessons from yeasts. *FEMS Microbiol Rev.* **38**, 185–200.
- Yu, H. G., & Koshland, D (2007). The Aurora kinase Ipl1 maintains the centromeric localization of PP2A to protect cohesin during meiosis. *J Cell Biol.* **176**, 911–918.
- Zhang, J., Shi, X., Li, Y., Kim, B. J., Jia, J., Huang, Z., Yang, T., Fu, X., Jung, S. Y., Wang, Y., Zhang, P., Kim, S. T., Pan, X., & Qin, J (2008). Acetylation of Smc3 by Eco1 is required for S phase sister chromatid cohesion in both human and yeast. *Mol Cell* **31**, 143–151.

Abbreviations

μ	micro
5'-FOA	5'-fluoroorotic acid
A	ampere
aa	amino acid
Ade	adenine
Amp	ampicillin
ATP	adenosine-5'-triphosphate
APC/C	anaphase promoting complex/cyclosome
APS	ammonium peroxydisulfate
bp	base pair
cc	coiled-coil
CDC	cell division cycle
CEN	centromere (centromeric DNA)
ChIP	chromatin immunoprecipitation
Chr	chromosome
CPC	chromosomal passenger complex
C-terminal	carboxy-terminal
D-box	destruction-box
DMSO	dimethyl sulfoxide
DNA	deoxyribonucleic acid
DIC	differential interference contrast
dNTP	deoxynucleoside triphosphate
DTT	dithiothreitol
EDTA	ethylenediaminetetraacetic acid
eGFP	enhanced green fluorescent protein
g	gram; gravitational constant
G1	gap 1 phase of the cell cycle
G2	gap 2 phase of the cell cycle
GFP	green fluorescent protein
EtBr	ethidium bromide

Abbreviations

h(s)	hour(s)
H2A/B	histone H2A/B
H3	histone H3
HA	HA human influenza hemagglutinin epitope
HRP	horseradish peroxidase
IN	input
IP	immunoprecipitation
k	kilo
kb	kilo base pairs
kDa	kilo Dalton
KT(s)	kinetochore(s)
l	liter
LB	lysogeny broth
MCS	multiple cloning site
m	milli
M	molar
<i>MAT</i>	mating type
min	minutes
mRNA	messenger RNA
MT(s)	microtubule(s)
MW	molecular weight
myc	human c-Myc protein derived epitope
n	nano
nt	nucleotides
N-terminal	amino-terminal
OD	optical density
ORF	open reading frame
PAGE	polyacrylamide gel electrophoresis
PAP	peroxidase anti-peroxidase
PBS	phosphate-buffered saline
PCR	polymerase chain reaction
PEG	polyethylene glycol
PMSF	phenylmethylsulfonyl fluoride

Abbreviations

PTM	posttranslational modification
qPCR	quantitative PCR
rDNA	DNA coding for ribosomal RNA
RNA	ribonucleic acid
rpm	rounds per minute
RT	room temperature
SAC	spindle assembly checkpoint
s	second
S-phase	DNA synthesis phase of the cell cycle
SC	synthetic complete
SD	standard deviation
SDS	sodium dodecyl sulfate
SEM	standard error of the mean
SIM	SUMO-interacting motif
SMC	structural maintenance of chromosomes
ssDNA	single stranded DNA
STUbL	SUMO-targeted ubiquitin ligase
SUMO	small ubiquitin-like modifier
TAP	tandem affinity purification
TBS	Tris-buffered saline
TCA	trichloroacetic acid
Tris	tris(hydroxymethyl)aminomethane
ts	temperature sensitive
U	unit
Ub	ubiquitin
V	volt
v/v	volume per volume
w/v	weight per volume
WT	wild type
YP	yeast bactopectone

Acknowledgements

First, I would like to sincerely thank my Ph. D. supervisor, Dr. Zuzana Storchová, for giving me the great opportunity to work on this challenging and interesting project as well as for her confidence and trust in my work. Thank you very much for your constant support, your vast creativity and your patience as well as for your scientific expertise and excellent guidance throughout my time in your lab.

In addition, I would like to thank Prof. Stefan Jentsch for his very generous and constant support as well as for providing such an excellent scientific environment to perform research in his department at the Max Planck Institute. Thank you also for being my official Ph. D. thesis supervisor at the faculty of biology of the LMU.

I further want to kindly acknowledge all members of my thesis committee at the LMU. Thus, I would like to thank Prof. Barbara Conradt, Dr. Ralf Heermann, Prof. Nicolas Gompel and Dr. Bettina Bölker for reading and evaluating my manuscript. In particular, I would like to thank Prof. Peter Becker for accepting to co-referee my work.

Furthermore, I want to express my sincere gratitude to Dr. Karolina Peplowska for all the knowledge, results and experience, which she generously shared with me during our work on Shugoshin. Thank you for your constant support and your patience during our endless discussions on our favourite protein.

Very special thanks go to all my colleagues in the Storchova lab for their constant support and helpful suggestions. I would like to thank Aline, Anastasia, Chris, Kasia, Krishna, Mario, Milena, Neysan, Silvia, Susanne, Verena and Yehui for the great pleasure it has been to work with them. In addition, I would like to acknowledge Claudio, Florian, Ivan, Jörg, Max, Sean, Susi and Tim for their helpful suggestions and scientific input (especially on ChIP experiments) as well as all other members of the MCB department. I further owe my thanks to Aline for her great technical support and to Massimo for preparing tons of media and plates. Additionally, I would like to thank Dr. Boris Pfander for the kind gift of the plasmid to tag endogenous yeast proteins with a C-terminal FLAG-tag as well as for all his suggestions and comments during our departmental seminars.

Furthermore, I want to express my sincere gratitude to my friends and family for their ongoing support and honest encouragement. In particular, I want to thank my parents, Anton and Maria, as well as my sister Maximiliane for everything they have done for me to make all this possible.

Finally, I would like to express my heartfelt thanks to Susie. I owe so much to all your open ears, your patience, your support and encouragement during the last years. It was my great pleasure to share them with you.

Curriculum Vitae

Personal Information

Name	Andreas Ulrich Wallek
Date of birth	17.03.1984
Place of birth	Munich
Address	Schönstr. 27a 81543 München

Education and professional experience

01/2011 –	Ph. D. student in the laboratory of Dr. Zuzana Storchová at the Max Planck Institute of Biochemistry (Martinsried)
10/2008 – 10/2010	Master of Science Biochemistry Ludwig-Maximilians-University Munich
10/2004 – 8/2008	Bachelor of Science Chemistry and Biochemistry Ludwig-Maximilians-University Munich
09/1994 – 06/2003	A-levels, secondary school Werner-Heisenberg-Gymnasium Garching

Publications

Peplowska, K.*, Wallek, A. U.*, & Storchová, Z (2014). Sgo1 regulates both condensin and Ipl1/Aurora B to promote chromosome biorientation. *PLoS Genet.* **10**, e1004411.

* these authors contributed equally to this work

Wirth, S., Wallek, A. U., Zernickel, A., Feil, F., Sztiler-Sikorska, M., Lesiak-Mieczkowska, K., Bräuchle, C., Lorenz, I. P., & Czyz, M (2010). Tautomerization of 2-nitroso-N-arylanilines by coordination as N,N'-chelate ligands to rhenium(I) complexes and the anticancer activity of newly synthesized oximine rhenium(I) complexes against human melanoma and leukemia cells in vitro. *J. Inorg. Biochem.* **104**, 774–789.

Stierstorfer, J., Wallek, A. U., & Klapötke, T. M (2008). Nitrogen-Rich Salts of 1-Methyl-5-nitrimino-tetrazolate: An Auspicious Class of Thermally Stable Energetic Materials. *Chem. Mater.* **20**, 4519–4530.